UNIVERSIDADE DA BEIRA INTERIOR
Ciências

Gellan microspheres application for capture or purification of plasmid DNA vaccine

Diana Vanessa Duarte Gomes

Dissertação para obtenção do Grau de Mestre em
Biotecnologia
(2º ciclo de estudos)

Orientadora: Profª. Doutora Ângela Maria Almeida de Sousa
Coorientador: Prof. Doutor Luís António Paulino Passarinha

Covilhã, novembro de 2019

“Anything is possible when
you have the right people
there to support you.”
Misty Copeland

To my amazing family.

Acknowledgements

Firstly, I would like to express my profound and sincere gratitude to Professor Doctor Ângela Sousa and Professor Doctor Luís Passarinha for all the support, patience, and guidance, for the scientific learning that you were able to provide me. You have always been ready to lend a hand, good advisors, so I need to say that it was a great pleasure and an enormous satisfaction to work with you this past year. And also, to Professor Doctor Diana Costa for kindly providing the PEI used in this project.

I would also like to acknowledge the Health Sciences Research Centre and the University of Beira Interior, for providing the adequate conditions that allowed me to develop this work.

Secondly, I would like to thank the Biotechnology and Biomolecular Sciences group, especially to Margarida Grilo, Jorge Ferreira and Margarida Almeida for their help, advice and knowledge shared with me.

To my friends since the beginning of my journey here in Covilhã, Leandro Madureira, Rita Vieira da Costa, Carolina Batista, Ana Nunes, Tiago Pereira, João Diogo, João Valente, Sofia Oliveira, André Cunha, Alexandre Santos a big thanks for the amazing years spent here, all the talks, funny moments, laughs, arguments, friendships, big decisions and especially to give me a second home here in Covilhã.

A big thanks to my lab colleagues and friends from this past year, Adriana Pinto, Diana Pereira, Raquel Neves, Rita Carapito, Micaela Riscado, Rita Proença, and the new ones, Pedro Vicente, Sofia Oliveira and Pedro Ferreira for all the advices, support, the talks about nothing and everything at the same time, all the shared breaks and also the “not so good moments”, because this has made us a family that I know I can always count on. THANKS!

Finally, to my amazing family for all the support, help provided and also for always believe that I was capable. To my parents, Clara Martins and Rui Gomes, my siblings, Catarina Gomes and Rui Gomes and also my grandparents, Adosinda Duarte e António Martins a huge thank you for always being there for me, for making every effort possible to give me the best, for all dedication and love. I would not have accomplished everything I have without you, I’m so grateful. I love you!

Resumo Alargado

O vírus do papiloma humano (HPV) é um vírus sexualmente transmissível e a persistência da sua infeção é considerada a maior causa para o desenvolvimento do cancro do colo do útero. Este potencial oncogénico do HPV está diretamente relacionado com a expressão das oncoproteínas E6 e E7, visto que estas têm a capacidade de interferir na desregulação do ciclo celular, indução da apoptose, entre outros fenómenos biológicos. O cancro do colo do útero corresponde à 4º maior causa de morte nas mulheres a nível mundial. No entanto, com as evoluções alcançadas ao nível científico tem sido possível melhorar e desenvolver novas terapias à base de DNA para tratar vários problemas de saúde como cancro e doenças genéticas. Sendo uma delas, as vacinas de DNA, uma vez que estas têm a capacidade de despoletar todos os tipos de imunidade desejada, através da resposta celular e resposta humoral, evitando a evolução da doença, o que é uma vantagem em relação às vacinas convencionais. Os vetores de DNA plasmídico (pDNA) codificantes de determinados antigénios têm sido muito explorados como vacinas de DNA, uma vez que apresentam baixa toxicidade e são mais simples de desenvolver. O processo biotecnológico de preparação do biofármaco de pDNA compreende etapas sequenciais de produção, clarificação e purificação com objetivo de obter a isoforma superenrolada (sc) com o grau de pureza recomendado pelas agências reguladoras, já que é considerada a conformação de pDNA biologicamente ativa. Contudo, este processo é bastante dispendioso para a indústria farmacêutica e apresenta um impacto ambiental acentuado, devido ao uso de elevadas quantidades de solventes orgânicos (isopropanol) e sais caotrópicos (sulfato de amónio e sulfato de sódio). Desta forma, é fundamental desenvolver novas estratégias de captura ou purificação do pDNA sc de modo a simplificar a amostra e evitar o uso de determinados reagentes, tornando o processo mais “green” e económico.

A goma gelana é um exopolissacárido microbiano aniónico que tem a capacidade de, em determinadas condições (presença de catiões, concentração de polímero, temperatura), alterar a sua estrutura conformacional e formar uma rede tridimensional dando origem a um gel termorreversível com diferentes características estruturais e propriedades, consoante o objetivo desejado. A gelana apresenta diversas aplicações na indústria alimentar (espessante, gelificante), farmacêutica (formulações oftálmicas), cosmética (loções, cremes), biotecnológica (substituinte do agar), e devido, a características como a sua biocompatibilidade, hidrofilicidade, porosidade e versatilidade tem vindo a ser explorada nos últimos anos como matriz cromatográfica. Recentemente foi explorada e otimizada por desenho experimental a formulação de microsferas de gelana através do método de emulsão água-em-óleo e reforço com iões divalentes para capturar proteínas em função da sua carga ou afinidade.

Assim, o objetivo central deste trabalho foi formular as microsferas de gelana e desenvolver uma estratégia de captura de pDNA sc a partir de um lisado bruto de *Escherichia coli* (*E. coli*) aplicando o método de batch. Para tal, a amostra de lisado foi obtida através de uma fermentação em *E. coli,* com posterior lise alcalina. As microesferas de gelana foram preparadas pelo método de emulsão água–em–óleo, reforçadas com alguns iões divalentes, cobre, níquel, zinco, cobalto, e algumas formulações foram posteriormente funcionalizadas com o polímero de polietilenoimina (PEI). O menor diâmetro das formulações foi obtido com 1.41 % de uma solução aquosa de gelana, previamente aquecida a 90 ºC que foi gotejada através de uma seringa para uma solução de óleo aquecida anteriormente a 100 ºC sob constante agitação de 750 rpm a uma velocidade de 75 µL/min. Ambas as formulações foram caracterizadas relativamente ao diâmetro médio (microscopia de semiótica), à morfologia (SEM), à carga global (potencial zeta) e à composição elementar (EDX e FTIR). Dos resultados obtidos quanto à morfologia, ambas as topologias de microesferas apresentam uma forma esférica e consistente. A estabilidade das duas formulações foi avaliada pela medição do diâmetro médio ao longo de vinte dias e ambas se apresentam estáveis ao longo do período em análise. Em relação ao diâmetro médio, as microesferas funcionalizadas com PEI apresentam um menor diâmetro que as microesferas reforçadas com cobre, o que pode ser devido à formação de uma ligação de coordenação entre o PEI e o cobre tornando a sua estrutura mais compacta. Esta ligação pode ter também um efeito na composição elementar pois, as microesferas reforçadas com cobre apresentam cerca de 9 % de cobre e as que foram funcionalizadas com PEI, apresentam 17 % de aminas e apenas 0.62 % de cobre. As microesferas reforçadas com cobre apresentam uma carga superficial de cerca de – 5 mV e as que que foram funcionalizadas com PEI, apresentam uma carga superficial de cerca de + 5 mV.

As estratégias de captura desenvolvidas tiveram por base a interação entre os iões metálicos reticulados nas microesferas e o pDNA presente no lisado celular, uma vez que a carga negativa do polímero de gelana repele os ácidos nucleicos. Após inúmeros estudos de otimização, as melhores condições de ligação do pDNA sc às microesferas de gelana reticuladas com cobre foram obtidas a pH 5.0 e a eluição com 200 mM NaCl em 10 mM Tris-HCl, 1 mM EDTA, pH 8.0, permitindo assim recuperar 15.61 % de pDNA sc com 2.42 % de pureza. Adicionalmente, outra estratégia desenvolvida para melhorar a captura de pDNA consistiu na precipitação do lisado de *E. coli* com 2,5 M de sulfato de amónio. Ao eliminar a maior parte das impurezas (RNA e proteínas) a quantidade de pDNA sc capturado aumentou para 32.41 % com um grau de pureza de 12.43 %. Por fim, as microesferas de gelana foram funcionalizadas com PEI, com objetivo de melhorar a captura de pDNA, tendo em conta o aumento de grupos funcionalizados para interagirem com DNA na superfície das microesferas. Nas microsferas funcionalizadas com PEI, o passo de ligação foi realizado com um tampão de 10 mM MES a pH 5.0 e a eluição com 200 mM NaCl em 10 mM Tris-HCl, 1 mM EDTA, pH 10.5. Nestas condições, foi possível a captura total do pDNA presente na amostra de lisado e uma recuperação/eluição 88.09 % de pDNA sc. Contudo, também ocorreu a retenção de grande parte do RNA da amostra que resultou num

decréscimo do grau de pureza para 3.18 %. Assim sendo, se o objetivo principal for a captura total de pDNA de lisados brutos sem recorrer a sais ou solventes orgânicos, a estratégia que apresenta grande potencial é aquela em que as microesferas foram funcionalizadas com PEI. Por outro lado, se o objetivo principal for a captura de pDNA com um grau de pureza mais elevado, é recomendado realizar um passo prévio de tratamento com sulfato de amónio antes do passo de captura, sendo que neste se pode aplicar as microesferas reticuladas com cobre ou também as funcionalizadas com PEI. Concluindo, estas estratégias simples e de baixo custo permitiram a clarificação do lisado sem ser necessário recorrer a solventes orgânicos como o isopropanol, visto que o lisado de *E. coli* normalmente apresenta cerca de 1.07 % de pDNA.

Palavras-chave

Infeção por HPV, método de batch, microesferas de gelana, passo de clarificação, polietilenimina, vacina pDNA.

Abstract

Cervical cancer is the 4th cause of death among women worldwide and is profoundly associated with HPV infection, due to apoptosis inhibition and uncontrolled cell proliferation caused by oncoproteins E6 and E7 action. At the moment, some prophylactic vaccines are available in the market, but that are only capable of preventing HPV infection. Thus, the development of effective treatment for HPV-infected individuals is fundamental. DNA vaccines emerged as a promising way to prevent and treat several diseases since it can stimulate both cellular and humoral immune responses. The biotechnological process for obtaining plasmid DNA (pDNA) includes several steps, which present an environmental impact and makes it quite expensive to the pharmaceutical industry. Therefore, it is crucial to explore new alternatives. In this work, copper-crosslinked gellan microspheres were produced through a water-in-oil emulsion in order to capture pDNA directly from the *Escherichia coli* (*E. coli*) lysate seeking a reduction in the recovery and clarification-associated costs. The lowest diameter of gellan microspheres was achieved with 1.41 % of an aqueous gellan gum solution, previously heated at 90ºC, and dripped through a syringe to the oil solution formerly heated at 100 ºC with constant stirring of 750 rpm at a flow rate of 75 µL/min. Afterwards batch method optimization, the gellan microspheres captured 15.61 % of pDNA with 2.42 % of purity by a strategy based on immobilized metal affinity chromatography (IMAC), by manipulating the pH and ionic strength of binding and elution buffers. Another strategy was developed in order to increase the pDNA capture by precipitating the *E. coli* lysate with ammonium sulfate. The elimination of major impurities improved the recovery percentage to 32.41 % and the purity degree to 12.43 %. Moreover, copper-crosslinked gellan microspheres were functionalized with polyethylenimine (PEI), in order to increase the pDNA capture by increasing the functional groups in the microspheres surface. This allowed an improvement in the recovery percentage to 88.09 %, but the same did not happen to the purity percentage, 3.18 %.

Thus, if the central aim is total pDNA capture from crude lysates without resorting to salts or organic solvents, the strategy in which the microspheres were functionalized with PEI showed great potential. On the other hand, if the main objective is to capture pDNA with higher purity, it is recommended to perform a prior step to the capture with ammonium sulfate, where copper-crosslinked microspheres may be applied or also the ones functionalized with PEI. In conclusion, these simple, fast and low-cost strategies allow lysate clarification since an *E. coli* lysate usually has 1.07 % of pDNA.

Keywords

HPV infection, pDNA vaccine, clarification step, gellan gum microspheres, batch method, polyethylenimine.

Index

CHAPTER 1 - INTRODUCTION 1
1.1 HUMAN PAPILLOMAVIRUS 1
1.1.1 HPV life-cycle and molecular biology *1*
1.1.2 E6 Oncoprotein *3*
1.1.3 E7 Oncoprotein *4*
1.1.4 Preventive and therapeutic vaccination *5*
1.2 DNA-BASED THERAPY 5
1.2.1 Gene Therapy *6*
1.2.2 DNA vaccines *7*
1.2.3 DNA delivery systems *9*
1.2.3.1 Viral Vectors *9*
1.2.3.2 Non-viral vectors *11*
1.3 PLASMID DNA 14
1.3.1 Upstream process *15*
1.3.2 Downstream process *16*
1.3.2.1 Clarification methods *17*
1.3.2.1.1 MEMBRANE PROCESSES 17
1.3.2.1.2 Precipitation *19*
1.3.2.1.3 Liquid-Liquid Extraction *20*
1.3.2.2 Chromatographic methods *21*
1.3.2.2.1 Size Exclusion Chromatography (SEC) *21*
1.3.2.2.2 Ion Exchange Chromatography (IEC) *22*
1.3.2.2.3 Hydrophobic Interaction Chromatography (HIC) *23*
1.3.2.2.4 Affinity Chromatography (AC) *24*
1.3.2.2.4.1 Immobilized Metal Ion Affinity Chromatography (IMAC) *25*
1.3.2.3 Batch Method *25*
1.4 GELLAN GUM 26
1.4.1 Molecular Structure *26*
1.4.2 Properties *28*
1.4.3 Applications *30*
CHAPTER 2 - OBJECTIVES **35**
CHAPTER 3 – MATERIALS AND METHODS **37**
3.1 MATERIALS 37
3.2 METHODS 37

3.2.1 Bacterial growth conditions and plasmid production *37*
3.2.2 Plasmid extraction *38*
3.2.3 Gellan microspheres production through water-in-oil emulsion *38*
3.2.3.1 Semi-optical analysis *38*
3.2.3.2 FTIR analysis *38*
3.2.3.3 SEM ANALYSIS 39
3.2.3.4 EDX analysis *39*
3.2.3.5 Global charge analysis through zeta potential *39*
3.2.4 Batch method for plasmid DNA capture *39*
3.2.4.1 Agarose gel electrophoresis *39*
3.2.4.2 Plasmid DNA quantification *40*
3.2.4.3 Total protein quantification *41*

CHAPTER 4 – RESULTS AND DISCUSSION 43

4.1 GELLAN MICROSPHERES PRODUCTION 43
4.2 STRATEGIES FOR PLASMID DNA CAPTURE THROUGH A BATCH METHOD 44
4.2.1 Screening of the batch method conditions *44*
4.2.1.1 Influence of different metal ions as crosslinkers *44*
4.2.1.2 Influence of pH and buffer *48*
4.2.2 Characterization of copper-crosslinked gellan microspheres *52*
4.2.2.1 Gellan microspheres stability analysis *53*
4.2.2.2 FTIR analysis *54*
4.2.2.3 SEM analysis *57*
4.2.2.4 EDX analysis *57*
4.2.2.5 Global charge analysis through zeta potential *58*
4.2.3 Study of the impurities influence by analysis of a pre-clarified E. coli lysate *58*
4.2.4 Study of the pDNA capture through functionalized microspheres *60*
4.2.5 Characterization of PEI-functionalized gellan microspheres *64*
4.2.5.1 Gellan microspheres stability analysis *65*
4.2.5.2 SEM analysis *66*
4.2.5.3 EDX analysis *66*

CHAPTER 5 - CONCLUSIONS AND FUTURE PERSPECTIVES 69

CHAPTER 6 – BIBLIOGRAPHY 71

List of figures

Figure 1 – HPV genome (adapted from (Durzynska, Lesniewicz et al. 2017)). 2

Figure 2 – Schematic representation of HPV infection (adapted from (Durzynska, Lesniewicz et al. 2017)). 3

Figure 3 - Schematic representation of the action mechanism of E6 oncoprotein (adapted from (Viarisio, Gissmann et al. 2017)). 4

Figure 4 - Schematic representation of the action mechanism of E7 oncoprotein (adapted from (Viarisio, Gissmann et al. 2017)). 4

Figure 5 - Mechanism of antigen presentation (a): Antigen presentation mediated directly by transfected myocytes; (b): Transfection of professional APCs; (c): Cross priming (adapted from (Hasson, Al-Busaidi et al. 2015)). 8

Figure 6 - Number of patents in the field of DNA vaccines (adapted from (Abdulrahman and Ghanem 2018))..... 9

Figure 7 - Models of non-viral nucleic acid delivery. (adapted from (Slivac, Guay et al. 2017))… 12

Figure 8 - Representation of upstream and downstream process of large-scale purification of supercoiled plasmid DNA (adapted from (Guilherme N.M. Ferreira 2000, Van Alstine, Jagschies et al. 2018)). 15

Figure 9 - Plasmid DNA expression vector (adapted from (Armando Tejeda-Mansir 2008))..... 16

Figure 10 – Different types of membranes and the respectively retained solute (adapted from (Aires-Barros and Azevedo 2017)). 18

Figure 11 – Normal flow filtration and tangential flow filtration processes (adapted from (Aires-Barros and Azevedo 2017, Liderfelt and Royce 2018)). 19

Figure 12 –Representation of precipitation methods - A: Elimination of proteins and high MW RNA by salt precipitation; B: Concentration of pDNA by addition of alcohols (adapted from (Thatcher 2018)).....19

Figure 13 - Schematic representation of target product recovery by ATPS (adapted from (Phong, Show et al. 2018)). 20

Figure 14 - Schematic representation of size exclusion chromatography (adapted from (Sciences 2015)). 22

Figure 15 - Schematic representation of ion-exchange chromatography (adapted from (Sciences 2016)). 23

Figure 16 - Schematic representation of hydrophobic interaction chromatography (adapted from (Sciences 2006)). 23

Figure 17 - Schematic representation of affinity chromatography (adapted from (Sciences 2016)). 24

Figure 18 - Representation of batch method steps. 26

Figure 19 - Chemical structure of native (A) and deacetylated (B) gellan gum (adapted from (Osmalek, Froelich et al. 2014)). 27

Figure 20 - Representation of the gelation process (adapted from (Morris, Nishinari et al. 2012)). 29

Figure 21 - Calibration curve obtained from the sc pDNA with a range of concentrations from 1 to 100 g/mL. 40

Figure 22 – A: Chromatographic profile of the *E. coli* lysate sample in the CIMac^{TM}pDNA analytical column. B: Chromatographic profile of the pDNA elution…. 40

Figure 23 - Calibration curve obtained with BSA standards (0-1200 µg/mL). 41

Figure 24 -Schematic representation of microspheres production. 44

Figure 25 – Agarose gel electrophoresis of the supernatants recovered from gellan microspheres prepared with different divalent ions…. 46

Figure 26 - Agarose gel electrophoresis of the supernatants recovered in the 2nd assay…. 49

Figure 27 – Representative image of copper-crosslinked gellan microspheres after its production obtained in the semiotic microscope (5x). 52

Figure 28 - Representative images of the copper-crosslinked gellan microspheres obtained in the semiotic microscope (5x). A – Snap taken at 0 days; B - Snap taken at 3 days; C - Snap taken at 10 days; D - Snap taken at 20 days. 53

Figure 29 - FTIR spectra: A - Gellan gum spectrum; B - Microspheres crosslinked with Cu^{2+} spectrum. 55

Figure 30 - FTIR spectra: A – Second derivative of the FTIR spectrum of the microspheres crosslinked with copper after the binding step; B - Microspheres crosslinked with Cu^{2+} spectrum. 56

Figure 31 - Representation of the copper-crosslinked gellan microspheres, visualized in SEM at a magnification of x70 (A) and x200 (B).....57

Figure 32 - Agarose gel electrophoresis of the supernatants recovered from the 3rd assay… ..59

Figure 33 – Zeta potential of the PEI-functionalized microspheres at different pH values. 61

Figure 34 - Agarose gel electrophoresis of the supernatants recovered from the 4th assay… ..62

Figure 35 - Image of (A) microspheres crosslinked with copper and (B) microspheres functionalized with PEI. 64

Figure 36 – Image of PEI-functionalized gellan microspheres after its production obtained in the semiotic microscope (5x).....64

Figure 37 - Images of the PEI-functionalized gellan obtained in the semiotic microscope (5x). A – Snap taken at 0 days; B - Snap taken at 3 days; C - Snap taken at 10 days; D - Snap taken at 20 days.....65

Figure 38 - Representation of the PEI-functionalized gellan microspheres, visualized in SEM at a magnification of x70 (A) and x200 (B).....66

List of tables

Table 1 – Viral protein functions and features (adapted from (Viarisio, Gissmann et al. 2017, Gupta, Kumar et al. 2018)). 2

Table 2 – Approved gene therapy products (adapted from (Ginn, Amaya et al. 2018)). 7

Table 3 - Advantages and disadvantages of viral vectors (adapted from (Ibraheem, Elaissari et al. 2014, Carter and Shieh 2015)). 10

Table 4 - Description of the different physical methods applied in gene delivery. 13

Table 5 - Chemical composition of different types of gellan (adapted from (loannis Giavasis 2000)). 27

Table 6 - Conventional applications of gellan gum in food. 31

Table 7 - Utility of gellan gum in the medical field through oral, nasal or ophthalmic formulations (adapted from (Prajapati, Jani et al. 2013, Osmalek, Froelich et al. 2014)). 32

Table 8 – Assessment of the sc pDNA concentration, total sc pDNA amount…. 47

Table 9 - Description of the equilibrium and elution conditions applied in the 2nd assay. 49

Table 10 - Assessment of the sc pDNA concentration, total sc pDNA amount… 50

Table 11 - Total protein amount of the E. coli lysate and supernatants recovered after the binding and elution step of the 1st and 2nd assays. 51

Table 12 – Copper-crosslinked gellan microspheres mean diameter considering the stability over time (n=5). 54

Table 13 - Chemical characterization of gellan microspheres crosslinked with copper through EDX. 58

Table 14 - Total protein amount of the crude E. coli lysate from 1st assay and of E. coli lysate precipitated with 2.5 M ammonium sulfate from the 3rd assay. 58

Table 15 – Assessment of the sc pDNA concentration, total sc pDNA amount… 60

Table 16 - Assessment of the sc pDNA concentration, total sc pDNA amount…. 63

Table 17 – PEI-functionalized gellan microspheres mean diameter considering the stability over time (n=5). 65

Table 18 - Chemical characterization of PEI-functionalized gellan microspheres through EDX. 67

List of acronyms

3D	Three-dimensional
AAV	Adeno-associated viruses
AC	Affinity chromatography
Al^{3+}	Aluminum (III) ion
APCs	antigen-presenting cells
APOBEC3	Apolipoprotein B mRNA editing enzyme catalytic polypeptide 3
ATPS	Aqueous two-phase systems
ATR	Attenuated total reflection
Ba^{2+}	Barium (II) ion
BAK	Bcl-2-antagonist killer
BCA	Bicinchoninic acid
BSA	Bovine serum albumin
Ca^{2+}	Calcium (II) ion
Cd^{2+}	Cadmium (II) ion
CDK2	cyclin dependent kinase 2
Cgas-STING	Cyclic GMP-AMP synthase-Stimulator of interferon genes
Co^{2+}	Cobalt (II) ion
CTAB	Cetyl trimethylammonium bromide
Cu^{2+}	Copper (II) ion
DLS	Dynamic light scattering
DMAEMA	n,n-dimethylaminoethyl methacrylate
DNA	Deoxyribonucleic acid
E. coli	*Escherichia coli*
E2F	Transcription factor
E2F1-3	Subclass of E2F factors
E2F4-5	Subclass of E2F factors
E6AP	E6 associated protein
EDTA	Ethylenediamine tetraacetic acid
EDX	Energy-dispersive X-ray spectroscopy
EMA	European Medicines Agency
EP	Electroporation
EPS	Exopolysaccharides
FDA	Food and Drug Administration
Fe^{3+}	Iron (III) ion
FTIR	Fourier-transform infrared spectroscopy
gDNA	Genomic DNA

GG	Gellan gum
HIC	Hydrophobic interaction chromatography
HPMC	Hydroxypropylmethylcellulose
HPV	Human papillomavirus
HR HPV	High-Risk HPV
HSV	Herpes simplex virus
IEC	Ion Exchange Chromatography
IFNα	Interferon α
IMAC	Immobilized Metal Ion Affinity Chromatography
IRF3	Interferon regulatory factor 3
K^+	Potassium ion
Kbp	Kilobase pair
KDa	Kilo Dalton
LB	Luria-Bertani
LCR	Long region control
ln	Linear isoform
MES	4-Morpholineethanesulfonic acid
MF	Microfiltration
Mg^{2+}	Magnesium ion
MHC	Major histocompatibility complex
MMP-9	Matrix metallopeptidase 9
Mn^{2+}	Manganese ion
MW	Molecular Weight
MWCO	Molecular Weight cut-off
Myc	intermediary proto-oncogene protein
Na^+	Sodium ion
NF	Nanofiltration
NFF	Normal flow filtration
Ni^{2+}	Nickel ion
Nm	Nanometer
O/W emulsion	Oil-in-water emulsion
oc	Open circular isoform
OD	Optical density
P300/CBP complex protein	CREB binding protein
PAMAM	Poly(amidoamine)
PBAE	Poly(ß-amino ester)s
Pd^{2+}	Palladium ion
pDNA	Plasmid DNA

PEG	Polyethylene glycol
PEI	Polyethylenimine
PLGA	Poly(lactic-co-glycolic acid)
PLL	Poly-l-lysine
polyDADMAC	Polydiallyldimethylammonium chloride
pRb	retinoblastoma protein
RNA	Ribonucleic acid
RO	Reverse Osmosis
Rpm	Revolutions per minute
sc	Supercoiled isoform
SCRIB	scribbled planar cell polarity protein
SD	Standard deviation
SDS	Sodium dodecyl sulfate
SEC	Size Exclusion Chromatography
SEM	Scanning electron microscope
siRNA	Silencing RNA
Sp1	Specificity protein 1
Sr^{2+}	Strontium ion
TAE	Tris-acetate-EDTA
TB	Terrific Broth
TFF	Tangential Flow Filtration
TLR9	Toll-like receptor 9
Tris	Tris(hydroxymethyl)aminomethane
UF	Ultrafiltration
VLPs	Virus-like particles
W/O emulsion	Water-in-oil emulsion
w/v %	Weight per volume percentage
WHO	World Health Organization
XRCC1	X-ray repair cross-complementing protein 1
Zn^{2+}	Zinc ion

List of communications

Oral communication:

- XIV Annual CICS-UBI Symposium, Covilhã, July 2019: Diana Gomes, Luís A. Passarinha, Ângela Sousa, Plasmid DNA capture from *E. coli* lysates applying gellan microspheres through a batch method.
- 13th International Meeting of the Portuguese Carbohydrate Group, Porto, September 2019: C. Gonçalves, D. Gomes, M. Grilo, A. Sousa, L.A. Passarinha, Gellan microsphere formulation for direct capture of Soluble catechol-O-methyltransferase from a *Komagataella pastoris* lysate.
- 13th International Meeting of the Portuguese Carbohydrate Group, Porto, September 2019: J. Coelho, D. Eusébio, D. Gomes, F. Frias, L.A. Passarinha, A. Sousa, Gellan exopolysaccharide biosynthesis and recovery to formulate microspheres optimized by Design of experiments.

Poster presentation:

- 13th International Meeting of the Portuguese Carbohydrate Group, Porto, September 2019: D. Gomes, L.A. Passarinha, A. Sousa, A new application of gellan microspheres for plasmid DNA capture from *E. coli* lysates through a batch method.
- III International Congress in Health Sciences Research: Towards Innovation and Entrepreneurship - Trends in Aging and Cancer, November 2019: Diana Gomes, Luís A. Passarinha, Ângela Sousa, A new insight of gellan microspheres application for *E. coli* lysates pDNA capture through a batch method.

List of publications

Coelho, J., D. Eusebio, D. Gomes, F. Frias, L. A. Passarinha and A. Sousa (2019). "Biosynthesis and isolation of gellan polysaccharide to formulate microspheres for protein capture." Carbohydr Polym **220**: 236-246.

C. Gonçalves, D. Gomes, M. Grilo, A. Sousa, L.A. Passarinha. “Strategies for direct capture of Soluble catechol-O-methyltransferase from a Komagataella pastoris lysate with gellan microspheres" (in preparation)

Chapter 1 - Introduction

1.1 Human Papillomavirus

Human papillomavirus (HPV) causes about 5% of all human cancers, (Martinez-Ramirez, Carrillo-Garcia et al. 2018) and it is responsible for 99% of cervical cancer cases, which is the fourth cause of cancer death among women worldwide. HPV is also involved in non-cervical malignancies such as vulvar, vaginal, penile, head and neck cancers (Lowy 2016, Gupta, Kumar et al. 2018). According to Globocan (Global Cancer Observatory), in 2018 there were 750 new cases and 340 deaths due to cervical cancer in Portugal.

Over 200 genotypes of human papillomavirus are known and they can be divided according to their potential to induce cellular transformation in high, intermediate or low risk and can also be classified phylogenetically (Durzynska, Lesniewicz et al. 2017, Viarisio, Gissmann et al. 2017). The alpha, beta and gamma genera contain the majority of the HPV types (Viarisio, Gissmann et al. 2017). The alpha genus causes mucosal and cutaneous lesions and the beta and gamma genus only cause cutaneous lesions. High-risk types, mainly found in the alpha genus, cause pre-and malignant lesions and the low-risk types cause benign lesions (Humans 2007). The most common and carcinogenic are HPV16 and HPV18, found in 60% and 15% of cervical cancer cases, respectively (Martinez-Ramirez, Carrillo-Garcia et al. 2018). Therefore, it is important to develop new therapeutic approaches against HPV-associated cancers, in order to reduce its incidence and mortality rates.

1.1.1 HPV life-cycle and molecular biology

HPVs are member of the *papillomaviridae* family and consist in small double-stranded circular DNA viruses with a length of about 8 Kb. HPV genome, represented in figure 1, is composed by a long control region (LCR), which contains *cis*-elements that are required for the replication and transcription of viral DNA, early genes (E1-E7), needed for viral replication and late genes, (L1-L2) that are necessary for virion assembly (Humans 2007, Durzynska, Lesniewicz et al. 2017, Viarisio, Gissmann et al. 2017, Martinez-Ramirez, Carrillo-Garcia et al. 2018).

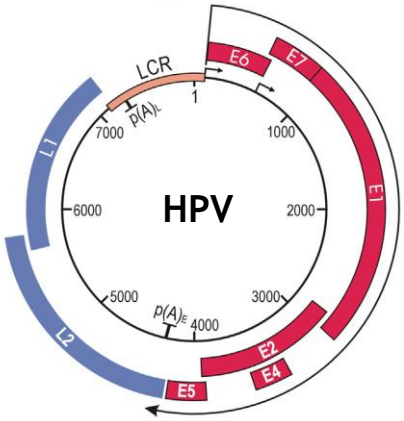

Figure 1 – HPV genome (adapted from (Durzynska, Lesniewicz et al. 2017)).

The viral E proteins are transcribed from the early promoter and the L proteins from the late promoter. The functions of these proteins (E and L) are described in table 1.

Table 1 – Viral protein functions and features (adapted from (Viarisio, Gissmann et al. 2017, Gupta, Kumar et al. 2018)).

Viral Protein	**Functions and Features**
E1	Forms a heterodimer complex with E2 and controls viral replication; Helicase function.
E2	Regulates early gene promoter and, together with E1, viral DNA replication; Genome segregation and encapsulation.
E3	Unknown function; present in only a few HPVs.
E4	May mediate the release of viral particles by destabilizing the cytokeratin network; Binds to cytoskeletal protein.
E5	Stimulates mitogenic signals of growth factors; Interaction with EGF/PDGF receptors.
E6	One of the major viral oncoproteins; interacts with and inactivates many cellular proteins.
E7	One of the major viral oncoproteins; interacts with and inactivates many cellular proteins.
L1	The major capsid protein; interacts with L2; the component of the HPV prophylactic vaccine.
L2	The minor capsid protein; involved in viral DNA encapsulation, facilitates viral entry and trafficking.

In figure 2 it is shown the establishment of HPV infection and neoplasia of cervical epithelium. The viral life cycle starts with the arrival of viral particles to the basal layer of the squamous epithelia through micro-abrasions allowing the replication of the HPV genome. At the beginning of the infection, low levels of E1, E2, E6, and E7 proteins are expressed, suspending normal

keratinocyte differentiation. Then, E2 recruits E1 in order to increase the number of copies of viral episomes, which continue increasing upon epithelium differentiation. In the upper differentiating epithelial layers, E6 and E7 are highly express leading to uncontrolled cell proliferation and when L1 and L2 proteins are expressed in the uppermost layer of the epithelium the viral life cycle is completed. So, the viral genome is encapsulated and occurs the release of mature virions (Mittal and Banks 2017, Martinez-Ramirez, Carrillo-Garcia et al. 2018). Although many women acquire an HPV infection, the majority are cleared or suppressed by the immune system within 1–2 years of exposure (Schiffman, Castle et al. 2007, Viarisio, Gissmann et al. 2017).

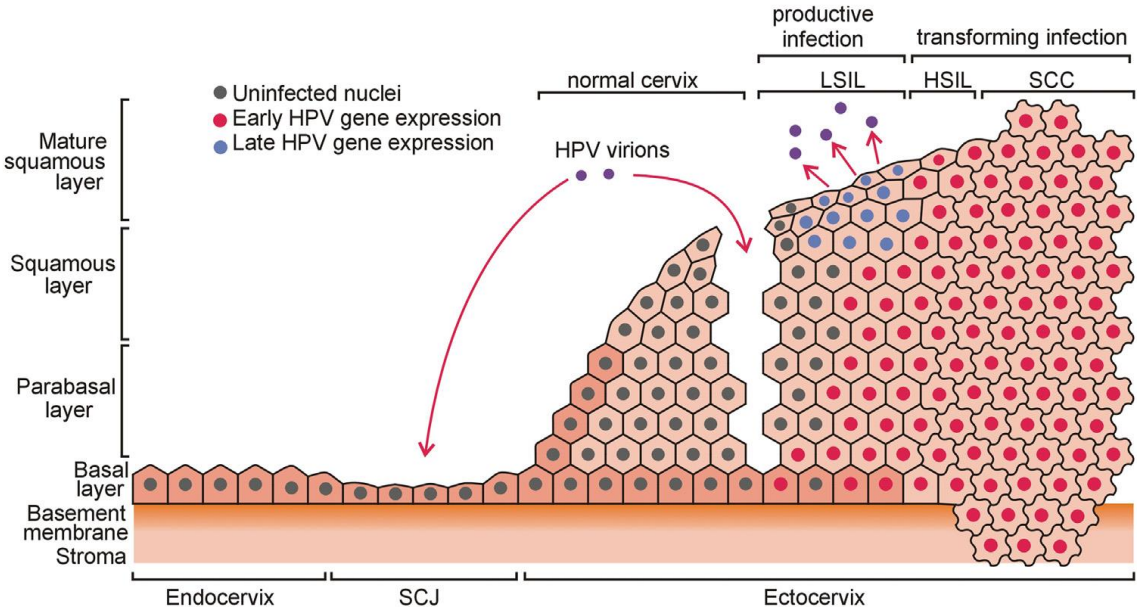

Figure 2 – Schematic representation of HPV infection (adapted from (Durzynska, Lesniewicz et al. 2017)).

Development of cervical lesions is connected with the establishment of a persistent infection, where the accumulation of DNA damage due to interactions of HR HPV E6 and E7 with p53 and pRb cause apoptosis inhibition and uncontrolled proliferation, which after a long time, may lead to the alteration of chronically infected cells into cancer cells (Viarisio, Gissmann et al. 2017, Martinez-Ramirez, Carrillo-Garcia et al. 2018).

1.1.2 E6 Oncoprotein

E6 is a protein constituted by 160 amino acids, two zinc-binding motifs and is essentially found in the nucleus-cell. It interacts with several host cell proteins and thus presents different functions, such as, escaping cell death (downregulation of p53 protein and Bak protein), deregulation of cell cycle (downregulation of P300/CBP complex protein and miR34a), immune system modulation (downregulation of IRF3 and IFNα), cell immortalization (upregulation of Myc and Sp1) genomic instability (upregulation of APOBEC3 and downregulation of XRCC1) and cell invasion (downregulation of SCRIB and miR-23b) (Estevao, Costa et al. 2019).

The most important function of the E6 oncoprotein is escaping cell death, through degradation of the p53 protein, which is represented in figure 3. It is known that p53 is a tumor suppressor

and acts in response to DNA damage or cellular stress, activating cellular processes in order to repair or eliminate cells with a damaged genome. In human cancers, this gene is often mutated (Zhang and Lozano 2017). In the particular case of cervical cancer, E6 interacts with the LXLL motif of E6 associated protein (E6AP), an E3 ubiquitin ligase that works as a connecting bridge between E6 and p53, inducing p53 degradation through proteasome pathway and consequently blocking p53 dependent apoptosis (Mittal and Banks 2017, Viarisio, Gissmann et al. 2017, Martinez-Ramirez, Carrillo-Garcia et al. 2018).

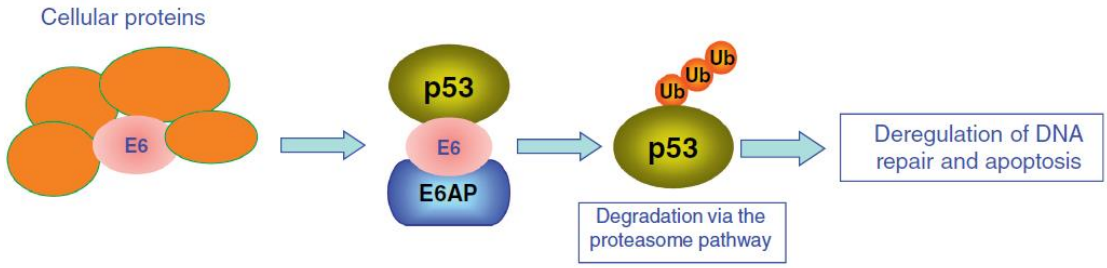

Figure 3 - Schematic representation of the action mechanism of E6 oncoprotein (adapted from (Viarisio, Gissmann et al. 2017)).

1.1.3 E7 Oncoprotein

E7 is a phosphoprotein with approximately 100 amino acid residues and three conserved regions, CR1, CR2, and CR3. Conserved region 2 contains the LXCXE (Leu-X-Cys-X-Glu) motif which is essential in the association with its targets and CR3 forms a zinc finger structure (Songock, Kim et al. 2017). This oncoprotein is found in the nucleus and interacts with several targets, presenting diverse functions, like, deregulation of cell cycle (pRB protein and p107/p130 downregulation), immune system modulation (blocking action of TLR9 and Cgas-STING), cell invasion (upregulation of MMP-9) and genomic instability (upregulation of CDK2) (Estevao, Costa et al. 2019).

One of the most important protein regulation mechanisms by E7 is through the retinoblastoma (pRb)/E2F system, which is presented in figure 4 (Mittal and Banks 2017, Songock, Kim et al. 2017).

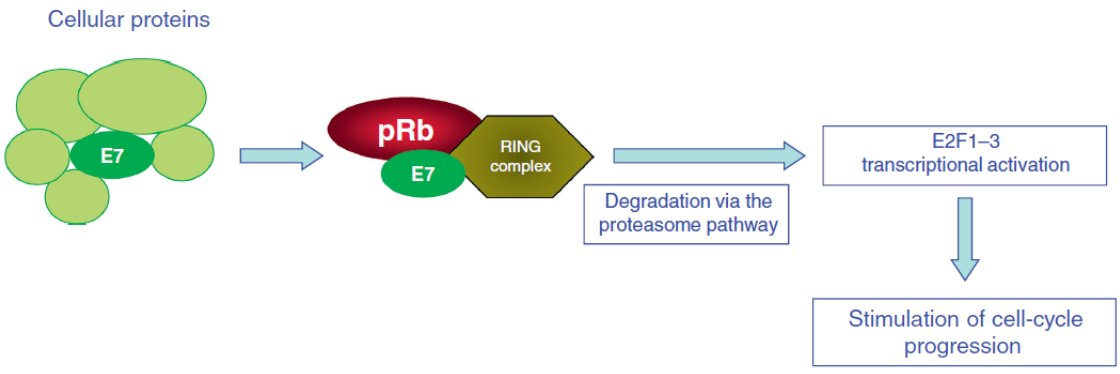

Figure 4 - Schematic representation of the action mechanism of E7 oncoprotein (adapted from (Viarisio, Gissmann et al. 2017)).

pRb family proteins are known as “pocket proteins,” function through binding to the activating E2F1-3 transcription factors and recruiting transcriptional inhibitory complexes to promoters (Songock, Kim et al. 2017). Association of E7 with pRb and the recruitment of the cullin2-RING ubiquitin ligase promotes pRb degradation via the proteasome pathway. As a consequence, this disrupts the interaction of pRb with E2F transcription factors, stimulating the G1/S phase cell cycle transition (Mittal and Banks 2017, Estevao, Costa et al. 2019).

In addition, E7 interacts with p105, p107 and p130 proteins through the same motif (LXCXE) that E7 interacts with pRb. p107 and p130 proteins function through binding to the inhibitory E2F4–5 transcription factors. In this way, occurs the degradation of p105 and p107, which control cell cycle entry in the basal layer, as well as p130, which is involved in cell cycle re-entry in the upper epithelial layer (Mittal and Banks 2017, Viarisio, Gissmann et al. 2017). So, this ensures that the cell remains in an S-phase-competent state which is vital for the viral life cycle.

1.1.4 Preventive and therapeutic vaccination

HPV infections worldwide continue to be extremely common, so the development of effective treatments is crucial in order to control existing HPV infections and their associated diseases (Yang, Jeang et al. 2016). Two prophylactic vaccines are available commercially for preventing HPV infection, Gardasil and Cervarix (Hung, Ma et al. 2008, Ken Lin 2010, Yeo-Teh, Ito et al. 2018). Both vaccines are made using virus-like particles (VLPs) that consist of L1 (Dochez, Bogers et al. 2014). Expression of L1 protein, the major component of the capsid, results in self- assemble of virus-like particles (VLPs), which are similar in shape and size to HPV virions but don’t have viral DNA (Ken Lin 2010). Gardasil is a quadrivalent vaccine containing recombinant L1 VLPs antigens for HPV types 6, 11, 16 and 18 whereas the bivalent vaccine, Cervarix, contains L1 VLPs antigens for HPV-16 and 18 (Ken Lin 2010, Dochez, Bogers et al. 2014, Yeo-Teh, Ito et al. 2018). These prophylactic vaccines have only been effective when administered in healthy patients, preventing the HPV infection and there is no evidence that they present therapeutic effects in treating or clearing established infections (Yang, Jeang et al. 2016).

Therefore, is still necessary the development of therapeutic vaccines to prevent and also treat existing HPV infections. Nowadays there are several groups developing and testing in preclinical and clinical trials different types of therapeutic HPV vaccines, in which the main target are E6 and E7 oncoproteins (Hung, Ma et al. 2008, Yang, Jeang et al. 2016, Yeo-Teh, Ito et al. 2018).

1.2 DNA-based therapy

DNA-based therapy has been evolving in the past century from an experimental technology into a sustainable strategy for developing therapeutics for several human disorders (Siddhesh D. Patil 2005). Since the discovery of the DNA double helix structure by Watson and Crick that it was possible to achieve a better comprehension of biological systems (Zimdahl 2015).

The discovery and understanding of the human genome made possible the identification of human genes involved in some diseases, which could help in the development and improvement of DNA-based drugs for gene therapy or DNA vaccines (Siddhesh D. Patil 2005). DNA-based therapeutics comprise plasmids for gene therapy or DNA vaccines, oligonucleotides, ribozymes, DNAzymes, aptamers and small interfering RNAs (siRNAs).

1.2.1 Gene Therapy

Nowadays, gene therapy is being studied and applied as a promising treatment option for a number of human diseases, such as inherited disorders, some types of cancer, and certain viral infections (Biswas, Kumar et al. 2018, Dunbar, High et al. 2018, Ginn, Amaya et al. 2018). Gene therapy is designed to introduce genetic material into target cells to replace the function of an abnormal or dysfunctional gene with a functioning variant (Sridharan and Gogtay 2016, Grace Hampson 2018, Vermeulen, Brans et al. 2018).

Normally, to deliver the gene has been used a vector, which is typically a virus, and this can be achieved through two approaches, the germline gene therapy, and somatic gene therapy. The first one implicates the introduction of the gene into the germ cells which passes through to the next generations whereas the latter consists of the transfer of the target gene to the somatic cells that are not inheritable (Sridharan and Gogtay 2016). A diversity of vectors and delivery procedures have been applied in gene therapy. The DNA vector function as a therapeutic gene expression cassette, which contains a promoter (guides the transcription of the gene), the gene of interest and a termination signal (finishes the transcription). The most commonly used are the viral vectors, however, the application of nonviral vectors has been increasing (Sridharan and Gogtay 2016, Ginn, Amaya et al. 2018).

The main challenge of gene therapy consists of the successful and safe target gene delivery due to the host's immune response directed against the vector and the transgene product. The research in the field of gene therapy has been increasing according to the frequent reports of therapeutic efficacy and recently approved products for the treatment of blindness by *in vivo* gene transfer and also for cancer (2017). All the approved products are presented in table 2 (Biswas, Kumar et al. 2018, Ginn, Amaya et al. 2018).

Table 2 – Approved gene therapy products (adapted from (Ginn, Amaya et al. 2018)).

Tradename	**Approval date**	**Approving agency**	**Indication**	**Manufacturer**
Genidicine (Adenoviral vector)	October 2003	State Food and Drug Administration of China	Head and neck squamous cell carcinoma	Shenzhen SiBiono GeneTech (Shenzhen, China)
Glybera® (alipogene tiparvovec) (adeno-associated viral vector)	November 2012	European Marketing Authorization (EMA)	Lipoprotein lipase deficiency	uniQure (Amsterdam, Netherlands)
Strimvelis™ (ϒ-retroviral vector)	June 2016	EMA	Adenosine desaminase deficiency (ADA-SCID)	GlaxoSmithKline (Midlesex, United Kingdom)
Kymriah™ (tisagenlecleucel) (lentiviral vector)	August 2017	Food and Drug Administration (FDA)	Acute lymphoblastic leukemia	Novartis Pharmaceuticals (Basel, Switzerland)
Yescarta™ (axicabtgene ciloleucel) (ϒ-retroviral vector)	October 2017	FDA	B-cell lymphoma	Kite Pharma, Incorporated (Santa Monica, California, USA)
Luxturna™ (voretigene neparvovec-rzyl) (adeno-associated viral vector)	December 2017	FDA	Retinal dystrophy (biallelic RPE65 mutation)	Spark Therapeutics, Inc. (Philadelphia, Pennsylvania, USA)

1.2.2 DNA vaccines

According to the World Health Organization (WHO), "a vaccine is a biological preparation that improves immunity to a particular disease" and the most licensed, since 1796, are conventional vaccines (Hasson, Al-Busaidi et al. 2015). This kind of vaccines include inactivated or live-attenuated microorganisms and (Hasson, Al-Busaidi et al. 2015, Kardani, Bolhassani et al. 2016) have been applied to prevent, treat, and even eradicate diseases such as smallpox, diphtheria, tetanus, poliomyelitis, leading to higher life quality and expectancy (Hasson, Al-Busaidi et al. 2015). Unfortunately, these vaccines present several problems related to the lack of safety and difficulty in the cultivation of the pathogenic microorganism, causing adverse immune reactions (Hasson, Al-Busaidi et al. 2015, Kardani, Bolhassani et al. 2016). In addition, they have the limitation of inducing only a prophylactic immune response being useful as a preventive vaccine but not as a therapeutic one.

Therefore, DNA vaccines emerged as a promising way to overcome the problems referred above by offering new approaches for the prevention and therapy of numerous diseases, since it can stimulate both cellular and humoral immune responses against parasites, bacteria and disease-causing viruses (Hasson, Al-Busaidi et al. 2015, Rappuoli and De Gregorio 2016, Lee, Arun Kumar et al. 2018). DNA vaccines are based on bacterial plasmids used to produce particular proteins (antigens) from a disease provoking pathogen (Ghanem, Healey et al. 2013, Hobernik and Bros 2018). The main advantage of such an approach is that the antigen is processed in a similar way to a viral infection. Thus, the antigen can be presented by three different pathways (figure 5): (a) plasmid DNA is internalized, then expressed by somatic cells (myocytes) and antigen presentation to CD8 T cells is made through MHC class I complex; (b) transfection of professional APCs, in which antigen presentation to T cells is accomplished through MHC class I and II complexes; (c) somatic cells transfected with pDNA are phagocytosed by APCs, resulting in cross-priming and antigen presentation to both CD4 and CD8 T cells (Hasson, Al-Busaidi et al. 2015, Lee, Yang et al. 2016, Lee, Arun Kumar et al. 2018).

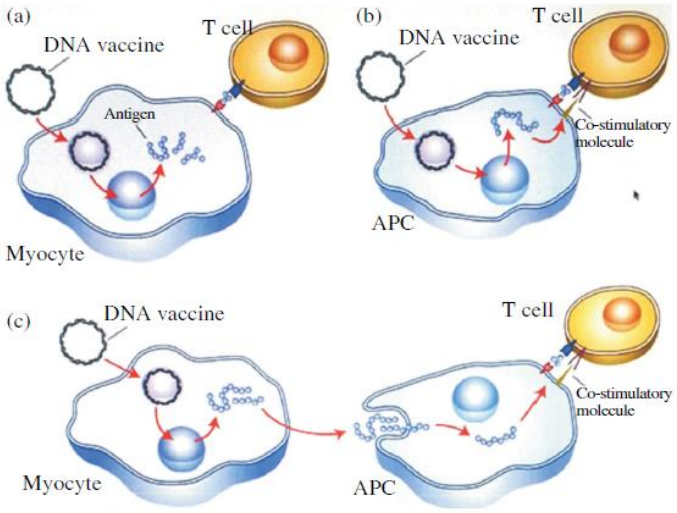

Figure 5 - Mechanism of antigen presentation (a): Antigen presentation mediated directly by transfected myocytes; (b): Transfection of professional APCs; (c): Cross priming (adapted from (Hasson, Al-Busaidi et al. 2015)).

Besides triggering either humoral or cellular immune responses, DNA vaccines can achieve this without the requirement of live vectors or complex biochemical manufacture procedures (Hasson, Al-Busaidi et al. 2015). In addition, DNA vaccines present other advantages such as improved stability in transportation and storage, stronger immune responses than traditional vaccines and longer-lasting production of the antigenic protein (Ghanem, Healey et al. 2013, Babiuk 2014, Lee, Arun Kumar et al. 2018). Moreover, it is possible to insert multiple variants of an antigen into a single plasmid vaccine, which reduces the number of vaccinations that must be administered (Hasson, Al-Busaidi et al. 2015). Thus, and as shown in figure 6, the number of patents in the field of DNA vaccines has been increasing (Abdulrahman and Ghanem 2018) which demonstrates the greatest interest in this new approach in therapy of cancer, allergies, autoimmune and infectious diseases (Hobernik and Bros 2018).

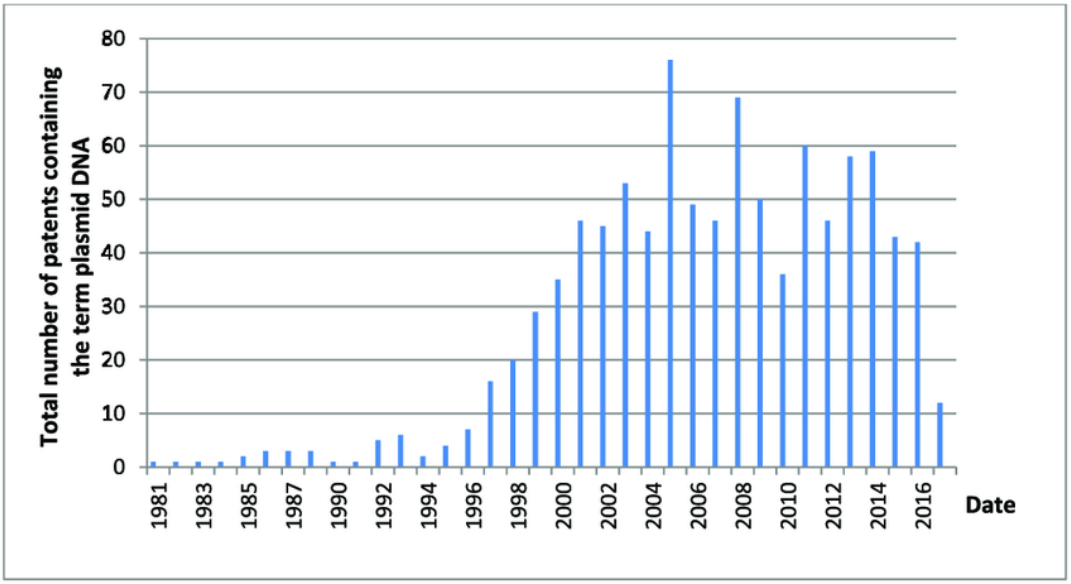

Figure 6 - Number of patents in the field of DNA vaccines (adapted from (Abdulrahman and Ghanem 2018)).

1.2.3 DNA delivery systems

Cellular environment is not favorable to DNA-based therapeutics entrance and its intracellular pathway until the cell-nucleus due to the extra and intra-cellular barriers. So, this inefficient internalization calls into question the exploration of the welfares of DNA-based therapeutics (Siddhesh D. Patil 2005). Therefore, to ensure that DNA can reach the nucleus without degradation it is necessary to use a delivery system that can protect it (Ibraheem, Elaissari et al. 2014). Delivery systems can be applied in the delivery of DNA vaccines, as well as in gene therapy and they can be divided into viral vectors and non-viral vectors.

1.2.3.1 Viral Vectors

The virus is composed of genetic material such as DNA and RNA, a protein coat that protects the genes and a lipid envelop around the protein coat (Yang, Liu et al. 2014). Through the virus-life cycle and its ability to reach the cell-nucleus of the host, express and replicate its own genetic material, they were used, as carriers, to delivery and guarantee protection to the therapeutic gene (Ibraheem, Elaissari et al. 2014). So, to make a virus a carrier of the therapeutic gene, it must be adapted by genetic engineering. This change consists in the removal of most genes coding for viral proteins and replacement by the desired gene (Giacca and Zacchigna 2012, Ibraheem, Elaissari et al. 2014).

There are several viruses that are used as viral vectors (retroviruses, adenoviruses, adeno-associated viruses (AAV), lentivirus, and herpes simplex virus) (Ibraheem, Elaissari et al. 2014, Foldvari, Chen et al. 2016). In table 3, are presented the main used, as well as their advantages and disadvantages (Ibraheem, Elaissari et al. 2014, Carter and Shieh 2015).

Table 3 - Advantages and disadvantages of viral vectors (adapted from (Ibraheem, Elaissari et al. 2014, Carter and Shieh 2015)).

Vector	**Advantages**	**Disadvantages**
Adenovirus	High transduction efficiency *ex vivo* and *in vivo* Transduces many cell types Transduces proliferating and nonproliferating cells Production easy at high titers	Remains episomal Transient expression Requires packaging cell line Immune-related toxicity with repeated administration Potential replication competence No targeting Limited insert size: 4-5 kb
Adeno-associated virus (AAV)	Integration on human chromosome 19 (wild-type only) to establish latent infection Prolonged expression Transduction does not require cell division Small genome, no viral genes	Not well characterized No targeting Requires packaging cell line Potential insertional mutagenesis Limited insert size: 5 kb
Herpes simplex virus (HSV)	Large insert size: 40-50 kb Neuronal tropism Latency expression Efficient transduction in vivo Replicative vectors available	Cytotoxic No targeting Requires packaging cell line Transient expression, does not integrate into genome
Lentivirus	Transduces proliferating and nonproliferating cells Transduces hematopoietic stem cells prolonged expression	Safety concerns: from human immunodeficiency virus origin Difficult to manufacture and store limited insert size: 8 kb Clinical experience limited
Retrovirus	Integration into cellular genome Broad cell tropism Prolonged stable expression Requires cell division for transduction Larger insert size: 9-12 kb	Inefficient transduction Insertional mutagenesis Requires cell division for transfection Requires packaging cell line No targeting Potential replication competence

Viral vectors are the most frequently used because they have shown the capability to reach a high level of transgene delivery in *in vivo* models and clinical trials, in spite of their weaknesses. These weaknesses can be summarized in (Ibraheem, Elaissari et al. 2014, Yang, Liu et al. 2014, Foldvari, Chen et al. 2016):

- The uncertainty of provoking an immune response that could be fatal;
- Problems with large-scale production of viral vectors and difficulty of packing large molecules, like nucleic acids;

- The limited size of the genetic materials that can be delivery by the virus;
- Transgene mis-insertion risks and resistance to repeated administration.

The use of viral vectors as delivery systems has been restricted and led to research on vectors that could be safer, cheaper and that could overcome the toxicity issues in delivery. Consequently, non-viral vectors have arisen as a promising alternative (Ibraheem, Elaissari et al. 2014, Yang, Liu et al. 2014, Slivac, Guay et al. 2017).

1.2.3.2 Non-viral vectors

Problems related to the safety and small cargo of therapeutic DNA of viral vectors made it necessary to research an alternative, and thus, have emerged vectors not based on viral systems (Ginn, Amaya et al. 2018). Non-viral vectors may provide quite a few advantages related to the safety profile, cost-effective manufacturing and they can carry large therapeutics and be repeatedly administered without provoking a noticeable immune response (Siddhesh D. Patil 2005, Foldvari, Chen et al. 2016).

Naked plasmid vectors are the simplest and popular non-viral delivery systems used in clinical trials because when injected directly in some tissues, are able to produce significant levels of gene expression (Ginn, Amaya et al. 2018). However, naked DNA has difficulty in pass through the extracellular environment due to the action of the nuclease and cross the cell membrane owing to the negative charge repulsion, which results in poor transfection efficiency. So, to overcome this limitation, non-viral delivery systems are developed through different methods and they can correspond to complexes or nanoparticles with the nucleic acid and a single or a mixture of materials (cationic lipids, surfactants, peptides, polysaccharides, metals) and synthetic polymers (PLGA, PEI, PAMAM) (Foldvari, Chen et al. 2016).

The delivery methods of DNA-based therapeutics can be divided into two groups (figure 7) (Ibraheem, Elaissari et al. 2014, Slivac, Guay et al. 2017):

1- Physical methods: these involve a physical force that disrupts the cell membrane to enable localized delivery of the naked DNA into the nucleus. They include needle injection, electroporation, gene gun, and ultrasound delivery.
2- Chemical methods: these can be prepared by electrostatic interaction between particulate carriers (polycationic derivatives) that bind to DNA forming condensed complexes or by encapsulation of DNA within biodegradable spherical structures leading to micro and nanoparticles or through DNA adsorption.

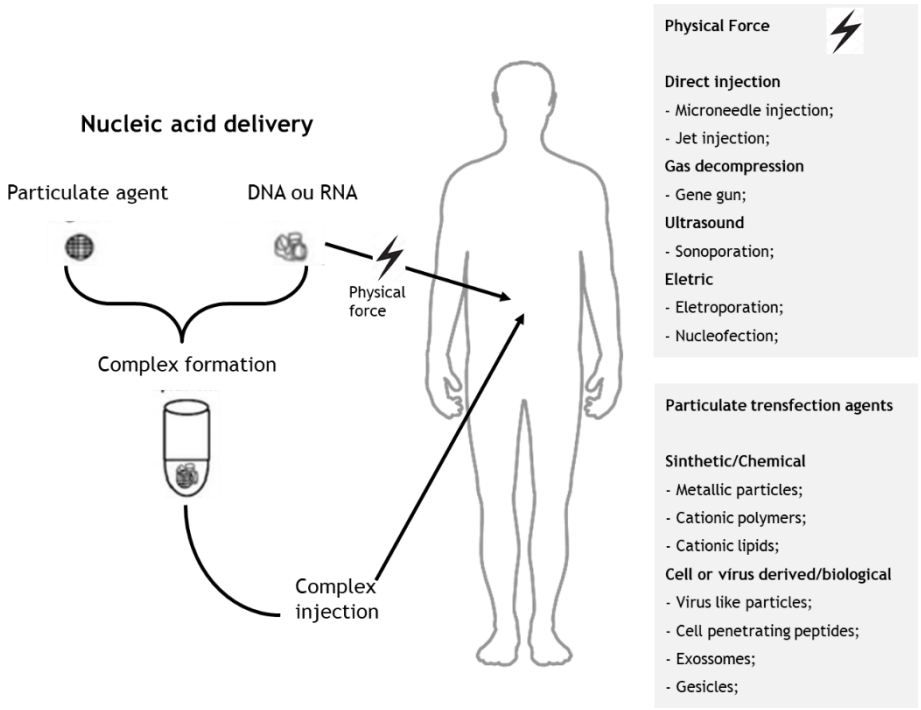

Figure 7 - Models of non-viral nucleic acid delivery. The nucleic acid delivery can be achieved in two ways: nucleic acid interacts with a particulate agent through mostly electrostatic interaction, forming a condensed complex capable of access the cells and the other method correspond to the delivery of naked DNA or RNA into the cells by using an external physical force that causes temporary permeabilization in the cell membrane. Then, the nucleic acid is introduced in the body and after reaching the target tissue will modify cells (adapted from (Slivac, Guay et al. 2017)).

Physical methods use mechanical, ultrasonic, electric, hydrodynamic or laser-based energy with the objective of creating momentary weak points in the target cell membrane, allowing the entrance of DNA by diffusion (Ibraheem, Elaissari et al. 2014, Slivac, Guay et al. 2017). Table 4 describes the fundamentals, advantages and disadvantages of the physical methods.

Table 4 - Description of the different physical methods applied in gene delivery.

Physical Methods	Fundamentals	Advantages/ Disadvantages	References
Microneedle technique	Direct injection of DNA into the desired tissue through a syringe.	Localized DNA delivery;	(Slivac, Guay et al. 2017)
Biobalistic (Gene gun)	DNA delivery into the target cell/tissue through metal nanoparticles (gold, tungsten, silver).	More efficient cellular uptake; Low efficiency; Sometimes requires surgery; May cause physical damage;	(Ibraheem, Elaissari et al. 2014, Carter and Shieh 2015, Jorritsma, Gowans et al. 2016, Slivac, Guay et al. 2017)
Electroporation	Application of an electric field causing permeabilization of the cell membrane, allowing DNA to easily enter the cell.	Improves DNA uptake; Leads in trials on DNA vaccination against viral infections; Ability to transfect cells in many different *in vivo* and *in vitro* environments;	(Carter and Shieh 2015, Jorritsma, Gowans et al. 2016, Slivac, Guay et al. 2017)
Sonoporation	Application of ultrasound waves to cause membrane permeabilization, allowing the DNA entrance into cells.	Safe; Non-invasive; Can reach internal organs without the necessity of surgery;	(Ibraheem, Elaissari et al. 2014, Slivac, Guay et al. 2017)

Chemical methods are proposed with the objective of improving DNA delivery into the cell-nucleus (Ibraheem, Elaissari et al. 2014, Slivac, Guay et al. 2017). In this way, they mask the negative charge of DNA, compact the DNA molecule to make it minor, and protect it against degradation caused by intracellular nucleases. In order to achieve these purposes the DNA is packed by electrostatic interaction among anionic DNA and polycations, or through encapsulation with biodegradable polymers, or, even, by adsorption (Ibraheem, Elaissari et al. 2014). Exploring the electrostatic interaction between DNA negatively charged and positively charged lipid or polymer, leads to the formation of a positively complex known as a lipoplex or polyplex, respectively (Abdelhamid Elaissari 1995). In lipoplexes, the cationic lipid is constituted by a hydrophobic anchor, a hydrophilic positively charged head and a spacer/linker, and it is used to protect DNA from nuclease and simplify endocytosis. They are formed when the lipid condenses with anionic DNA and the charge density, as well as the spacer of the lipid, have an important role in the delivery of DNA (Ibraheem, Elaissari et al. 2014, Yang, Liu et al. 2014). Besides the low efficiency in vivo, cytotoxicity caused by the positive charge of lipoplex is the main problem related to its application (Ibraheem, Elaissari et al. 2014).

Polymers have shown to be a promising alternative to use as a vector for DNA delivery due to their potential for structural diversity and flexible functionality (Yang, Liu et al. 2014). Polyplexes consist of the use of a cationic polymer to condense the negatively charged DNA into a small (nano-sized) complex through electrostatic interactions. By decreasing size, it facilitates DNA entrance into the cell, which leads to an increase in transfection efficiency (Zhang, Xu et al. 2004). However, this approach presents some disadvantages related to poor efficiency, toxicity, and safety, which differ due to the structures of polymers (Yang, Liu et al. 2014). Among the most studied cationic polymers is polyethyleneimine (PEI), with high amino group density (Foldvari, Chen et al. 2016, Slivac, Guay et al. 2017), which has a strong buffering potential (Slivac, Guay et al. 2017), and presents higher nucleic acid binding and delivery capacity. Additional polymers explored are poly-l-lysine (PLL), n,n-dimethylaminoethyl methacrylate (DMAEMA), and poly(ß-amino esters) (Foldvari, Chen et al. 2016). At present, available polymer-based DNA carriers do not fulfill the necessities of DNA delivery for clinical applications, which demands continuous improvements (Shi, Zheng et al. 2017, Xiang, Oo et al. 2017).

The encapsulation of DNA with biodegradable polymers (e.g. PLGA, PBAE, and protonated polyamines) (Luten, van Nostrum et al. 2008, Jorritsma, Gowans et al. 2016) is a promising alternative to DNA condensed with polycations and can overcome limitations of the latter. This method consists in the formation of nano or micro-sized circular structures of hydrolytically degradable polymers incorporating DNA. It presents advantages such as easiness in removal from the body and great DNA protection (Ibraheem, Elaissari et al. 2014). Nevertheless, also presents some drawbacks like poor encapsulation efficiency and partial release of DNA, which causes low DNA bioavailability (Fu, Pack et al. 2000).

In the case of biodegradable polymers, DNA adsorption combines two procedures referred above, electrostatic interaction and encapsulation. It is based on the use of biodegradable particles containing cationic polymers adsorbed to its surface, and, therefore the anionic DNA can be linked through electrostatic interactions (Manmohan Singh 2000). It is possible to improve the bioavailability of DNA, but as DNA is adsorbed to the surface of the particle it is exposed to enzymes that could damage it (Kasturi, Sachaphibulkij et al. 2005, Munier, Messai et al. 2005).

1.3 Plasmid DNA

The interest in pDNA for therapeutics, such as vaccination and gene therapy, has been increasing in the past years leading to the improvement of biopharmaceutical pDNA production methods (Blom, Bennemo et al. 2010). Plasmids are highly negatively charged, circular double-stranded DNA molecules and the size can vary from 1 to 200 Kbp, allowing large amounts of DNA to be loaded (Alex Xenopoulos 2014, Tolmasky 2017, Abdulrahman and Ghanem 2018). They are usually produced in recombinant *Escherichia coli* (*E. coli*) host and can pass from one cell to another through transformation, transduction or conjugation (Ghanem, Healey et al.

2013, Abdulrahman and Ghanem 2018). The pDNA has different conformations, open-circular (oc), linear (ln), supercoiled (sc) and denatured conformations, which present different charge distribution, size and base exposure. The supercoiling phenomenon of the sc isoform increases its base exposure and its charge in comparison with other isoforms, however, the sc isoform may convert into other pDNA isoforms depending on the physical and chemical procedures applied (Diogo, Queiroz et al. 2005, Abdulrahman and Ghanem 2018). The isoform that has interest in research is sc pDNA since several reports proved that this isoform has better biological performance and is more efficient for transfection than the other isoforms because the latter could present damage in the expression cassette (Valente, Sousa et al. 2014, Valente, Sousa et al. 2018).

The manufacturing of pDNA comprehends two main steps, an upstream process, and a downstream process, which are represented in figure 8 (Aires-Barros and Azevedo 2017).

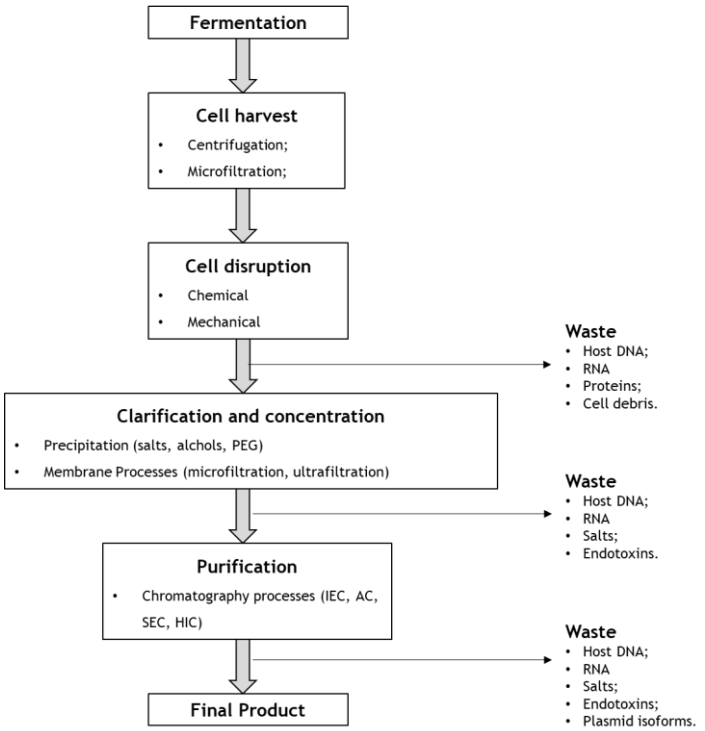

Figure 8 - Representation of upstream and downstream process of large-scale purification of supercoiled plasmid DNA (adapted from (Guilherme N.M. Ferreira 2000, Van Alstine, Jagschies et al. 2018)).

1.3.1 Upstream process

The upstream process consists in the construction, production, and isolation of the desired plasmid. First, occurs the plasmid construction and the selection of a specific strain that allows the cloning process (Abdulrahman and Ghanem 2018, Lindskog 2018). The plasmid should have the necessary elements to propagate in the host and to express the interest gene. Therefore, it must contain bacterial elements (selection marker and replication region) and eukaryotic elements (promoter, transgene, and a transcriptional terminator) as shown in figure 9 (Bower and Prather 2009). The selection marker allows selective growth of *E. coli* cells normally in the

presence of an antibiotic (such as Kanamycin) and the replication region replicates the plasmid independently of the host machinery increasing its number of copies per cell. The eukaryotic elements are composed of an expression cassette in which the promoter drives the transgene expression and the transcription terminator finishes the transgene expression (Armando Tejeda-Mansir 2008, Carson, Miller et al. 2019).

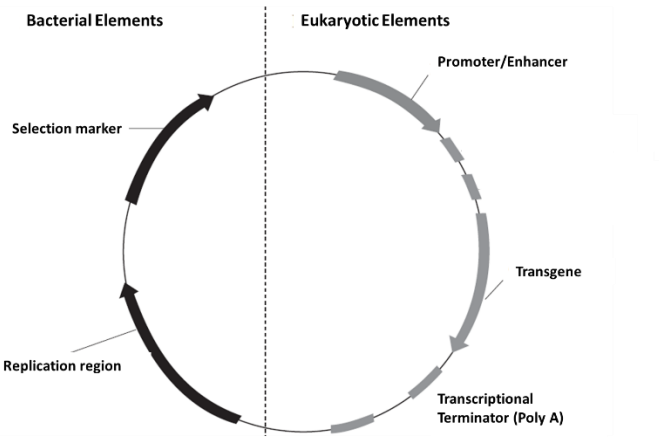

Figure 9 - Plasmid DNA expression vector (adapted from (Armando Tejeda-Mansir 2008)).

Escherichia coli is still the most used system in biotechnology because it is well characterized and due to its safety, ease of handling and high productivity (Eva K. Lindskog 2018). Thus, the pDNA replication occurs by a process called fermentation, in which the conditions should be carefully selected since pDNA production is influenced by the plasmid type/size, *E. coli* strains, growth conditions, culture type and medium composition (Islas-Lugo, Vega-Estrada et al. 2016).

1.3.2 Downstream process

The major goal of the downstream process is elimination of cell impurities and pDNA obtaining in conditions that meet the pharmaceutical specification (Abdulrahman and Ghanem 2018). This process is normally divided into three steps: recovery, intermediate purification, and polishing.

The main objective of the first step is the target product release, the solid compounds removal and the sample concentration (Aires-Barros and Azevedo 2017). So, at the end of pDNA production, the *E. coli* cells are harvested usually by centrifugation or microfiltration (Alex Xenopoulos 2014, Besnard, Fabre et al. 2016, Abdulrahman and Ghanem 2018). At laboratory scale is mainly used centrifugation, but at large scale, the use of centrifugation could be costly and hard to perform, so the use of filtration has been increasing (Nunes, Morão et al. 2012, Padilla-Zamudio, Guerrero-German et al. 2015, Besnard, Fabre et al. 2016). After bacterial harvest, the cells are lysed to liberate the pDNA. The lysis techniques applied could be mechanical, physical, alkaline or thermal (Voß 2007, Chunsheng, Qinglin et al. 2011, Baumann and Hubbuch 2017, Abdulrahman and Ghanem 2018), however in pharmaceutical plasmid production the most used is based on the alkaline lysis developed by Birnboim and Doly (J.Doly

1979, Voß 2007, Chunsheng, Qinglin et al. 2011, Carson, Miller et al. 2019). Alkaline lysis causes cell membrane disruption through the use of high pH, a detergent (SDS) and a strong base like NaOH, leading to pDNA release as well as all cell components (Alex Xenopoulos 2014, Carson, Miller et al. 2019). The *E. coli* extract presents several impurities that need to be eliminated, like cell debris, RNA, gDNA, endotoxins, proteins and also the desired pDNA that only corresponds to a very small percentage of the extract (Voß 2007, Ghanem, Healey et al. 2013, Alex Xenopoulos 2014). Thus, normally the solid-liquid separation is achieved through cross-flow filtration or tangential-flow filtration (TFF) and also bag filters at industrial scale (Alex Xenopoulos 2014, Besnard, Fabre et al. 2016). After the removal of solid debris, it is performed a reduction of sample volume (sample concentration) by using alcohols as nucleic acid precipitating agents. And finally, a clarification step is normally applied for the impurity precipitation usually with chaotropic salts, like ammonium sulfate or with other precipitating agents like PEG and calcium chloride, in order to remove impurities such as gDNA, high molecular weight RNA, proteins and endotoxins (Luechau, Ling et al. 2009, Alex Xenopoulos 2014). The pDNA fraction could be increased before the purification with an adequate chromatography step (Sousa, Sousa et al. 2012). And finally, the goal of the polishing step consists in the removal of the remaining impurities (Aires-Barros and Azevedo 2017). However, this represents a big challenge because supercoiled pDNA is very similar in size, structure, and charge to RNA, gDNA and open-circular pDNA (Ghanem, Healey et al. 2013, Alex Xenopoulos 2014).

1.3.2.1 Clarification methods

Clarification consists in the removal of undesirable materials, such as cells or cell debris, allowing the recovery of the desired product (Besnard, Fabre et al. 2016, Aires-Barros and Azevedo 2017). Despite the efficiency of the clarification step has a direct influence on the purification performance, this step is often undervalued. Diverse technologies are used for different operations due to the diversity of products and in order to achieve the desired clarification (Besnard, Fabre et al. 2016).

1.3.2.1.1 Membrane Processes

Membrane technology has been used in recent years for biomolecule separation and concentration of process fluids, due to its flexibility, simplicity, being environmentally friendly and cost-effective (Aires-Barros and Azevedo 2017). In the process, membrane acts as a barrier retaining the bigger molecules and allowing the small ones to pass through the pores. The membrane processes, represented in figure 10, could be divided according to their pore size in microfiltration (MF), ultrafiltration (UF), nanofiltration (NF), reverse osmosis (RO).

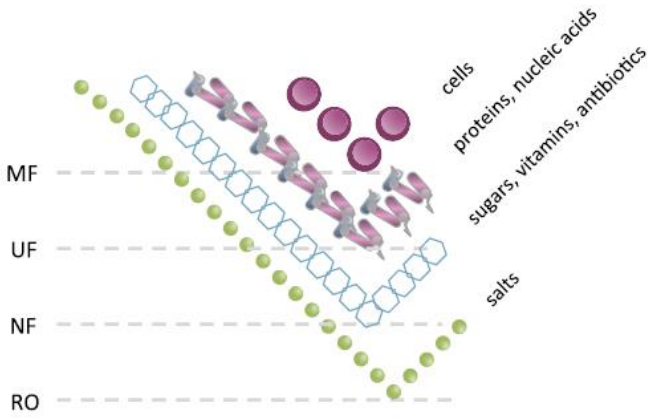

Figure 10 – Different types of membranes and the respectively retained solute (adapted from (Aires-Barros and Azevedo 2017)).

The microfiltration process is used for suspended material retention and works with a pore size range from 0.1-10 µm. Thus, large particles like cell debris will not pass through the membrane, whereas smaller particles like proteins, vitamins, and salts will pass. The membranes can be symmetric or asymmetric, the most used are the ones with a pore size of 0.1, 0.22, and 0.45 µm. Ultrafiltration allows nucleic acids, proteins and colloids retention and the membrane pore size range varies from 1 to 50 nm, but usually, the membranes are characterized by the molecular weight cut-off (MWCO). Commercially there are available membranes with MWCO from 3 to 500 KDa. Ultrafiltration membranes can only be asymmetric and generally contain an ultrathin active layer on the top of a sublayer. Nanofiltration membranes are asymmetric with pore size range from 0.2 to 10 nm, allowing retention of sugars, vitamins and polyvalent ions (Aires-Barros and Azevedo 2017, Liderfelt and Royce 2018). Reverse osmosis is mainly used in the desalinization of seawater, since almost all substances are retained, only allowing water and a few organic molecules passage (Liderfelt and Royce 2018).

Initially, the membrane processes were performed in dead-end-mode (normal flow filtration), this means that the feed flows perpendicularly through the membrane, but since it could occur deposition of particles, sharp pressure drops and precipitation of molecules on the surface or in the filter pores, leading to a cake formation, nowadays is more used tangential flow filtration (TFF), figure 11. Tangential flow filtration or cross-flow filtration gained more attention in the industry because the feed flows tangentially to the membrane, reducing the cake formation to a thinner layer (Aires-Barros and Azevedo 2017, Liderfelt and Royce 2018). However, the membranes used in filtration present some problems related to membrane clogging/fouling (Prather, Sagar et al. 2003) and also the supernatant can be poorly clarified when there are large amounts to be processed (Van Alstine, Jagschies et al. 2018).

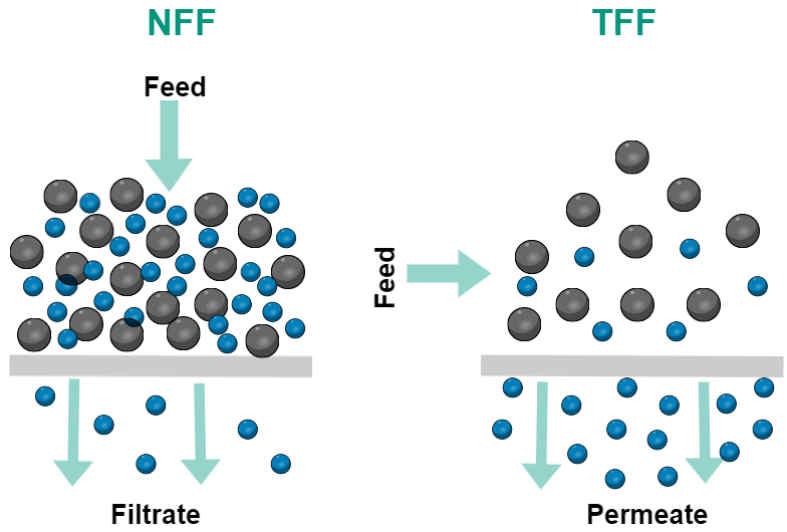

Figure 11 – Normal flow filtration and tangential flow filtration processes (adapted from (Aires-Barros and Azevedo 2017, Liderfelt and Royce 2018)).

1.3.2.1.2 Precipitation

In a complex mixture, precipitation can be applied to separate biological products by precipitating the target molecules or the impurities, with the final aim of concentrate the product. To achieve precipitation it must be added a precipitating agent or change the solubility conditions of the solution. For example, proteins can be precipitated by the addition of high concentrations of salts, because the salt will promote the exposure of hydrophobic zones leading to hydrophobic interactions between proteins, which consequently facilitates protein aggregation followed by precipitation (Aires-Barros and Azevedo 2017). Therefore, proteins and high molecular weight (MW) RNA can be eliminated by the addition of salts to the lysates, in which ammonium sulfate and sodium sulfate are the most used, figure 12.

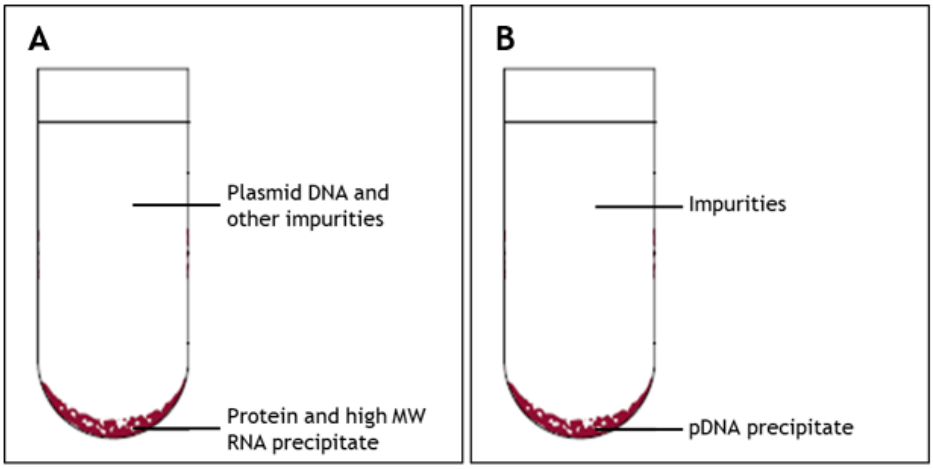

Figure 12 –Representation of precipitation methods - A: Elimination of proteins and high MW RNA by salt precipitation; B: Concentration of pDNA by addition of alcohols (adapted from (Thatcher 2018)).

In large scale production, most of the processes use organic solvents like alcohols, especially ethanol and isopropanol, and also a high concentration of salt to precipitate and concentrate the plasmid DNA because pDNA is insoluble in alcohols, figure 12 (Prather, Sagar et al. 2003,

Andreou 2013, Thatcher 2018). The addition of alcohols and salt to the solution will promote an electrical attraction between phosphate groups and positive ions, which form strong and stable ionic bonds leading to pDNA precipitation. In addition, it has been reported that pDNA has also been precipitated from the clarified alkaline lysate by using the detergent Cetyl Trimethylammonium Bromide (CTAB) and polydiallyldimethylammonium chloride (polyDADMAC), a cationic polymer. Nevertheless, the addition of precipitating agents could represent a problem for the pharmaceutical industry because it is necessary to confirm and validate their removal and also due to the toxicity associated with the use of organic solvents (Alex Xenopoulos 2014, Pruthu 2014).

1.3.2.1.3 Liquid-Liquid Extraction

Liquid-Liquid extraction consists of the partitioning of the product between two immiscible phases: an aqueous phase and the solvent phase (Aires-Barros and Azevedo 2017). Aqueous two-phase systems (ATPS) have been applied in the separation and purification of biomolecules such as proteins, enzymes, phytochemicals, nucleic acids, and pigments. In the past twenty years, the interest in ATPS has been increasing due to their ability in eliminating several impurities during the recovery process, the capacity to extract the target product through its separation into one of the phases, and at the same time promote its concentration by partitioning into the smaller volume of the extraction phase (Phong, Show et al. 2018). In figure 13 it is represented a scheme of product recovery by ATPS.

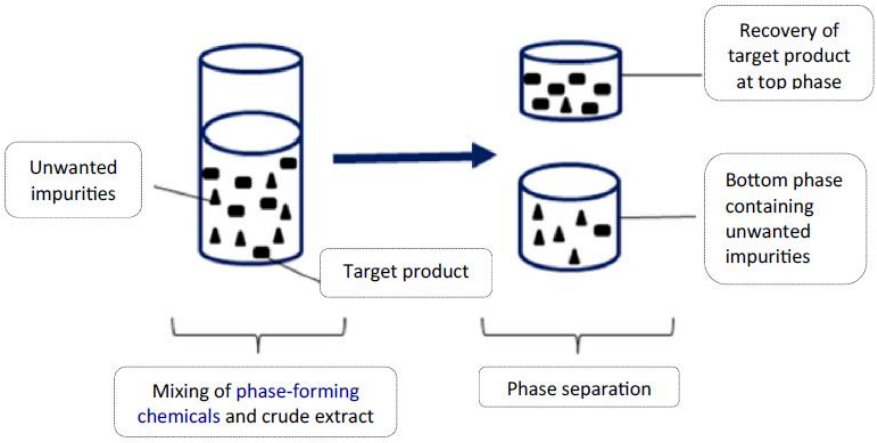

Figure 13 - Schematic representation of target product recovery by ATPS (adapted from (Phong, Show et al. 2018)).

Aqueous two-phase systems using polyethylene glycol (PEG) and di-potassium hydrogen phosphate have been studied for primary capture of plasmid DNA and removal of some RNA, which could be used as a concentration step preceding to chromatography (Luechau, Ling et al. 2010). Phong and co-workers recently described an ATPS composed of 12% polyethylene glycol, 12% sodium sulfate, and an affinity ligand to recover pDNA from an alkaline bacterial cell lysate, achieving about 67% of pDNA recovery in the top phase (Phong, Show et al. 2018). These aqueous systems present advantages in comparison with traditional processes by

combining two or more early steps such as cell debris removal, concentration, separation, and pre-purification, which makes the procedure more energy-efficient and cost-effective (Luechau, Ling et al. 2009, Phong, Show et al. 2018). Although ATPS demonstrate a great combination of yield and purity degree the operational costs are much higher than other techniques applied in the industry like TFF, due to the high use of chemicals (Alex Xenopoulos 2014). Moreover, the poor application of ATPS in the industry is mostly due to the difficulty and complexity in understanding the interactions between ATPS components and the driving mechanism of phase formation (Phong, Show et al. 2018).

1.3.2.2 Chromatographic methods

Chromatography was first described by Mikhail Tswett in 1903 to separate plant pigments (Hage 2018, Nesterenko and Palamareva 2019) and is still the foremost method applied in biopharmaceuticals purification due to its several advantages (Aires-Barros and Azevedo 2017) and This technique separates the components of a mixture based on the differential interaction with two chemical or physical phases, mobile and stationary phase. The mobile phase passes through the system while the stationary phase is confined in a support, usually a column. The components pass through the system and the ones that have stronger interactions with the stationary phase are more retained and therefore, slowly flow through the system, while the components with weaker interactions spend more time in the mobile phase (Hage 2018).

There are several chromatographic methods that have been employed to purify pDNA-based vaccines, based on differences in size (SEC), charge (IEC), hydrophobicity (HIC) and affinity (AC) of different molecules in the clarified lysate (Ghanem, Healey et al. 2013). The purification stage must guarantee 97% of purity in the obtained sample of pDNA, in which at least 80% corresponds to supercoiled isoform and should not contain more than 1% of gDNA, host proteins, RNA and endotoxins, according to regulatory agencies, FDA and EMA (Ghanem, Healey et al. 2013, Abdulrahman and Ghanem 2018).

1.3.2.2.1 Size Exclusion Chromatography (SEC)

Size exclusion chromatography was first described in 1955 for the separation of peptides from amino acids by Lindqvist and Storgárdst, but was only after 1959 that gained more attention (J. Porath 1959, Aires-Barros and Azevedo 2017). The size exclusion mechanism is based on size, in which the stationary phase consists of inert porous material and also has a range of pore dimensions that are similar to the size of the compounds that will be separated (Hage 2018, Nesterenko and Palamareva 2019). Thus, the small molecules are able to penetrate in the pores

whereas the larger ones only flow through the column, allowing the mixture separation, since the small ones flow more slowly than the larger ones, figure 14 (Aires-Barros and Azevedo 2017).

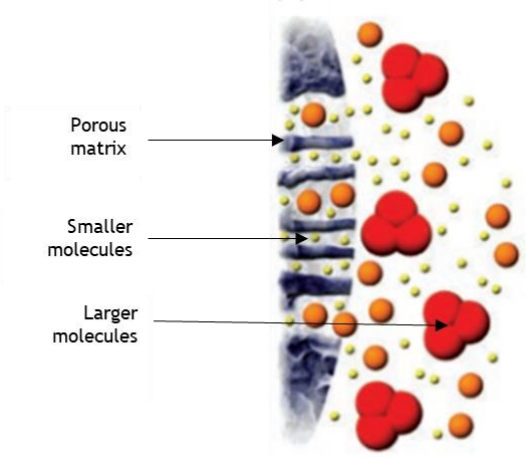

Figure 14 - Schematic representation of size exclusion chromatography (adapted from (Sciences 2015)).

In pDNA purification, this chromatographic mode is not used as a first purification step, but as a polishing step enabling removal of residual contaminants (endotoxins, gDNA, RNA) and separation of sc pDNA from oc pDNA with simultaneous buffer exchange into an appropriate formulation or storage buffer (Ghanem, Healey et al. 2013). SEC can also be applied to desalt or buffer-exchange a certain solution and also to estimate molar mass by using calibration standards (Aires-Barros and Azevedo 2017).

1.3.2.2.2 Ion Exchange Chromatography (IEC)

Ion exchange chromatography it is probably the most used for biological products purification due to its simplicity, low cost when compared with other chromatographic techniques and wide applicability (separation and purification of several molecules with ionizable or charged groups, like nucleic acids, proteins, vitamins, etc) (Aires-Barros and Azevedo 2017). It is based on the electrostatic interaction between the ligands and the charge of pDNA, so the separation occurs due to differences in the surface net charge (Nesterenko and Palamareva 2019). The equilibrium of the stationary phase is made with a binding buffer that presents a certain pH and ionic strength that will ensure that when the mixture is added, the biotarget binds to the stationary phase and the impurities do not bind. The elution of the bound molecules usually is achieved through the increase in ionic strength (salt concentration) or by changing the buffer pH. When the salt is added, the ions compete with the bound molecules forcing them to elute.

The stationary phase can have ionic groups with negative (cation-exchange) or positive charge (anion-exchange) (Aires-Barros and Azevedo 2017). Anion-exchange chromatography, represented in figure 15, is used for pDNA separation due to interaction between the positive groups of the stationary phase with negatively charged phosphate groups on the pDNA backbone (Abdulrahman and Ghanem 2018). The pDNA isoforms have similarities but possess different conformations and different local charge densities, therefore the elution order is related to the chain length and consequently with the number of charged phosphate groups (Ghanem, Healey

et al. 2013). Supercoiled pDNA has a higher charge density than the other isoforms, so it has stronger interactions with the stationary phase, eluting later than other topologies (Ghanem, Healey et al. 2013, Abdulrahman and Ghanem 2018). Nonetheless, this chromatographic mode presents poor selectivity between pDNA and impurities from the lysate, requiring the combination with other purification techniques.

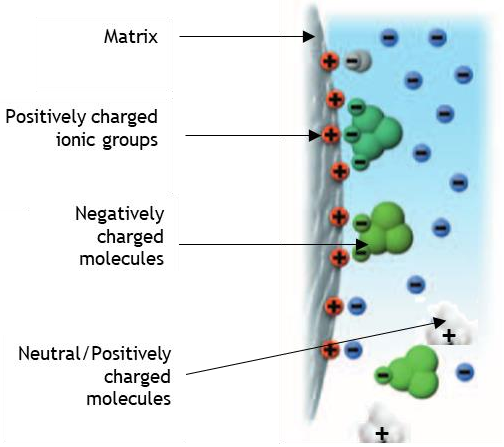

Figure 15 - Schematic representation of ion-exchange chromatography (adapted from (Sciences 2016)).

1.3.2.2.3 Hydrophobic Interaction Chromatography (HIC)

HIC promotes the separation of the molecules based on the interaction that occurs between the hydrophobic groups at the biomolecule surface and the hydrophobic ligands, figure 16.

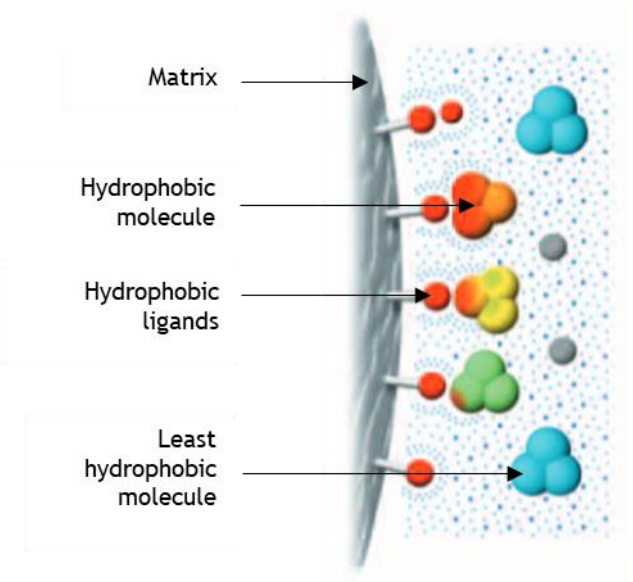

Figure 16 - Schematic representation of hydrophobic interaction chromatography (adapted from (Sciences 2006)).

Biomolecules, like nucleic acids are hydrophilic, but usually, have a few hydrophobic groups at their surface. So in the binding, it is applied high salt concentration to expose the hydrophobic groups and allow the interaction between the ligands and the target molecules, and the elution is achieved by the decrease of salt concentration in the buffer (Aires-Barros and Azevedo 2017,

Abdulrahman and Ghanem 2018). The molecules elute in increasing order of their hydrophobicity. It is usually applied to separate biomolecules according to their hydrophobicity or to eliminate very hydrophobic (e.g., RNA or endotoxins from DNA preparation) or hydrophilic molecules (Ghanem, Healey et al. 2013, Aires-Barros and Azevedo 2017). Despite these applications, the use of high salt concentration denotes a drawback due to high costs and environmental hazards (Abdulrahman and Ghanem 2018).

1.3.2.2.4 Affinity Chromatography (AC)

Affinity chromatography is based on a specific interaction between an immobilized ligand and a particular site of the target biomolecule, figure 17 (Aires-Barros and Azevedo 2017, Abdulrahman and Ghanem 2018, Hage 2018).

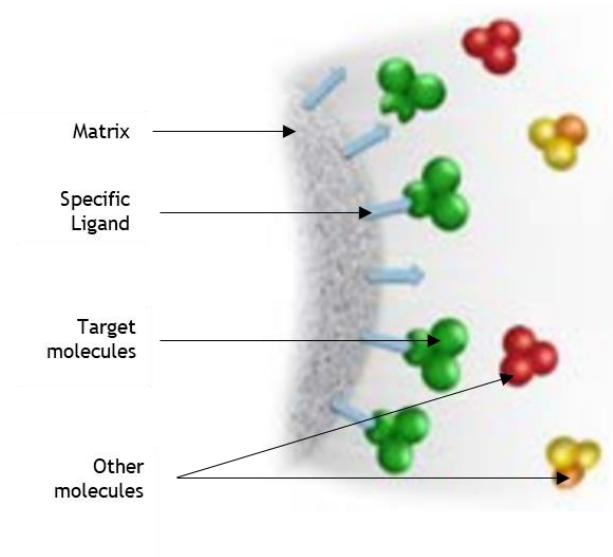

Figure 17 - Schematic representation of affinity chromatography (adapted from (Sciences 2016)).

Affinity techniques are usually divided into two main groups, biospecific interactions and pseudoaffinity interactions. The first one is based on highly specific interactions between two molecules, like interactions between enzyme and substrate or antibody and antigen, while the last one is based on the interaction between the ligand and a group of the biomolecule instead of a single well-defined site (Aires-Barros and Azevedo 2017). However, the interactions established between the ligand and the target molecule can be a combination of previously referred interactions, as well as hydrogen bonds, cation-π interactions, π-π interactions, Van der Waals forces, among others (Sousa, Sousa et al. 2012).

Initially, the ligand is coupled to a support, followed by the sample addition under conditions that are favorable for the specific binding of the molecule to the immobilized ligand and finally the elution may be achieved specifically using a competitive ligand, or nonspecifically through pH, ionic strength or polarity change (Hage, Anguizola et al. 2012, Hage 2018). AC can also be applied to concentrate substances that are present in low amounts and to separate proteins based on their biological function. However, AC has disadvantages associated with ligand leaking and also with the high cost of the resin (Aires-Barros and Azevedo 2017).

1.3.2.2.4.1 Immobilized Metal Ion Affinity Chromatography (IMAC)

IMAC was introduced in 1975 for the isolation of histidine-containing proteins through affinity interaction with transition metal ions. This technique is based on the specific interaction that can happen between immobilized metal ions and proteins, peptides or nucleic acids. The metal ions (Ni^{2+}, Zn^{2+}, Cu^{2+}, Co^{2+}, Fe^{3+}) are immobilized into a column due to the use of chelating agents like iminodiacetic acid or nitrilotriacetic acid (Hage, Anguizola et al. 2012, Aires-Barros and Azevedo 2017). After the sample is added to the column and the target molecule interacts with immobilized metal ion being retained. Then, the elution can be performed by the addition of a competing agent or by changing the pH (Hage, Anguizola et al. 2012). The supercoiling phenomenon of the sc pDNA contributes to the higher base exposure and local charge density, which could contribute to higher interaction with the ligand when compared with oc isoform (Abdulrahman and Ghanem 2018). Even so, this chromatographic procedure presents some concerns related to metal ions leakage because it may interfere with the purity and shelf-life of the obtained product (Hage, Anguizola et al. 2012).

1.3.2.3 Batch Method

Chromatography techniques are very used in industry for pDNA purification (Diogo, Queiroz et al. 2005) providing high-resolution separations, however, these methods cannot manage 'dirty'/complex samples since colloidal impurities commonly plug the packed-bed columns (Tüzmen, Akdoğan et al. 2010).

The batch method has been used for the determination of adsorption and desorption isotherms, for monitoring sorption kinetics of proteins on beaded materials (Hlady 1999, Mesgari-Shadi, Sarrafzadeh et al. 2018) and for studying the purification of a crude alkaline lysate applying cell beads (Deshmukh and Lali 2005). The batch method is composed of three steps, the adsorption or binding, washing and elution steps (Mesgari-Shadi, Sarrafzadeh et al. 2018), as shown in figure 18. First, the equilibrium buffer is added to the particles to set the particles in the best conditions for the binding step, in which the solution is added to the beads and the biomolecule will interact with the ligand on the particles. In the washing step, the non-adsorbed biomolecules or impurities will be removed by the equilibrium buffer and finally, in the elution step the interaction between the biomolecule and the particles is interrupted by the elution buffer (Hlady 1999, Mesgari-Shadi, Sarrafzadeh et al. 2018).

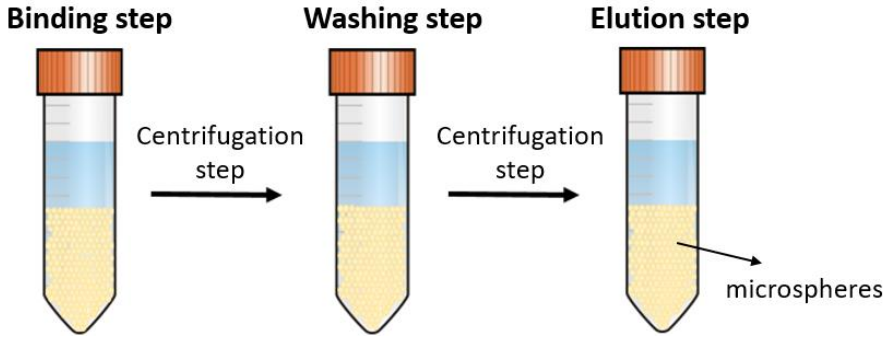

Figure 18 - Representation of batch method steps.

These steps are performed under stirring to achieve particle suspension in the added solution. Usually, the non-adsorbed components are separated from the one adsorbed on the particles through centrifugation steps (Hlady 1999). In comparison with the column procedure, this method is faster and cheaper and allows us to handle "dirty" samples (Don J. Brenner 1969, Tüzmen, Akdoğan et al. 2010).

According to Vladimir and co-workers, the batch method is well suited for beaded materials, like gel beads (Hlady 1999). Recently, polymers prepared from natural resources have become more and more essential due to their low cost, availability, water-solubility, biocompatibility, biodegradability, and gel-forming ability (Reis, Neufeld et al. 2006, Malviya, Sharma et al. 2016). For example, alginate that is a polysaccharide found in all species of brown algae is much explored in food and pharmaceutical industry due to its biocompatibility and non-toxic properties. Moreover, alginate can form gel beads in case of being crosslinked with cations, like calcium or zinc (Reis, Neufeld et al. 2006). One application of alginate microspheres was described by Neufeld and co-workers for DNA immobilization which was achieved with high encapsulation efficiency (T. Alexakis 1995). Another natural polysaccharide very similar to alginate is gellan gum that also has be ability to be crosslinked with divalent cations to form microspheres (Abbas and Marihal 2014).

1.4 Gellan Gum

Microbial exopolysaccharides (EPS) have a vast range of applications in food, pharmaceutical, cosmetics among other industries, due to their physical properties. Some of these applications consist of its use as emulsifiers, gelling agents, film formers and stabilizers (Ishwar B. Bajaj 2007, Prajapati, Jani et al. 2013). EPS are water-soluble polymers and may be ionic or non-ionic. Xanthan gum, gellan gum, and kefiran are the most studied and important heteropolysaccharides (Ishwar B. Bajaj 2007, Pérez-Ramos, Nácher-Vázquez et al. 2016).

1.4.1 Molecular Structure

Gellan gum is a linear and anionic polysaccharide that was named before as S-60 and PS-60 (BeMiller 2019). It is produced by the bacteria *Sphingomonas paucimobilis*, *Sphingomoas elodea*

(formerly known as *Pseudomonas elodea*) and *Azotobacter chroococcum* (Pérez-Ramos, Nácher-Vázquez et al. 2016). This molecule is composed of a tetrasaccharide unit of two residues of ß-D-glucose, one of ß-D -glucuronate and one of α-L-rhamnose, this means approximately 60% of glucose, 20% of rhamnose and 20% of glucuronate. It also contains non-polysaccharide material such as cell protein and ash. The chemical composition of different types of gellan is presented in table 5 (Prajapati, Jani et al. 2013).

Table 5 - Chemical composition of different types of gellan (adapted from (loannis Giavasis 2000)).

Gellan gum	**Neutral sugars Glc/Rha = 6/4**	**Uronic acid %**	**Acetyl group %**	**Protein %**	**Ash %**
Native	69	11	3	10	7
Deacetylated	62	13	0	17	8
Deacetylated and clarified	66.5	22	0	2	9.5

There are two types of gellan gum, native gellan gum, known as high acyl gellan gum and deacetylated gellan gum. Its chemical structure is illustrated in figure 19.

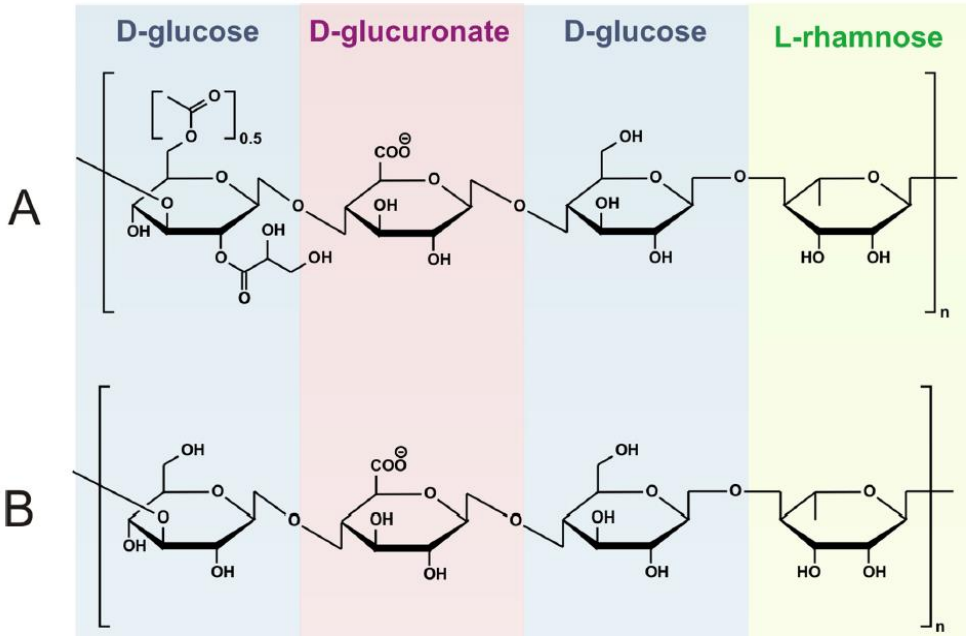

Figure 19 - Chemical structure of native (A) and deacetylated (B) gellan gum (adapted from (Osmalek, Froelich et al. 2014)).

The native gellan gum contains two ester groups, acetate, and glycerate bound to the same glucose residue. There is approximately one glycerate on O2 per tetrasaccharide repeat unit and one acetate on O6 for every two repeat units. When native gellan is exposed to high temperatures and alkaline treatment, both acyl groups are hydrolyzed and produce deacetylated gellan gum, low acyl gellan gum. The removal of acyl groups has an intense effect on the properties of gels produced with gellan (BeMiller 2019), results in a transformation from

soft, elastic thermoreversible gels (with textures similar to gel made with mixtures of xanthan and locust bean gum) to harder (tougher, rigid), brittle gels (with textures similar to gels made with agar and carrageenan) with greater thermal stability and optimal gelling conditions (Ishwar B. Bajaj 2007, Fialho, Moreira et al. 2008, BeMiller 2019).

1.4.2 Properties

Gellan gum can produce firm and translucent gels that are stable at low pH. This gelling property it's a function of the presence and type of cations in solutions, pH, temperature and polymer concentration during gelation (Zia, Tabasum et al. 2018). Moreover, this also affects the physical properties of gellan (Fialho, Moreira et al. 2008).

The gelation process has two parts that take place when a gellan gum solution is heated and then cooled. These sol-gel transitions are considered as a phase transition, in which the molecules of gellan gum go through roughly coiled shape to highly ordered double helices (Ishwar B. Bajaj 2007, Zia, Tabasum et al. 2018). The temperature at which the transition occurs was described as approximately 30ºC, however, the transition to double helix and following aggregation of helices is strongly influenced by the presence of cations and the polymer concentration (Prajapati, Jani et al. 2013). The addition of cations to the gellan solution has an effect on the aggregation of the double-helical segments to form a 3D network. Divalent cations addition, such as Mg^{2+} and Ca^{2+}, form gels stronger than the ones formed with monovalent cations, such as Na^{+} and K^{+} (Ishwar B. Bajaj 2007, Zia, Tabasum et al. 2018). So, first, the gellan molecules will look like random coil polymers when dispersed in water and heated (>60º). Through hydrogen bonds and van der Waals with the proximate chain, these coils create double-helical structures on cooling. In second, the double helices aggregate and form the cation-mediated junction zone in the presence of gel-promoting cations (figure 20). These cross-linkages will lead to the construction of strong gel channels (Ishwar B. Bajaj 2007, Zia, Tabasum et al. 2018).

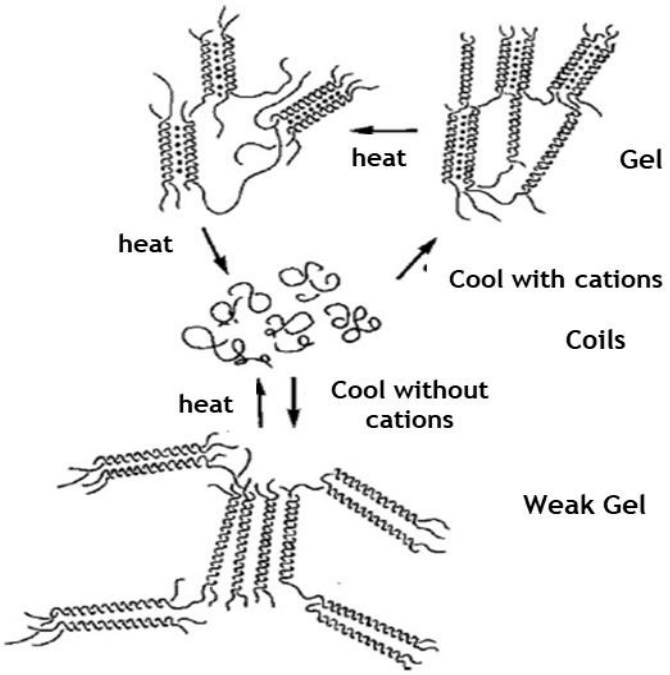

Figure 20 - Representation of the gelation process (adapted from (Morris, Nishinari et al. 2012)).

Gellan requires the presence of cations to form gels, and the gel can be modified through the type and concentration of the cation (Kang 1993). So the addition of monovalent or divalent cations during cooling significantly increases the number of salt bridges at junction zone, making the gels more resistant to temperature and improving the gelling potential of gellan gum. Besides the type and presence of cations, the acetyl group has a substantial effect on the properties of the gel of GG. The deacetylation of GG changes it from soft, flexible and drab gels into strong, firm and bright gels with high thermal stability (Ishwar B. Bajaj 2007, Zia, Tabasum et al. 2018).

In addition, gellan solutions suffer viscosity changes that are thermally reversible. The viscosity diminishes with increasing temperature, however with cooling the viscosity returns to its original value (Kang 1993). It was also reported that the gel strength increases within a pH range of 3.5 to 8, which is the natural pH range of most foods, but a change in pH affects the melting temperature in some cases (Ishwar B. Bajaj 2007).

Gellan gum has the capability to stand the heat and acid stress conditions during its production. Some of the best properties of gellan gum are its gelling property, malleability, textures, excellent thermal and acid stability. Additionally, gellan is biocompatible, biodegradable, non-toxic, has adjustable gel elasticity and high transparency (Fialho, Moreira et al. 2008, Zia, Tabasum et al. 2018).

1.4.3 Applications

Gellan gum is commercially available in 4 forms: Kelcogel, Gelrite, Gel-Gro and Phytagel (Ishwar B. Bajaj 2007, Fialho, Moreira et al. 2008, Prajapati, Jani et al. 2013). Kelcogel is available in two forms: high acyl and low acyl gellan gum (Prajapati, Jani et al. 2013). It is used in the food industry as a thickening and gelling agent and is also incorporated in lotions, creams, toothpaste (personal care) as a stabilizer and suspending agent. Gelrite, Gel-Gro and Phytagel are used as gelling agents too and to use in place of agar in media for microbial growth and plant tissue culture (Ishwar B. Bajaj 2007). Gel-Gro has the ability to form transparent gels in the presence of cations and presents hardness similar to agar, thermal stability, and compatibility with additives (Prajapati, Jani et al. 2013). Gelrite bears several autoclave cycles and is resistant to a variety of enzymes (Ishwar B. Bajaj 2007). Moreover, it shows potentiality in environmental applications such as in the biodegradation of gasoline and for the transportation of gel encapsulated bacteria in order to treat contaminated aquifers through a process called bioaugmentation (Fialho, Moreira et al. 2008).

Gellan gum is widely used due to its unique properties. Since it was approved by the FDA, in 1992, to be used as a food additive, therefore this is the most well-known/explored application of gellan gum. In table 6 are exemplified the potentials of gellan gum in several food products.

Table 6 - Conventional applications of gellan gum in food.

Food area	Products	Agents	References
Water-based gels	Dessert gels, aspic	Gelatin, alginate, carrageenan	(loannis Giavasis 2000, Ishwar B. Bajaj 2007)
Confectionery	Pectin jellies, fillings, marshmallow	Pectin, gelatin, starches, agar, xanthan, locust bean gum	(loannis Giavasis 2000, Ishwar B. Bajaj 2007, Prajapati, Jani et al. 2013)
Jams, marmalades, and jellies	Diet jams, imitation jams, bakery fillings, jellies	Pectin, carrageenan, starches	(loannis Giavasis 2000, Ishwar B. Bajaj 2007, Prajapati, Jani et al. 2013)
Pie fillings and puddings	Desserts, pie fillings, canned/precooked puddings	Alginate, carrageenan, starches	(loannis Giavasis 2000, Ishwar B. Bajaj 2007, Prajapati, Jani et al. 2013)
Fabricated foods	Restructured meat, fruits, and vegetables	Alginate, carrageenan, locust bean gum	(loannis Giavasis 2000, Ishwar B. Bajaj 2007)
Pet foods	Canned/gelled pet foods	Alginate, carrageenan, locust bean gum	(loannis Giavasis 2000, Ishwar B. Bajaj 2007)
Dairy products	Yogurt, milkshakes, gelled milk, ice cream, low fat spread, dips	Alginate, carrageenan, gelatin	(loannis Giavasis 2000, Ishwar B. Bajaj 2007, Prajapati, Jani et al. 2013)
Beverages	Fruit, milk-based, soy and carbonated drinks	Xanthan, gum tragacanth, gum arabic	(loannis Giavasis 2000, Saha and Bhattacharya 2010)
Films/coatings	Batter, breadings, coatings, adhesion systems	Acid ascorbic	(Prajapati, Jani et al. 2013)

Adding gellan gum to confectionary and bakery products provides structure, reduces the setting time of the starch jellies and prevents moisture fluctuations in sugary foods. Further, the necessary gellan gum concentration to produce the products mentioned above corresponds simply to one-fifth of the used agar. Gellan gum can also substitute pectin in jam and gelatin in water-based gels being efficacious at low concentrations. Moreover, gellan is used to provide the structure through the partial replacement of starches in pie fillings and puddings and to give form to fabricated food (pet food, fabricated fruit pieces or meat chunks), since GG does not melt during pasteurization, which allows the maintenance of their characteristics (Ishwar B. Bajaj 2007). According to the applications discussed above, gellan can be considered as an excellent multifunctional agent since it is tolerant of several environmental conditions.

Gels of gellan gum can also be used to replace agarose in electrophoresis. To prepare the gel to separate de DNA fragments based on size, the required concentration of gellan is only 0.125% compared to 1% of agarose. However, these electrophoresis gels must include a second polymer like hydroxymethylcellulose to reduce electroosmosis (Ishwar B. Bajaj 2007).
For biomedical and pharmaceutical fields gellan has been blended with different polymers and applied in gene therapy (gellan was grafted with PEI), as protein carrier, biological signaling, in scaffolds for bone regeneration, in wound healing cell adhesion and as a pharmaceutical excipient for nasal, ocular, gastric and colonic drug delivery (table 7) (Fialho, Moreira et al. 2008, Zia, Tabasum et al. 2018).

Table 7 - Utility of gellan gum in the medical field through oral, nasal or ophthalmic formulations (adapted from (Prajapati, Jani et al. 2013, Osmalek, Froelich et al. 2014)).

Formulation type	Active Pharmaceutical Ingredient	Function/Application
Oral Formulations		
Gellan capsules and beads	Theophylline	Phosphodiesterase inhibitor
Gellan beads	Propranolol hydrochloride	Beta-blocker
	Cephalexin	Antibiotic
	Rifabutin	
In situ gelling system	Theophylline	Phosphodiesterase inhibitor
	Paracetamol	Analgesic, antipyretic
In situ floating gel	Levofloxacin hemihydrates	Helicobacter pyroli infections, peptic ulcers
	Naproxen	Rheumatic arthritis, Inflammation
Gellan granules	Ephedrine hydrochloride	Sympathomimetic
In situ gelling floating gellan system; Gellan macrobeads; Gellan beads coated with chitosan	Amoxicillin	Antibiotic
Gum cordia/gellan beads; Acrylamide-grafted gellan gum tablets	Metformin hydrochloride	Antidiabetic
Immediate release gellan tablets	Metoclopramide hydrochloride	Antiemetic gastroprokinetic
Gellan gum tablets; Floating beads	Metronidazole	Antibacterial
	Acetohydroxamic acid	
Oil filled gellan buoyant beads blended by carbopol 934 or HPMC	Clarithromycin	Antibiotic
Microcapsules of gellan gum and egg albumin; Hydrogel microspheres	Diltiazem – resin complex	Antihypertensive
	Carvedilol	
Gellan beads gelated by Al^{3+} and cross-linked by glutaraldehyde	Glipizide	Type 2 diabetes mellitus
Carboxymethyl gellan beads	Metformin	Antidiabetic
Ophthalmic Formulations		
Sustained delivery ophthalmic system	Methylprednisolone	
Soluble bioadhesive ocular insert	Gentamicin	Antibiotic for veterinary use

Albumin nanoparticles with gellan for ophthalmic use	Pilocarpine	Anti-glaucoma
In situ gelling ophthalmic solution	Pilocarpine	Anti-glaucoma
	Sezolamide, dorzolamide	
	Carteolol hydrochloride	
	Timolol maleate	Glaucoma
	Indomethacin	Anti-inflammatory
	Piroxicam	
	Gatifloxacin sesquihydrate	Antibiotic
	Pefloxacin mesylate	
	Gatifloxacin	Bacterial conjunctivitis
	Matrine	Anti-inflammatory bacterial conjunctivitis, bacterial keratitis
Ocular insert	Ciprofloxacin hydrochloride	Bacterial conjuctivitis
	Gatifloxacin	
In situ gelling ophthalmic nanoemulsion	Terbinafine hydrochloride	Fungal keratitis
Nasal formulations		
In situ nasal gel	Fluorescein dextran	Epithelial uptake testing
	Scopolamine hydrobromide	Nausea, motion sickness prevention
	Momethasone furoate	Anti-inflammatory
		Allergic rhinitis
Intranasal microparticles	Metoclopramide hydrochloride	
In situ nasal gel based on thiolated gellan	Dimenhydrinate	Motion sickness prevention

According to Prajapati, Osmalek and co-workers gellan can be employed in the production of easy-to-swallow solid dosage forms, such as gels and coated tablets and also in oral drug delivery essentially as a disintegrating agent in instantaneous release tablets (Prajapati, Jani et al. 2013, Osmalek, Froelich et al. 2014). Hydrocolloids beads based on gellan gum are easily used for controlled, nonstop or slow release of several drugs through the modification of the release rate of active ingredients (Ishwar B. Bajaj 2007, Fialho, Moreira et al. 2008, Zia, Tabasum et al. 2018).

In ophthalmological applications, it was shown that gellan-based ophthalmic solutions have a bigger residence time in tear fluid than saline solutions. So gellan gum can be used for controlled bioavailability of ophthalmic formulations (Ishwar B. Bajaj 2007). In the tissue engineering field, gellan gum has been applied in cartilage reconstruction due to its mechanical properties and in 3D scaffolds through the production polycaprolactone-based blends (Fialho, Moreira et al. 2008). Lately, gellan is being explored as injectable carriers for autologous cells like bone marrow cells or chondrocytes since it is capable of gelling inside the body and efficiently adapting to the deficiency site to renovate the cartilage (Prajapati, Jani et al. 2013, Osmalek, Froelich et al. 2014). Besides that, gellan can be incorporated in wound dressing

designed in order to prevent postsurgical adhesion and scar formation, due to biocompatibility and non-toxic properties (Osmalek, Froelich et al. 2014).

In our research group, gellan has been studied as a potential chromatographic matrix to purify biomolecules since it presents properties like porosity, hydrophilicity, high binding capacity, and negative charge. These characteristics are regarded as a key to achieve the best performance of a chromatographic matrix and allow gellan to interact with positively charged biomolecules (Goncalves, Rocha et al. 2014).

All of these applications or possible uses of gellan highlight its versatility and its advantage over other polymers in different situations. It can be argued that gellan became one of the most significant commercialized EPS through the high number of patent filing.

Chapter 2 - Objectives

The main purpose of this work consists in the application of gellan microspheres reinforced with a counter-ion for the capture of plasmid DNA from *E. coli* complex lysates. Thus, in order to achieve this aim, it was necessary the development of some tasks.

The tasks to achieve the main aim include:

1. Gellan microspheres production through a water-in-oil emulsion, followed by its reinforcement with the addition of a divalent cation solution.
2. Gellan microspheres characterization, in which it was studied the stability of gellan microspheres formulations through a semiotic microscope, the confirmation of the microspheres reinforcement through energy-dispersive X-ray spectroscopy (EDX) and Fourier-transform infrared spectroscopy (FTIR), the global charge of the microspheres through zeta potential analysis and lastly the gellan microspheres morphology through scanning electron microscopy (SEM).
3. Application of gellan microspheres in a batch method in order to establish a capture strategy of pDNA from *E. coli* complex lysates.

Chapter 3 – Materials and Methods

3.1 Materials

For microspheres production, Gellan gum (Gelzan ®) was purchased from Sigma-Aldrich Co. (St Louis, USA) and copper sulfate anhydrous ($CuSO_4$) from Acros Organics (Geel, Belgium). The plasmid pMC.CMV-MCS-EF1-GFP-SV40Poly A with the resistant gene to Kanamycin was acquired from Addgene, USA and it was previously cloned with the gene E7 (pDNA-E7) by our research group. For the bacterial cultures, tryptone and yeast extract were obtained from Bioakar Diagnostics and Luria-Bertani (LB) medium in PanReac. Agar and kanamycin were purchased from Thermo Fisher Scientific (Waltham, USA). For alkaline lysis was used a protocol optimized by our research group with 3 solutions, solution A (50 mM glucose, 25 mM Tris-HCl and 10 mM EDTA at pH 8.0), solution B (200 mM NaOH and 1% (w/v) SDS) and solution C (3 M potassium acetate at pH 5.0). In the batch assays, Tris-base and sodium chloride (NaCl) were purchased from Thermo Fisher Scientific (Waltham, USA) and MES hydrate and MES sodium salt were obtained from Sigma-Aldrich Co. (St Louis, USA). In electrophoresis, GreenSafe reagent (GreenSafe Premium) was obtained from NZYTech Lda (Lisbon, Portugal) and agarose was acquired from Hoefer (San Francisco, USA). Ultrapure reagent-grade water, purified with a Milli-Q system from Millipore (Billerica, MA, USA) was used to prepare all the solutions.

3.2 Methods

3.2.1 Bacterial growth conditions and plasmid production

The pDNA-E7 was amplified through *E. coli* Top10 fermentation. Firstly, in LB-agar plates with 50 µg/mL of kanamycin the bacteria were inoculated and its growth occurred overnight at 37ºC. Then it was performed a pre-fermentation in which some colonies were transferred to an Erlenmeyer containing Terrific Broth (20 g/L tryptone, 24 g/L yeast extract, 4 mL/L glycerol, 0.017 M KH_2PO_4 and 0.072 M K_2HPO_4), supplemented with kanamycin 50 µg/mL and left to grow at 37ºC with 250 rpm shaking until an optic density (OD) of almost 2.6. After that, a specific volume of this medium was transferred to 4 erlenmeyers with TB medium to start the fermentation with OD of 0.2 and the growth was suspended after 16-18h at late log phase (OD≈9). Cells were recovered by centrifugation at 4500 rpm for 10 min at 4 ºC, and the pellets were stored at -20 ºC.

3.2.2 Plasmid extraction

In order to extract de plasmid, it was performed the cell lysis through the modified alkaline method (M. M. Diogo 2000). Thus, bacterial pellets from 250 mL of fermentation were resuspended in 20 mL of solution A (50 mM glucose, 25 mM Tris-HCl and 10 mM EDTA at pH 8.0) and then the volume was divided into two centrifuge tubes adding 10 mL of solution B (200 mM NaOH and 1% (w/v) SDS), followed by 5 minutes of incubation at room temperature to promote cell lysis. In order to stop cell lysis, it was added 10 mL of solution C (3 M potassium acetate at pH 5.0) and incubated on ice for 20 minutes. After the tubes were centrifuged twice at 20 000 g for 30 minutes at 4 ºC to eliminate major cell debris, gDNA and proteins, and the supernatant was stored at -20 ºC until use.

3.2.3 Gellan microspheres production through water-in-oil emulsion

The gellan microspheres were produced by a water-in-oil emulsion technique. Initially, 1.41 % of gellan gum was dissolved in water under stirring and heated at 100 ºC for 15 minutes. After, the gellan solution was transferred to a syringe with a 21G needle attached to a Harvard apparatus. The solution was dripped at 20 cm height with a flow rate of 75 µL/min into a 100 % vegetable cooking oil solution under constant stirring of 750 rpm and heating at 100 ºC. The microspheres were stabilized by adding 200 mL of 200 mM divalent cation solution to the mixture, maintaining the stirring of 750 rpm for 30 minutes at room temperature. After, the microspheres were washed with ethanol 70 % and dried with distilled water in a vacuum filtration system with a filter paper (VWR, USA). The copper-crosslinked gellan microspheres were recovered and some were functionalized with 6.15 % PEI through 2 h of agitation at room temperature. Lastly, each formulation of the microspheres was conserved in 10 mM MES buffer, pH 6.2, at 4 ºC.

3.2.3.1 Semi-optical analysis

After gellan microspheres production, the stability of each formulation was evaluated for 20 days through mean diameter determination using semi-optical microscopy. The microspheres were put in microscope slides and were visualized at 5x magnification lens. Five different images were captured to obtain the mean diameter at 0, 3, 10 and 20 days.

3.2.3.2 FTIR analysis

Fourier-transformed Infrared Spectroscopy (FTIR) was used to confirm the microspheres reticulation with Cu^{2+} and to validate its interaction with plasmid DNA. The samples were freeze-dried and the spectra were acquired using an FTIR spectrophotometer (Nicolet iS10) (Thermo Scientific, Waltham, USA) operated in ATR mode with an average of 120 scans on a wavenumber ranging from 400 to 4000 cm^{-1}, at a resolution of 32 cm^{-1}. It was also acquired the gellan gum spectrum and the data was processed in the OMNIC Spectra software (Thermo Scientific).

3.2.3.3 SEM analysis

Each formulation was visualized through scanning electron microscopy (SEM), Hitachi S-3400 N (Tokyo, Japan), in order to analyze its morphology and geometry. The microspheres were removed from the MES buffer and placed into aluminum support with a carbon base, and then frozen at -20 ºC. The images were acquired at different magnifications, with the BSE 3D detector.

3.2.3.4 EDX analysis

Chemical elements present in the copper-crosslinked microspheres and in the beads functionalized with PEI were identified by energy-dispersive X-ray spectroscopy (EDX) through a Bruker 129 eV (Bruker, USA). The microspheres in the frozen state, after SEM analysis, were analyzed to also confirm the copper presence through a QUANTAX 400 (Bruker, USA).

3.2.3.5 Global charge analysis through zeta potential

The zeta-potential of the copper-crosslinked microspheres, of the gellan microspheres functionalized with PEI and also of gellan gum microspheres was determined by Dynamic Light Scattering (DLS), at 25 ºC, using a Zetasizer Nano ZS (Malvern Instruments, UK). Therefore, microspheres were added to 1 mL of ultra-pure grade water used as a dispersant and it was evaluated the global charge through a folded capillary cell (DTS 1070) placed into the Zetasizer (n = 3). The data were obtained with the Malvern Zetasizer software v 6.34.

3.2.4 Batch method for plasmid DNA capture

The batch method was applied to capture pDNA from complex *E. coli* lysates using copper-crosslinked gellan microspheres and functionalized with PEI. This method consisted of the equilibrium of the microspheres and then follow by three characteristic steps, binding, washing, and elution intercalated by a centrifugation step. Therefore, it was performed several strategies to optimize the applied conditions to maximize the pDNA capture. In general, the microspheres were equilibrated with 10 mM MES buffer pH 5.2 at 4ºC, then the binding of pDNA to the microspheres was achieved by the addition of 10 mL of *E. coli* lysate, under constant stirring at 4 ºC for 2 hours. Then the supernatant was collected and in order to remove the unbound species, it was performed a washing step with 10 mM MES buffer pH 5.2. The elution of pDNA bound to microspheres was achieved by increasing pH to 8.0 in Tris-EDTA buffer and also by NaCl presence (200 mM and 1 M) for 1h under constant stirring. The supernatants were recovered and analyzed by agarose gel electrophoresis.

3.2.4.1 Agarose gel electrophoresis

The agarose gel electrophoresis was run with the supernatants recovered from the batch method by horizontal gel electrophoresis. It was performed using a 15 cm long 1% (w/v) agarose gel at 110 V for 30 minutes in TAE buffer (40 mM Tris base, 20 mM acetic acid, 1 mM EDTA, pH

8.0), stained with Greensafe (1 µL/mL). After, the gel was visualized under UV light using Firereader software version 15.15 of UVITEC.

3.2.4.2 Plasmid DNA quantification

The purity and recovery of sc pDNA were evaluated using a CIMac™ pDNA analytical column. It was performed a calibration curve with pDNA-E7 previously purified with Qiagen Kit,which concentrations vary from 1 to 100 g/mL, as shown in figure 21.

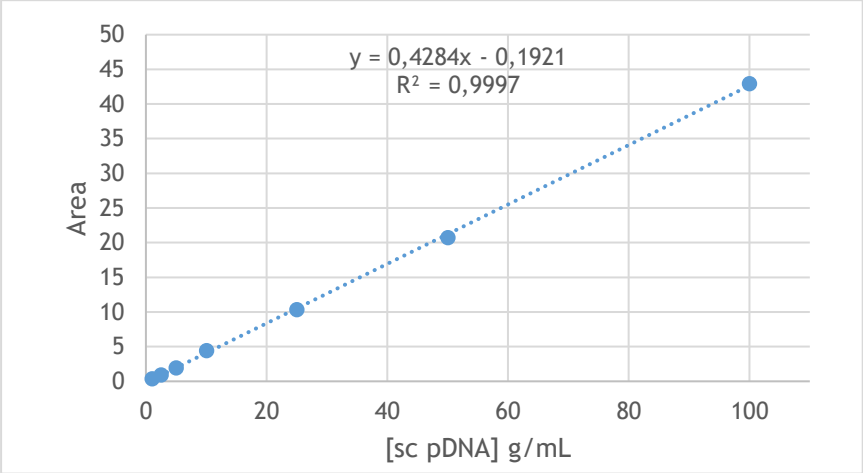

Figure 21 - Calibration curve obtained from the sc pDNA with a range of concentrations from 1 to 100 g/mL.

The analytical column was equilibrated with 600 mM NaCl in 200 mM Tris-HCl (pH 8.0), then the lysate and the supernatant which corresponds to pDNA elution from the batch method were injected and it was applied a linear gradient from 600 mM to 700 mM NaCl in 200 mM Tris for 10 minutes, leading to elution of RNA and DNA species. The peaks presented in the chromatogram, figure 22 were integrated allowing the calculation of purity degree and recovery percentage.

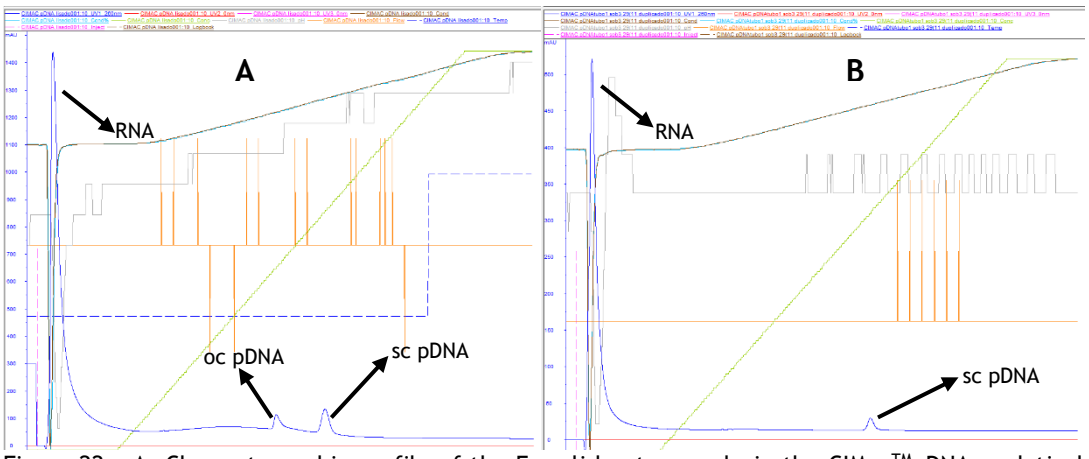

Figure 22 – A: Chromatographic profile of the E. coli lysate sample in the CIMac™pDNA analytical column. B: Chromatographic profile of the pDNA elution step recovered during the batch method in the CIMac™pDNA analytical column. RNA species eluted in the flowthrough and oc and sc pDNA isoforms separated during the linear gradient. Mobile phase: Buffer A – 200 mM Tris-HCl buffer (pH 8.0); Buffer B – 1 M NaCl in 200 mM Tris-HCl buffer (pH 8.0).

The first peak that appears on the chromatogram corresponds to RNA, so this means that it does not interact with the column. Then, by increasing the salt concentration, the pDNA isoforms are eluted separately, first eluting the open circular isoform (oc pDNA) and then the supercoiled isoform (sc pDNA) (Sousa, Almeida et al. 2014). The percentage of sc pDNA recovered and the purity degree was calculated with the two equations presented below:

$$\%\, recovery = \frac{sc\ pDNA\ mass\ from\ the\ assessed\ sample}{sc\ pDNA\ mass\ from\ the\ lysate\ sample} \times 100 \quad (1)$$

$$\%\, purity = \frac{sc\ pDNA\ peak\ area}{\sum all\ peak\ areas} \times 100 \quad (2)$$

The amount of sc pDNA recovered was calculated taking into account the concentration and volume applied in the assay. The percentage of recovery, equation 1 corresponds to the amount of sc pDNA from the sample relative to the amount of sc pDNA in the lysate sample. The purity degree is obtained through the peak areas, as shown in equation 2.

3.2.4.3 Total protein quantification

The protein content in the samples was measured using the Pierce BCA Protein Assay Kit (Thermo Scientific, USA). In summary, 1 µL of each sample, 19 µL of water and 80 µL of working reagent were prepared in a 96 well microplate, in triplicate. The microplate was manually homogenized and incubated in the dark at 37ºC for 30 minutes. Then, the absorbance was recorded at 562 nm in a xMarkTM Microplate Absorbance Spectrophotometer (Bio-Rad, USA). After, a calibration curve was constructed using bovine serum albumin (BSA) as standard, in which concentrations vary from 0 to 1.2 µg/mL, figure 23.

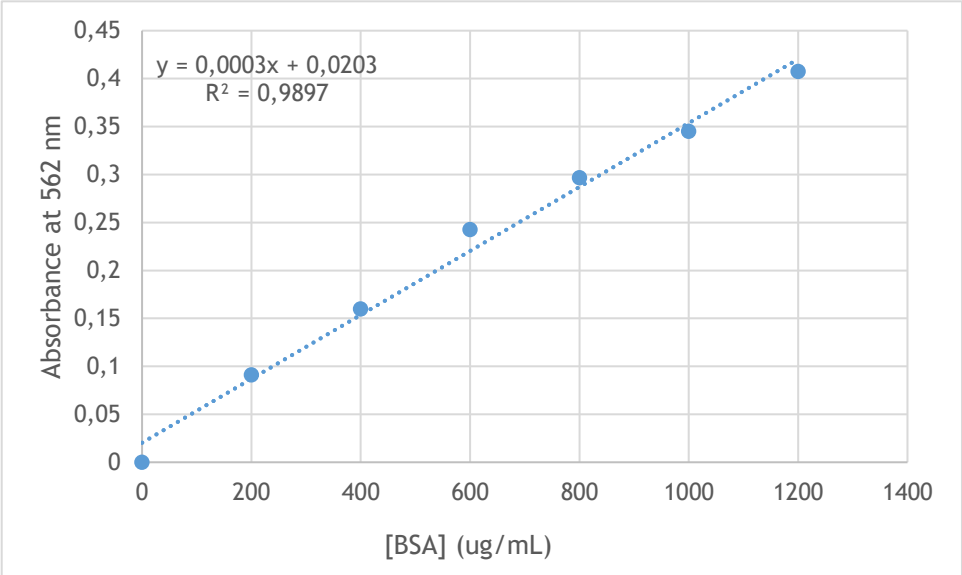

Figure 23 - Calibration curve obtained with BSA standards (0-1200 µg/mL).

Chapter 4 – Results and discussion

4.1 Gellan microspheres production

Emulsions consist on the mixture of two immiscible liquids in which one of the liquids is dispersed as small spherical droplets in the continuous phase being therefore widely applied in microparticles formation (Aguero, Zaldivar-Silva et al. 2017). Emulsions can be divided into two groups, oil-in-water (O/W) and water-in-oil (W/O) types. In the first system water is the continuous phase and in the second one corresponds to the dispersion phase (Yamashita, Miyahara et al. 2017). Equally, the concept is apply to oil but in a reverse mode. In general, the water-in-oil emulsion is the basis for alginate microparticles formation, since it is easy to scale-up where the high-speed stirring allows the achievement of smaller particle size (Aguero, Zaldivar-Silva et al. 2017). After the W/O emulsion, the biopolymer in the water droplets is crosslinked to form hydrogel particles and this can be achieved by different methods, including temperature manipulation, or addition of ions, acids, bases, or cross-linking agents depending on the biopolymer gelation mechanism (Joye and McClements 2014).

Gellan gum is a polymer that displays a thermoreversible conformational transition during the cooling of its heated solutions (Yang, Hou et al. 2019), requiring the presence of cations to form gels (Kang 1993). When gellan is heated the molecules are in a disordered state (single coil) and upon cooling, the molecules suffer a transformation into an ordered state (double helix). The cations addition promotes an electrostatic interaction between them and the gellan carboxylic groups, increasing the double helices aggregation which leads to the formation of a stronger 3D network (Zia, Tabasum et al. 2018, Yang, Hou et al. 2019).

Gellan microspheres were obtained through a W/O emulsion, where the main conditions were previously optimized by our research group (Coelho, Eusebio et al. 2019), as schematized in figure 24. A gellan gum solution 1.41 % (w/v) was heated until 90 ºC under constant stirring, 300 rpm. At the same time, 300 mL of vegetable oil was heated at 100 ºC under stirring of 750 rpm. Then, the gellan solution was transferred to a syringe and dripped into the cooking oil solution through a 21G needle at a flow rate of 75 µL/min. A divalent cation solution (200 mM) was added to the emulsion at room temperature under stirring to reinforce and stabilize the microspheres. After 30 minutes of agitation, the microspheres were filtered, washed with ethanol 70 % and stored in 10 mM MES buffer pH of 6.2.

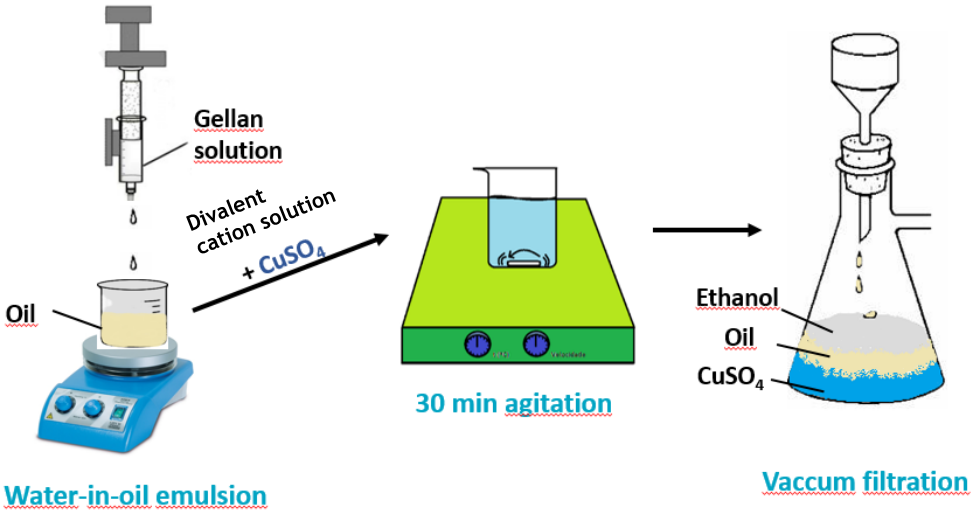

Figure 24 -Schematic representation of microspheres production.

4.2 Strategies for plasmid DNA capture through a batch method

4.2.1 Screening of the batch method conditions

Since the major aim of this dissertation is the application of the gellan microspheres in a batch method to capture plasmid DNA from *E. coli* lysates, it is necessary to explore the best conditions for the capture strategy. Therefore, it was made a screening of conditions for pDNA capture by gellan microspheres, in which it was studied the influence of the crosslinker, the influence of pH in the binding and elution steps, the influence of the impurities in pDNA capture through the analysis of a pre-clarified lysate and lastly the effect of microspheres functionalized with positive groups in the capture of pDNA.

4.2.1.1 Influence of different metal ions as crosslinkers

Nucleic acids and gellan gum are both negatively charged, so it is expected that the interaction of nucleic acids occurs with the crosslinked divalent cations present in the microspheres, probably mimic the retention mechanisms of an immobilized metal affinity chromatography (IMAC). According to several authors, in IMAC different transition metal ions are used as ligands, such as Co^{2+}, Mn^{2+}, Cu^{2+}, Ni^{2+}, Zn^{2+}, Fe^{3+}(Jason C. Murphy 2003, Tan, Kim et al. 2007, Igor Tadeu Lazzarotto Bresolin 2009). Thus, in the first assay, the microspheres were reinforced with the following solutions: $CuSO_4$, $NiCl_2$, $CoCl_2$, $ZnCl_2$, $CuCl_2$, and $FeCl_3$ in order to understand the influence of the divalent cation in the pDNA capture. For that, 20 mL of the gellan microspheres crosslinked with different ions were equilibrated in 10 mM Tris-HCl, 1 mM EDTA at pH 8.0 and stirred for 15 minutes at 4 °C. Thereafter, it was performed a centrifugation step at 500 g for

5 minutes, the supernatant was discard and 10 mL of crude alkaline lysate, pH 5.0 (binding solution) was added and incubated for 2 hours on the roller shaker at 4 ºC. New centrifugation of 100 g for 5 minutes was performed, collecting the supernatant that contained the molecules that did not bind to the microspheres. Then, it was performed a washing step with the equilibrium buffer (10 mM Tris-HCl, 1 mM EDTA at pH 8.0), followed by centrifugation for 5 minutes at 100 g, and the supernatant was recovered. Afterward, it was added 10 mL of the 1st elution buffer (200 mM NaCl, 10 mM Tris-HCl, 1 mM EDTA, pH 8.0) incubated 1 hour on the roller shaker at 4 ºC. The supernatant containing the eluted molecules was recovered after the centrifugation step and once again a washing step was applied, but at this time, by using the 1st elution buffer. Finally, it was added 10 mL of the 2nd elution buffer (1 M NaCl, 10 mM Tris-HCl, 1 mM EDTA, pH 8.0), repeating the previous incubation step, and the supernatant was collected after the centrifugation step. All the supernatants were analyzed through agarose gel electrophoresis as shown in figure 25.

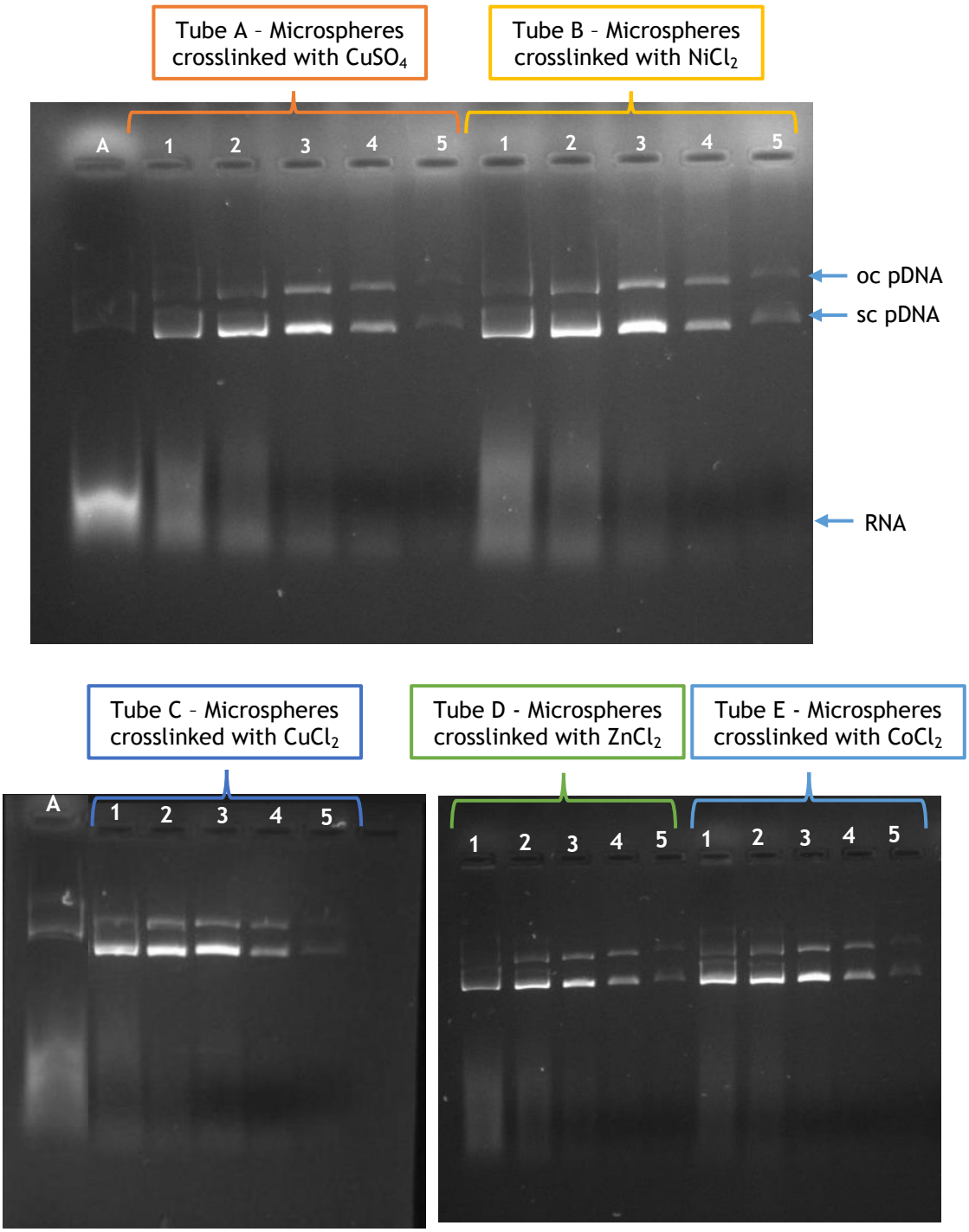

Figure 25 - Agarose gel electrophoresis of the supernatants recovered from gellan microspheres prepared with different divalent ions. Tube A -microspheres crosslinked with $CuSO_4$; Tube B - microspheres crosslinked with $NiCl_2$; Tube C -microspheres crosslinked with $CuCl_2$; Tube D - microspheres crosslinked with $ZnCl_2$; Tube E -microspheres crosslinked with $CoCl_2$; A - E. coli lysate used in the binding step; 1 - E. coli lysate that did not bind to the gellan microspheres; 2 - Washing with 10 mM Tris-HCl, 1 mM EDTA, pH 8.0; 3 - first elution with 200 mM NaCl in 10 mM Tris-HCl, 1 mM EDTA, pH 8.0; 4 - Washing with 200 mM NaCl in 10 mM Tris-HCl, 1 mM EDTA, pH 8.0; 5 - final elution with 1 M NaCl in 10 mM Tris-HCl, 1 mM EDTA, pH 8.0.

Gellan microspheres require the addition of a reinforcement solution containing cations to stabilize them, and divalent cations are more effective than monovalent cations for this purpose (Kang 1993, Goncalves, Rocha et al. 2014). In figure 25, it is not shown the analysis of the gellan microspheres reinforced with $FeCl_3$ because it was not possible to produce them with normal characteristics (round shape). In general, it seems that all microspheres favor the pDNA retention in comparison to RNA since the RNA band in the eluted samples (lane 3) is less evident than in fractions of non-bound sample (figure 25). Among all types of microspheres, the microspheres crosslinked with $CuCl_2$ (tube C) seem to retain less sc pDNA due to higher density in sc pDNA band of lane 1 and 2 of figure 25. Observing the lane 3 from all experiments of figure 25, which corresponds to sc pDNA elution with 200 mM NaCl in 10 mM Tris-HCl, 1 mM EDTA, pH 8.0, it is suggested that the electrostatic interaction established between the pDNA and the divalent cations present in the microspheres, was destabilized by an increase of the ionic strength in the elution buffer, resulting in the pDNA elution. However, by the analysis of the agarose gel electrophoresis, it was only possible to perform a qualitative evaluation of these assays, thus hindering a realistic and comparative analysis of the influence of the different types of gellan microspheres in the sc pDNA capture. Thus, to overcome this limitation, the *E. coli* lysate and the supernatants from the sc pDNA elution step with 200 mM NaCl (lane 3) were analyzed in an analytical column CIMac^{TM}pDNA in order to quantify the amount of sc pDNA. The results are presented in table 8.

Table 8 – Assessment of the sc pDNA concentration, total sc pDNA amount, percentage of recovery and purity percentage of the E. coli lysate and the supernatants from the sc pDNA elution with 200 mM NaCl (n = 2) of the 1st assay in which gellan microspheres were reinforced with different metal ions solutions ($CuSO_4$, $NiCl_2$, $CoCl_2$, $ZnCl_2$, $CuCl_2$).

Samples	[sc pDNA] (µg/mL)	Total sc pDNA amount (µg)	Recovery Percentage (%)	Purity Percentage (%)
E. coli lysate, pH 5 (binding solution)	8.65	86.5	-	3.66
Elution of sc pDNA from Microspheres reinforced with $CuSO_4$	**1.35**	**13.5**	**15.61**	**2.42**
Elution of sc pDNA from Microspheres reinforced with $NiCl_2$	0.82	8.2	9.48	1.48
Elution of sc pDNA from Microspheres reinforced with $CuCl_2$	0.88	8.8	10.17	1.81
Elution of sc pDNA from Microspheres reinforced with $ZnCl_2$	0.83	8.3	9.60	1.59
Elution of sc pDNA from Microspheres reinforced with $CoCl_2$	0.81	8.1	9.36	1.62

The *E. coli* lysate has a sc pDNA concentration of 8.65 µg/mL, which corresponds to about 86.5 µg present in 10 mL of applied sample and the supernatant that presents the highest amount of sc pDNA recovered, 13.5 µg, was eluted from gellan microspheres crosslinked with copper

sulfate. The sc pDNA eluted from gellan microspheres reinforced with copper also has the highest purity (2.42 %) between all the supernatants recovered. The results obtained from the other gellan microspheres formulations had recovery percentage around 9.36 % - 10.17 %, and the purity percentage about 1.48 % - 1.81 %. Considering table 8, it is possible to order the interaction of transition metal ions with sc pDNA taking into account the amount of sc pDNA that was eluted/recovered from different gellan microspheres in $CuSO_4$ > $CuCl_2$ > $ZnCl_2$ > $NiCl_2$ > $CoCl_2$.

As stated by Anastassopoulou, the positively charged metal ions interact directly or indirectly with sites characterized by high electron density or negatively charged DNA residues (Anastassopoulou 2003). These sites may be the negatively charged phosphate groups and the electron-donating atoms present in the nitrogenous bases of DNA, such as nitrogen (N) and oxygen (O). The major mode of interaction is with N7 and O6 of guanine and N7 and N1 of adenine and the N3 of pyrimidines (cytosine and thymine) (Anastassopoulou 2003). Duguid and co-workers described that ions preferentially bind to the bases over phosphates of DNA in the following order: Pd^{2+} > Cu^{2+}, Co^{2+} > Ni^{2+}, Cd^{2+}, Mn^{2+} > Ca^{2}, Sr^{2+}, Ba^{2+} (John Duguid 1993). In addition, Murphy and co-workers claimed that immobilized copper ions are superior in nucleic acid binding than nickel ions, suggesting that the interaction occurs mainly through the nitrogens present in the bases (Jason C. Murphy 2003). Based on the literature referred above, copper (II) is the one that most interacts with sc pDNA, which supports the results described in table 8, since the microspheres reinforced with copper sulfate retained the largest amount of pDNA, 13.5 μg, in relation to RNA, being reflected in the highest purity, 2.42 %. Therefore, in the following assays, the microspheres were reinforced with $CuSO_4$.

4.2.1.2 Influence of pH and buffer

The *E. coli* lysate sample is obtained through alkaline lysis, in which the first buffer (P1) is added to the cells allowing its resuspension. Cell disruption is accomplished by the addition of a strong base such as NaOH and detergent, SDS, from the second buffer pH 12.5 (P2) that denatures proteins present in the cell wall. This step induces the release of all host components (proteins, nucleic acids, and endotoxins) and cellular debris into the extracellular medium. This solution is neutralized by the addition of the 3rd buffer pH 5.5 (P3) containing potassium acetate, which aids in the precipitation of gDNA and cellular debris (G-Biosciences , Alex Xenopoulos 2014). According to the procedure mentioned above the final pH of the lysate sample is about 5.0. By this reason, for carrying out the 2nd assay, the lysate sample was subjected to a pH adjustment of 5.2, since at this pH the MES buffer is stable to perform the batch method, and 8.0, in order to understand whether different pHs influenced the binding and elution conditions. The equilibrium and elution conditions of the strategies studied are presented in table 9. In tube A the strategy consisted of using a pH 5.2, once the *E. coli* lysate has a pH around 5.0. In tube B it was evaluated the influence of pH 8.0.

Table 9 - Description of the equilibrium and elution conditions applied in the 2nd assay.

Strategy	Equilibrium buffer	Elution buffer
Tube A: pH 5.2	10 mM MES pH 5.2	200 mM NaCl and 1 M NaCl in 10 mM MES pH 5.2
Tube B: pH 8.0	10 mM Tris-HCl, 1 mM EDTA, pH 8.0	200 mM NaCl and 1 M NaCl in 10 mM Tris-HCl, 1 mM EDTA pH 8.0

The supernatants recovered from this 2nd assay were analyzed in agarose gel electrophoresis, as illustrated in figure 26.

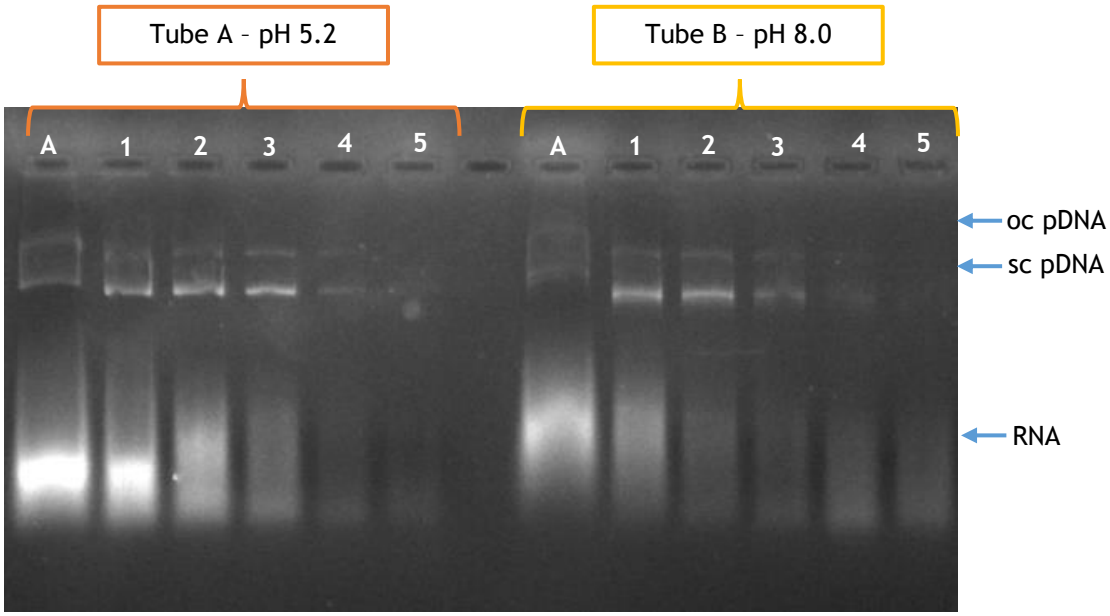

Figure 26 - Agarose gel electrophoresis of the supernatants recovered in the 2nd assay. Tube A - Assay performed at pH 5.2 with 20 mL of copper-crosslinked gellan microspheres and 10 mL of E. coli lysate. Tube B - Assay performed at pH 8.0 with 20 mL of copper-crosslinked gellan microspheres and 10 mL of E. coli lysate. A - E. coli lysate applied in which tube; 1 - E. coli lysate that did not bind to the gellan microspheres; 2 - Washing with the equilibrium buffer; 3 - elution of E. coli lysate with first elution buffer; 4 - Washing with first elution buffer; 5 - final elution of E. coli lysate with second elution buffer.

Analyzing figure 26, the band that corresponds to RNA becomes faint in both tubes, suggesting a decrease in RNA content during several steps of the batch method. This decrease is more noticeable after lane 3 in tube A, assay performed at pH 5.2 and in lane 2, tube B, assay performed at pH 8.0. In relation to pDNA retention and elution in the assay performed at pH 5.2 (tube A), the band of sc pDNA presents similar densities in lane 1 (molecules that did not bind to gellan microspheres) and lane 3 (pDNA elution), whereas in the lane 3 of the assay performed at pH 8.0 (tube B) the band is rather faint. These results indicate that at pH 8.0 the sc pDNA elution is less evident. Therefore, the *E. coli* lysate and the supernatant that corresponds to the sc pDNA elution with 200 mM NaCl, lane 3, of both tubes were analyzed in the analytical column CIMac™ pDNA, as described in the 1st assay. The results are presented in table 10, which also contains the results obtained for the pDNA elution from the microspheres

reinforced with $CuSO_4$ of the 1st assay (table 8) for comparison since the binding step was promoted at pH 5.0 and the elution step with pH 8.0.

Table 10 - Assessment of the sc pDNA concentration, total sc pDNA amount, percentage of recovery and purity percentage of the E. coli lysate and the supernatants from the sc pDNA elution with 200 mM NaCl (n = 2) of the 2nd assay and comparison with the sc pDNA elution of the 1st assay.

Samples	[sc pDNA]	Total sc pDNA amount (µg)	Recovery Percentage (%)	Purity Percentage (%)
E. coli lysate (binding solution)	8.65	86.5	-	3.66
Elution of sc pDNA with 200 mM NaCl in 10 mM MES, pH 5.2 (Tube A – 2nd assay)	0.59	5.9	6.82	2.03
Elution of sc pDNA with 200 mM NaCl in 10 mM Tris-EDTA, pH 8.0 (Tube B – 2nd assay)	0.05	0.5	0.58	1.28
Elution of sc pDNA with 200 mM NaCl in 10 mM Tris-EDTA, pH 8.0 (1st assay)	1.35	13.5	15.61	2.42

According to the table 10, in strategies where it was explored both binding and elution steps at pH 5.2 (tube A) or pH 8.0 (tube B), the concentration of the eluted sc pDNA was low (0.59 µg/mL and 0.05 µg/mL) as well as the purity percentage (2.03 % and 1.28 %), respectively. The highest amount of eluted sc pDNA (13.5 µg) and recovery percentage (15.61 %) was found in the 1st assay in which the binding step was performed at pH 5.0 and the elution step at pH 8.0.

The *E. coli* lysate sample used in 1st and 2nd assays was not clarified, so it presents a great complexity of biomolecules, like RNA, gDNA, proteins, pDNA, endotoxins and other impurities (Guilherme N.M. Ferreira 2000). Proteins have a specific isoelectric point and by manipulating the medium pH it is possible to change their surface charge between negative, neutral and positive. Endotoxins, as well as RNA, are negatively charged, so these biomolecules can compete with sc pDNA for binding to metal ions (Sousa, Sousa et al. 2012). Based on this information, the total protein quantification was performed through the BCA method of the *E. coli* lysate, the supernatant that did not bind to the microspheres and the supernatant obtained in the first elution step with 200 mM NaCl of both strategies from the 1st and 2nd assays with copper-crosslinked microspheres. The results are presented in table 11.

Table 11 - Total protein amount of the E. coli lysate and supernatants recovered after the binding and elution step of the 1st and 2nd assays.

Samples	[protein] (µg/mL)	Protein amount (µg)
E. coli lysate (binding solution)	6046.67	1209.33
E. coli lysate that did not bind to the microspheres, pH 5.0 (1st assay)	3602.22	720.44
Elution of sc pDNA with 200 mM NaCl in 10 mM Tris-EDTA, pH 8.0 (1st assay)	-	-
E. coli lysate that did not bind to the microspheres, pH 5.2 (Tube A – 2nd assay)	1024.44	204.89
Elution of sc pDNA with 200 mM NaCl in 10 mM MES, pH 5.2 (Tube A – 2nd assay)	1380.00	276.00
E. coli lysate that did not bind to the microspheres, pH 8.0 (Tube B – 2nd assay)	1024.44	204.89
Elution of sc pDNA with 200 mM NaCl in 10 mM Tris-EDTA, pH 8.0 (Tube B – 2nd assay)	-	-

The *E. coli* lysate has 1209.33 µg of total protein amount according to table 11. In the strategy performed at pH 5.2, the content that did not bind to the microspheres contains 204.89 µg of total protein amount and the supernatant that corresponds to the elution of sc pDNA has 276.00 µg of total protein amount. Bolanos-Garcia and Davies stated that the *E. coli* proteins usually co-purified in IMAC present an isoelectric point between 5 and 7, so at pH 5.2 the proteins have positive/neutral charge and at pH 8.0 the proteins are negatively charged (Bolanos-Garcia and Davies 2006). This means that at pH 5.2 most of the proteins are positively charged so some biomolecules can interact with the negative charge of gellan microspheres since it was possible to quantify them in the supernatant of sc pDNA obtained in the elution at pH 5.2. Nevertheless, at pH 5.2 it seems that the proteins have no interference in the pDNA interaction with copper ion. This hypothesis can be related to the fact that at this pH, *E. coli* proteins present the same charge of the copper ions leading to a repulsion between both, being the coper ions available to interact with pDNA.

In the strategy performed at pH 8.0, it was only possible to quantify proteins in the supernatant of the *E. coli* lysate that did not bind to the microspheres, 204.89 µg. At pH 8.0 most of the proteins present negative charge, so they could compete with pDNA for the metal ion interaction during the binding step, which corroborates with the results obtained in pDNA quantification analysis since this strategy recovered less sc pDNA. The elution at pH 8.0 with 200 mM NaCl seems to favor the pDNA elution due to the increment of ionic strength, maintaining proteins bound to the gellan microspheres, they can elute with the increase of the

ionic strength to 1 M NaCl, but this supernatant was not quantified once there was no pDNA. In the 1st assay, it was only possible to quantify proteins in the *E. coli* lysate that did not bind to the microspheres at pH 5.0 (about 720.44 µg), indicating once more that at this pH the proteins interact with the negative charge of the gellan, not interfering with the pDNA interaction with copper. The pDNA elution occurs by the increase of the ionic strength but is favored by the application of Tris buffer pH 8.0 instead of MES buffer pH 5.2, once that Tris salt weakly competes with the biomolecule of interest for the binding site, thus favoring its desorption (Patrick P. Berna 1997, Igor Tadeu Lazzarotto Bresolin 2009).

Based on previous results, it can be concluded that at pH 5.0, the pDNA binding is favored in relation to pH 8.0 and the pDNA elution is favored by the application of Tris buffer at pH 8.0. After understanding that the use of copper-crosslinked gellan microspheres and the binding and elution steps performed at pH 5.0 and 8.0, respectively, were the best conditions to capture pDNA from *E. coli* lysates it was performed the microspheres characterization in terms of morphology, stability, elemental composition, and charge.

4.2.2 Characterization of copper-crosslinked gellan microspheres

The copper-crosslinked gellan microspheres were analyzed in the semiotic microscope in order to determine the mean diameter. So, it was taken 5 snaps and the respective diameter measures. Figure 27 is an example of a snap obtained in the semiotic microscope after the production of the microspheres.

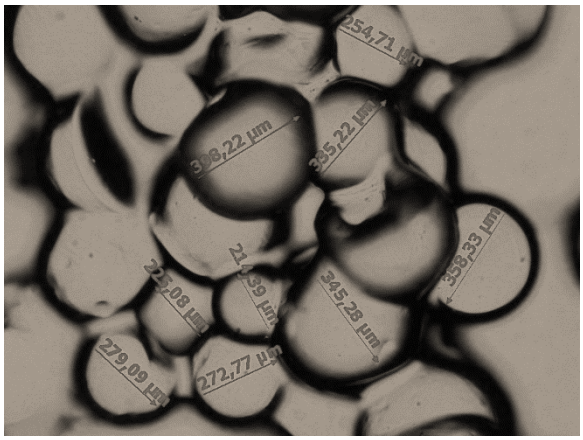

Figure 27 – Representative image of copper-crosslinked gellan microspheres after its production obtained in the semiotic microscope (5x).

In general, the microspheres present a round shape, suggesting that the water-in-oil emulsion allows a suitable formulation of microspheres. The mean diameter of copper-crosslinked microspheres is about 365.34 ± 17.24 µm, according to five images obtained in the microscope. In comparison with the mean diameter of the copper-crosslinked microspheres described by Coelho and coworkers, 308.21 ± 16.65 µm, the mean diameter obtained in the copper-crosslinked microspheres is a little higher (Coelho, Eusebio et al. 2019). This difference could be attributed to the gellan gum concentration applied in the microspheres formulation, because

in the article was applied 1.27 % (w/v) (Coelho, Eusebio et al. 2019) and in this work the concentration was about 1.41 % (w/v). According to Abbas and Mariah and also to Bhattacharya and co-workers, higher gellan concentration promotes an increase in the ability of water absorption, leading to a higher diameter of the microspheres (Bhattacharya, Banerjee et al. 2013, Abbas and Marihal 2014). Nevertheless, several authors prepared gellan beads through the ionotropic method, using $CaCl_2$ as a crosslinker, and it was obtained a diameter range between 380 µm to 2340 µm (Chakraborty, Jana et al. 2014, Fan, Yi et al. 2017, Nandi, Nandi et al. 2018, Lyu, Liu et al. 2019). In the present work, the copper-crosslinked microspheres present a lower diameter, which is an advantage since it increases the contact surface area with the target molecule, which could increasing the number of target binding molecules (Thomas 2012).

4.2.2.1 Gellan microspheres stability analysis

The microspheres stability was studied over time, through evaluation of the mean diameter in the semiotic microscope, mainly, after its production 0, 3, 10 and 20 days. Among the analyzed samples, 5 snaps were taken for each day and the mean diameter was calculated. Figure 28 demonstrates an example of the measures made for the copper-crosslinked gellan microspheres over time. Table 12 summarizes the mean diameters obtained from the 5 snaps (n = 5) for each sample over time.

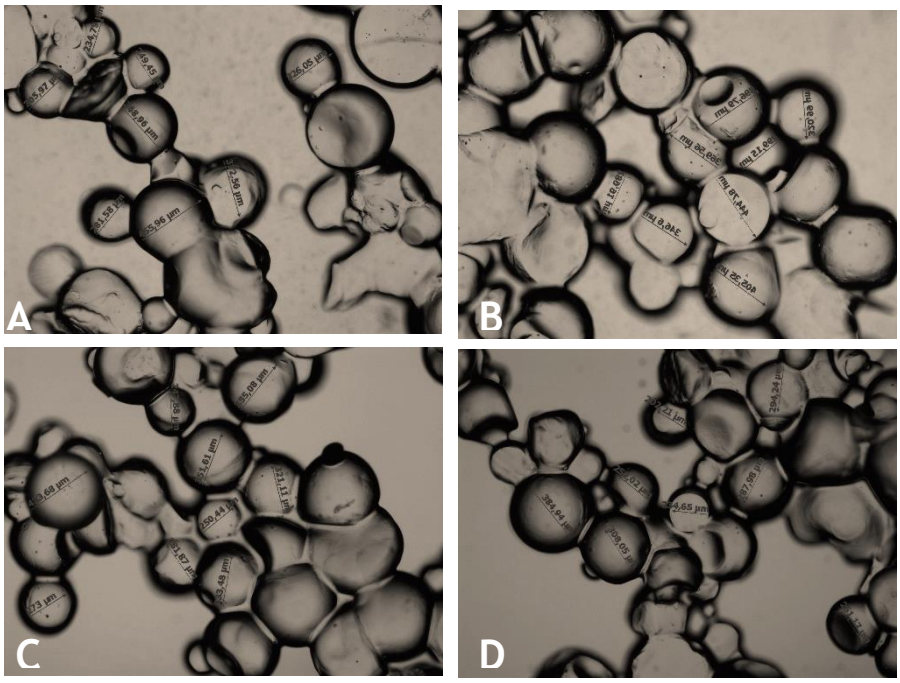

Figure 28 - Representative images of the copper-crosslinked gellan microspheres obtained in the semiotic microscope (5x). A – Snap taken at 0 days; B - Snap taken at 3 days; C - Snap taken at 10 days; D - Snap taken at 20 days.

Table 12 – Copper-crosslinked gellan microspheres mean diameter considering the stability over time (n=5).

Days	Mean diameter (µm ± SD)
0	365.34 ± 17.24
3	322.28 ± 9.43
10	300.82 ± 20.92
20	285.08 ± 11.40

The results presented in figure 28 and table 12 indicate that the microspheres mean diameter diminishes over time. This behavior can be related to the disintegration of the biggest microspheres over time, only remaining intact the smallest ones, probably due to the swelling phenomenon (Coelho, Eusebio et al. 2019). Nevertheless, there are a lot of microspheres with uniform size, which suggest that in these formulation conditions the microspheres stability is higher than 20 days.

4.2.2.2 FTIR analysis

The characterization of microspheres by FTIR was used to confirm the interaction between gellan microspheres and the copper ion and also between the copper-crosslinked microspheres and the pDNA. Therefore, it was acquired the spectrum of the gellan gum/gellan microspheres crosslinked with copper (figure 29) and the spectrum of microspheres crosslinked with copper after the binding step (figure 30).

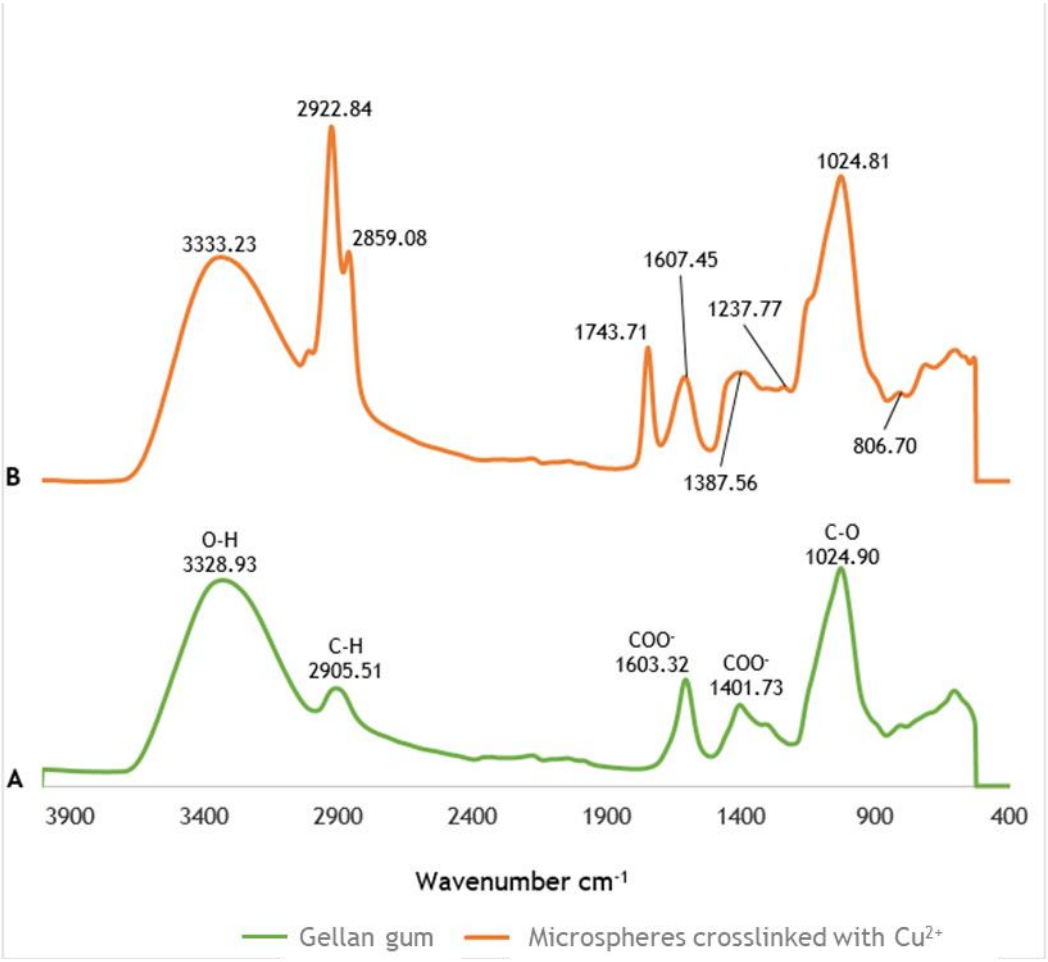

Figure 29 - FTIR spectra: A - Gellan gum spectrum; B - Microspheres crosslinked with Cu^{2+} spectrum.

The gellan gum spectrum (figure 29-A) shows a characteristic peak at 3328.93 cm^{-1} due to the stretching vibration of hydroxyl groups (-OH) existing in the glucopyranose ring, it also has a band at 2900.51 cm^{-1} which is attributed to the stretching vibration of –CH2 group. The bands at 1603.32 cm^{-1} and 1401.73 cm^{-1} are assigned to the presence of carboxylate anions (COO^-). The peak at 1024,90 cm^{-1} is due to the C-O stretching (Dhanka, Shetty et al. 2018). According to Derun and co-workers, the copper sulfate FTIR spectrum shows characteristic peaks at 3114, 1667, 1067 and 860 cm^{-1} (E. Moroydor Derun 2014). The FTIR spectrum of copper-crosslinked gellan microspheres (Figure 29-B) demonstrates the same five characteristic peaks present in the gellan gum spectrum with small variations and one new peak at 1743.71 cm^{-1} which could suggest an interaction between gellan gum and copper.

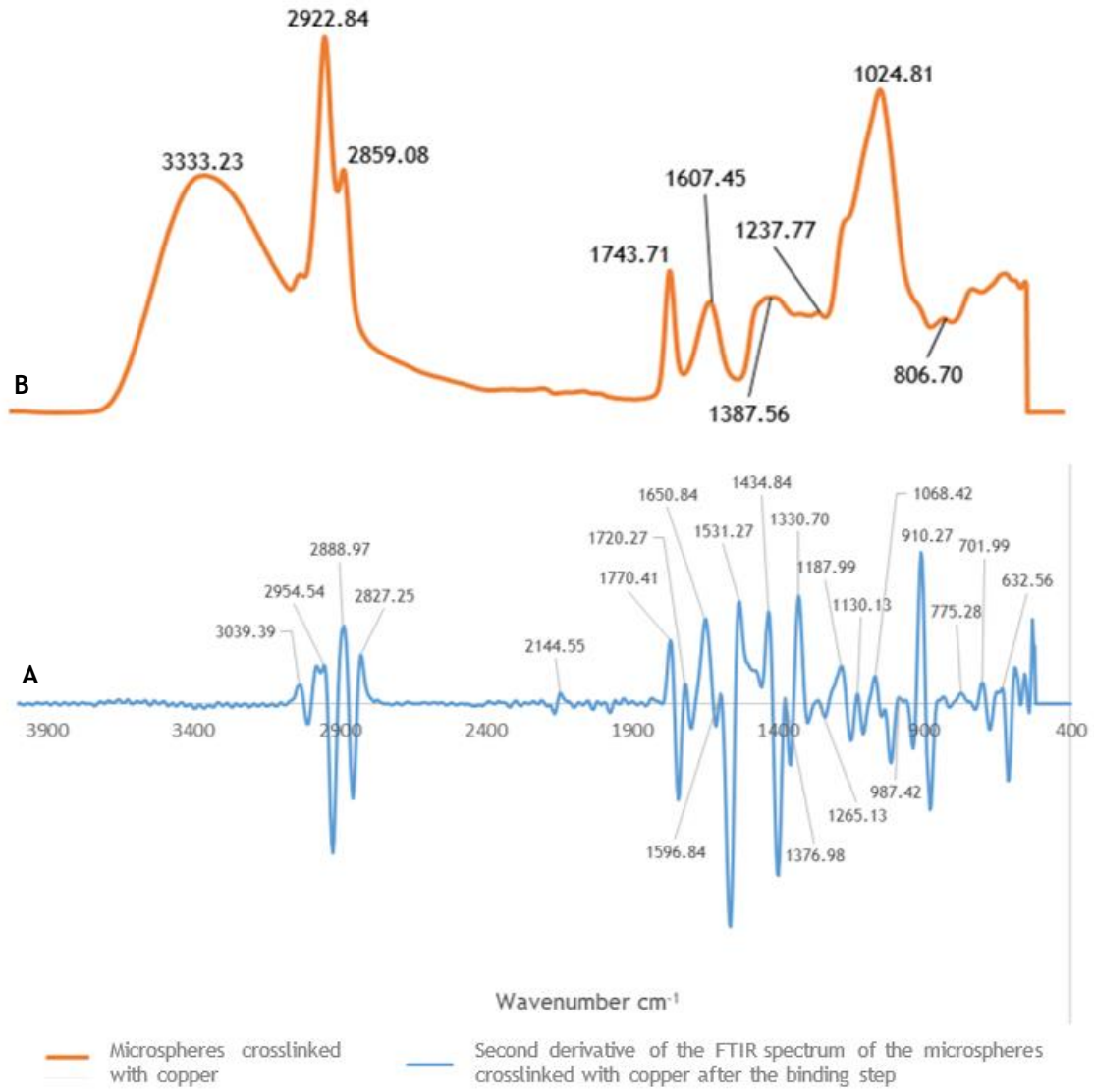

Figure 30 - FTIR spectra: A – Second derivative of the FTIR spectrum of the microspheres crosslinked with copper after the binding step; B - Microspheres crosslinked with Cu^{2+} spectrum.

It was also performed the FTIR analysis of the copper-crosslinked microspheres after the binding step in order to understand if the pDNA would interact with the microspheres. However, the information of the original spectrum was not very clear, so in figure 30-A is represented the second derivative of this FTIR spectrum which improves the resolution (Lucimara A. Forato 1997) and allows a higher precision of the characteristic spectral of the groups (Leal 2018). Thus, it is possible to obtain a more detailed identification of small and close lying absorption peaks, which are not resolved in the original spectrum (Rieppo, Saarakkala et al. 2012). The FTIR spectrum of the second derivative presents the same characteristic peaks as the one of copper-crosslinked microspheres, so the presence of new peaks, especially in the region of the 1800-1500 cm^{-1} can indicate an interaction with pDNA. According to Charak and Mehroka and also to Zaman and co-workers, the adsorption peaks between 1531.27 cm^{-1} and 1770.41 cm^{-1} are assigned to nitrogenated bases of plasmid, purines and pyrimidines, (Charak and Mehrotra

2013, Zaman, Arif et al. 2017). Specifically, the peaks at 1720.27 cm^{-1}, 1650.84 cm^{-1}, and 1596.84 cm^{-1} could be due, respectively, to the presence of guanine, thymine and adenine. Moreover, this FTIR spectrum presents a peak at 987.42 cm^{-1} that is indicative of the DNA existence (Mohsen 2011). So, it seems that the plasmid is capable of establishing interactions with the copper-crosslinked microspheres.

4.2.2.3 SEM analysis

The morphology and geometry of copper-crosslinked gellan microspheres were evaluated through SEM. Figure 31 illustrates the SEM images captured at different degrees of magnification.

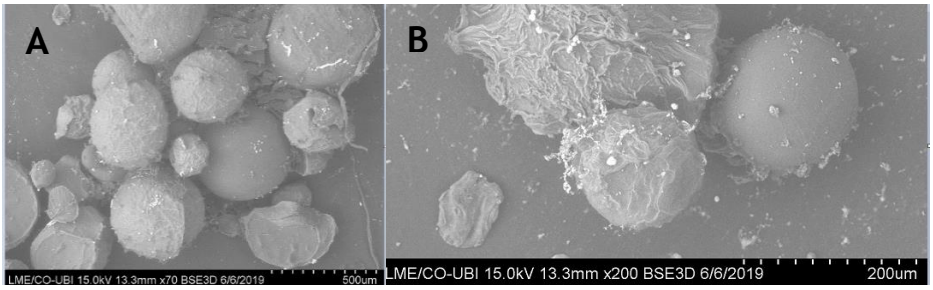

Figure 31 - Representation of the copper-crosslinked gellan microspheres, visualized in SEM at a magnification of x70 (A) and x200 (B).

Considering the SEM images, the copper-crosslinked gellan microspheres are spherical in shape and present a consistent structure, in which most have small cavities at the surface. The rough surface morphology can be associated with the cavities found in the surface of the microspheres (Coelho, Eusebio et al. 2019). Although the microspheres present a rough surface, it has no sharps edges, which diminishes the occurrence of the "egg-beater effect" during the batch method (Hlady 1999). The microspheres do not have inner pores which suggest that the binding of the target molecule will only occur with the surface of the microspheres. Moreover, the morphology described by (Narkar, Sher et al. 2010) for the gellan microspheres produced by ionotropic gelation method using $CaCl_2$ as a crosslinker is very similar to the one observed in figure 31.

4.2.2.4 EDX analysis

Copper-crosslinked gellan microspheres after SEM analysis were examined through energy-dispersive X-ray spectroscopy (EDX) in order to identify the principal elements and also to confirm the presence of the crosslinker, copper. The results are represented in table 13, in which are expressed in normalized concentration by weight percentage of each element (C norm. [wt. %]), in atomic concentration by atomic percentage of each element (C Atom. [at. %]) and there is also represented the error related to the weight percentage at the 2 Sigma level (C Error (2 sigma) [wt. %]).

Table 13 - Chemical characterization of gellan microspheres crosslinked with copper through EDX.

Element	C norm. [wt. %]	C Atom. [at. %]	C error (2 sigma) [wt. %]
Carbon	38.64	48.63	9.56
Oxygen	52.03	49.15	12.45
Copper	9.33	2.22	0.78
Total	100.00	100.00	

According to the elementary analysis, the copper-crosslinked gellan microspheres have two major constituents, carbon and oxygen, which was expected since gellan gum is a polysaccharide constituted by a tetrasaccharide unit of two residues of ß-D-glucose, one of ß-D-glucuronate and one of α-L-rhamnose (Prajapati, Jani et al. 2013). Moreover, the microspheres reinforcement was proven successful since it was found 9.33 % of copper in the copper-crosslinked microspheres.

4.2.2.5 Global charge analysis through zeta potential

The zeta potential was measured through Zetasizer Nano ZS, evaluating the global charge of the copper-crosslinked gellan microspheres. Thus, 1 mL of the gellan microspheres were placed in a folded capillary cell and it was prepared 3 replicates. The obtained values for the copper-crosslinked gellan microspheres vary from -3 mV to -7 mV, indicating that although microspheres are reinforced with copper, the global charge is negative, which it was expectable as gellan gum is an anionic polymer presenting a zeta potential between -25 mV and -35 mV (Coelho, Eusebio et al. 2019).

4.2.3 Study of the impurities influence by analysis of a pre-clarified *E. coli* lysate

The 3rd assay aimed to verify if impurities present in the *E. coli* lysate, such as proteins and RNA, could interfere in the interaction of pDNA with the transition metal ion. In this way, the *E. coli* lysate was clarified by precipitation with 2.5 M ammonium sulfate. The supernatant was recovered and desalted by passing through PD-10 desalting columns to perform the total protein quantification in order to understand if the protein content decreased in comparison to the crude lysate. These results are presented in table 14.

Table 14 - Total protein amount of the crude E. coli lysate from 1st assay and of E. coli lysate precipitated with 2.5 M ammonium sulfate from the 3rd assay.

Samples	[protein] (µg/mL)	Protein amount (µg)
Crude *E. coli* lysate (binding solution) (1st assay)	6046.67	1209.33
E. coli lysate precipitated with 2.5 M ammonium sulfate (3rd assay)	4468.89	893.77

In fact, the lysate precipitated with ammonium sulfate has a lower protein content than the crude lysate (893.77 µg and 1203 µg, respectively), which can facilitate the interaction of pDNA with copper ions during the capture procedure. Thus, 3rd assay was performed applying the same steps described previously and the recovered supernatants were analyzed by agarose gel electrophoresis as shown in figure 32.

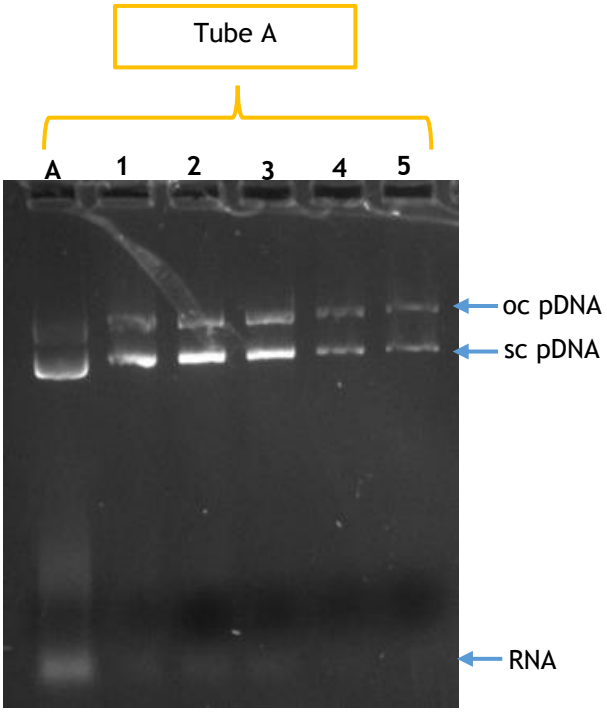

Figure 32 - Agarose gel electrophoresis of the supernatants recovered from the 3rd assay (20 mL of copper-crosslinked gellan microspheres and 10 mL of E. coli lysate precipitated with 2.5 M ammonium sulfate). A – E. coli lysate treated with ammonium sulfate; 1 – E. coli lysate that did not bind to the gellan microspheres; 2 – Washing with 10 mM MES, pH 5.2; 3 – first elution of E. coli lysate with 10 mM Tris, 1 mM EDTA, 200 mM NaCl pH 8.0; 4 – Washing with 10 mM Tris, 1 mM EDTA, 200 mM NaCl pH 8.0; 5 – final elution of E. coli lysate with 10 mM Tris, 1 mM EDTA, 1 M NaCl pH 8.0

In figure 32, it is noticeable that the precipitation of the *E. coli* lysate with 2.5 M ammonium sulfate also causes a decrease in the RNA content, especially in the RNA of high molecular weight, and it seems that this strategy allows the binding and elution of higher amount sc pDNA than in the previous assays. Due to the presence of ammonium sulfate in the lysate sample and in the supernatant of pDNA elution with 200 mM NaCl, these samples were desalted through PD-10 desalting columns once it could interfere with the analysis performed in the analytical column. The results of this 3rd assay are presented in table 15, as well as, the results of the 1st assay since it was applied the same conditions in the binding and elution steps.

Table 15 – Assessment of the sc pDNA concentration, total sc pDNA amount, percentage of recovery and purity percentage of the E. coli lysate precipitated with ammonium sulfate and the supernatant from the sc pDNA elution with 200 mM NaCl (n = 2) of the 3rd assay and comparison with the crude E. coli lysate and the sc pDNA elution of the 1st assay.

Samples	[sc pDNA] (µg/mL)	Total sc pDNA amount (µg)	Recovery Percentage (%)	Purity Percentage (%)
E. coli lysate precipitated with 2.5 M ammonium sulfate (3rd assay)	7.90	79.0	-	11.67
Elution of sc pDNA with 200 mM NaCl in 10 mM Tris-EDTA, pH 8.0 (3rd assay)	2.56	25.6	32.41	12.43
E. coli lysate (binding solution) (1st assay)	8.65	86.5	-	3.66
Elution of sc pDNA with 200 mM NaCl in 10 mM Tris-EDTA, pH 8.0 (1st assay)	1.35	13.5	15.61	2.42

The elimination/reduction of impurities like RNA, endotoxins, and proteins could be achieved by the lysate precipitation with chaotropic salts, such as ammonium sulfate (Alex Xenopoulos 2014). So, the *E. coli* lysate was precipitated with this salt in order to understand if the impurities interfered in the pDNA interaction with the copper ion. The results present in table 15 suggest that some sc pDNA was precipitated with the ammonium sulfate since the initial concentration of sc pDNA in the lysate decreases from 8.65 µg/mL to 7.90 µg/mL. However, the reduction of impurities in the lysate due to the precipitation with ammonium sulfate, such as proteins and RNA, allowed the binding and consequently the elution of higher amount of sc pDNA from 13.5 µg to 25.6 µg, which was reflected in the recovery percentage from 15.61 % to 32.41 %. In addition, in this 3rd assay, the purity percentage also increased from 2.42 % to 12.43 % once that its calculation considers the impurities present in the lysate. These results confirmed that mainly RNA and proteins affect the interaction between pDNA and the copper ion.

4.2.4 Study of the pDNA capture through functionalized microspheres

The 4th assay was performed using copper-crosslinked microspheres and functionalized with PEI in order to study the effect of microspheres surface functionalization with positive groups in the capture of plasmid DNA from the *E. coli* lysates. After the copper-crosslinked gellan microspheres production it was added 6.15 % of branched PEI 25 kDa in 0.1 M sodium acetate pH 4.5, under constant stirring for 2 h. PEI is a cationic polymer that contains primary, secondary, and tertiary amines in their backbone (Pandey and Sawant 2016), so with the PEI addition it can be possible that the surface charge of the microspheres becomes positive. The zeta potential of PEI-functionalized microspheres was analyzed and indicated an overall charge

between -3 mV and +10 mV, which confirms that the polycation addition increases the charge of gellan microspheres to positive, due to the presence of amino groups (Hu, Hu et al. 2015). It was also studied the influence of the pH in the zeta potential of the microspheres functionalized with PEI, since the amino groups of PEI could be or not protonated depending on the buffer pH (Antila, Harkonen et al. 2015). In figure 33 it is represented the microspheres zeta potential obtained for different pH values.

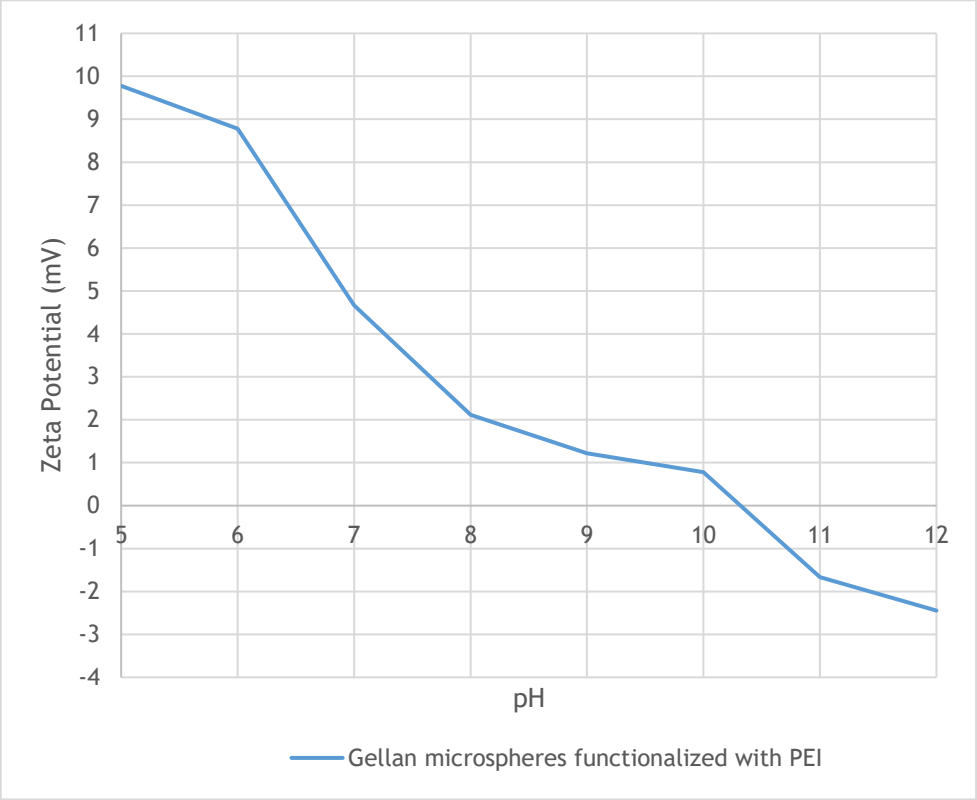

Figure 33 – Zeta potential of the PEI-functionalized microspheres at different pH values.

The surface charge of the PEI-functionalized microspheres is positive in the pH range of 5 – 10, being more positive to lower pH, and at higher pH value, i.e., 10.5 < pH < 12, the surface shifts to negative charge. These results can be attributed to PEI composition, mostly due the presence of amino groups and also to its pKa, which is around 7.9-9.6 (Virgen-Ortíz, dos Santos et al. 2017). When the pH decreases from the pKa of PEI, the [H^+] increases, resulting in the protonation of the amino groups, which leads to a higher zeta potential of the microspheres (Hu, Hu et al. 2015). In addition, these results suggest that the surface charge of the PEI-functionalized gellan microspheres at a pH range of 5 - 8 is favorable for DNA interaction and the application of higher pH can favor the DNA desorption.

Thus, this 4th assay was performed using a pH around 5.0 for the binding step and the elution was achieved with an increment of NaCl concentration in 10 mM Tris-HCl, 1mM EDTA pH 10.5. The pH in the elution buffer was changed to 10.5, once that at this pH the microspheres present neutral/negative charge, which can facilitate the DNA desorption by diminishing the

electrostatic attraction between the PEI and the DNA (Sun, Zhu et al. 2010). The supernatants recovered from the 4th assay were treated with sodium heparin (25 000 UI) and exposed for 1h at 60ºC to allow the pDNA decomplexation from PEI and also its analysis in agarose gel electrophoresis, figure 34.

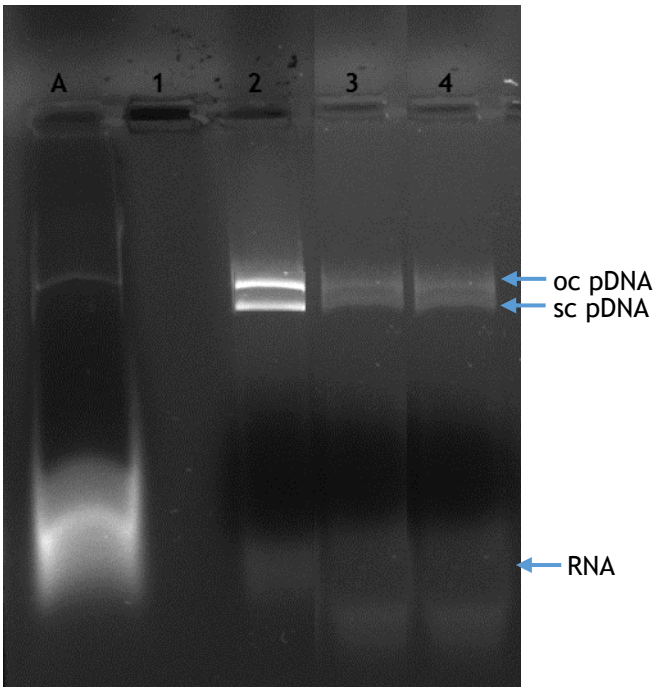

Figure 34 - Agarose gel electrophoresis of the supernatants recovered from the 4th assay (20 mL of PEI-functionalized gellan microspheres and 10 mL of E. coli lysate. A – E. coli lysate; 1 – E. coli lysate that did not bind to the gellan microspheres; 2 – first elution of E. coli lysate with 10 mM Tris, 1 mM EDTA, 200 mM NaCl pH 10.5; 3 – second elution of E. coli lysate with 10 mM Tris, 1 mM EDTA, 300 mM NaCl pH 10.5; 4 – final elution of E. coli lysate with 10 mM Tris, 1 mM EDTA, 1 M NaCl pH 10.5.

Considering the figure 34, it is possible to notice that in lane 1 was not detected pDNA or RNA, which suggests that at pH 5.0 all the nucleic acids bound to the functionalized microspheres, which could be explained by the strong electrostatic attraction to the PEI present in the microspheres surface (Sun, Zhu et al. 2010). In the lanes 2 - 4 it was implemented several increasing NaCl concentrations (200 mM; 300 mM and 1 M) expecting the elution and separation of the binding nucleic acids. Although the major quantity of pDNA was eluted with 200 mM of NaCl (lane 2), it seems some co-elution of RNA. The *E. coli* lysate and the supernatant of pDNA elution with 200 mM NaCl were analyzed in the analytical column. The results of this 4th assay are presented in table 16, as well as, the results of the 1st assay and the 3rd assay in order to compare the purity degree and the recovery percentage of the eluted pDNA.

Table 16 - Assessment of the sc pDNA concentration, total sc pDNA amount, percentage of recovery and purity percentage of the E. coli lysate and the supernatant from the sc pDNA elution with 200 mM NaCl (n = 2) of the 4th assay and comparison with the pDNA elution of the 1st assay and of the 3rd assay.

Samples	[sc pDNA] (µg/mL)	Total sc pDNA amount (µg)	Recovery Percentage (%)	Purity Percentage (%)
E. coli lysate (binding solution)	8.65	86.5	-	3.66
Elution of sc pDNA with 200 mM NaCl in 10 mM Tris-EDTA, pH 8.0 (1st assay)	1.35	13.5	15.61	2.42
Elution of sc pDNA with 200 mM NaCl in 10 mM Tris-EDTA, pH 8.0 (3rd assay)	2.56	25.6	32.41	12.43
Elution of sc pDNA with 200 mM NaCl in 10 mM Tris-EDTA, pH 10.5 (4th assay)	**3.81**	**76.2**	**88.09**	**3.18**

According to table 16, the higher amount of eluted pDNA (76.2 µg) was achieved in the 4th assay in which the microspheres were functionalized with PEI and corresponds to 88.09 % of the recovered pDNA. Since all the nucleic acids were retained in the binding step (lane 1 of figure 34) the remaining 12 % of pDNA was eluted in the subsequent elution steps with 300 mM and 1 M of NaCl (lanes 3 and 4 of figure 34). This significant improvement of the pDNA capture could be explained by the presence of amino groups in the surface of functionalized microspheres responsible to promote stronger electrostatic interactions with the pDNA (Sun, Zhu et al. 2010). However, a decrease in the purity percentage of the pDNA (3.18 %) was obtained in comparison to the 3rd assay (12.43 %), since PEI amino groups strongly retain the pDNA and also the RNA. In comparison with the pDNA eluted in the 1st assay (copper-crosslinked microspheres), the microspheres functionalized with PEI show a great improvement in the recovery percentage (15.61 % to 88.09 %) and also a slight increase in the purity degree (2.42 % to 3.18 %). Regarding the satisfactory improvement of pDNA capture with the PEI-functionalized gellan microspheres, it was performed their characterization in terms of mean diameter, stability, chemical composition, and morphology.

4.2.5 Characterization of PEI-functionalized gellan microspheres

The copper-crosslinked microspheres have light blue color due to the presence of copper ion and when the PEI was added to the microspheres, the color changed to dark blue as can be seen in figure 35. PEI is composed of amino groups and since it was dissolved in 0.1 M sodium acetate buffer pH 4.5, the amino groups are positively charged. So, the blue dark color of the PEI-functionalized microspheres could be attributed to the formation of a coordinate bond between the copper ion and the amino groups (Dong, Du et al. 2019) and also by the influence of the pH in this crosslinking reaction.

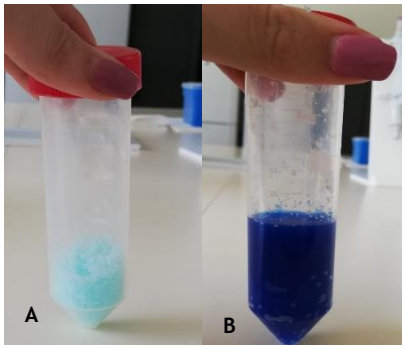

Figure 35 - Image of (A) microspheres crosslinked with copper and (B) microspheres functionalized with PEI.

The PEI-functionalized gellan microspheres were analyzed in the semiotic microscope in order to determine the mean diameter. So, it was taken 5 snaps and the respective diameter measures. Figure 36 is an example of a snap obtained in the semiotic microscope after the production of each formulation of the microspheres.

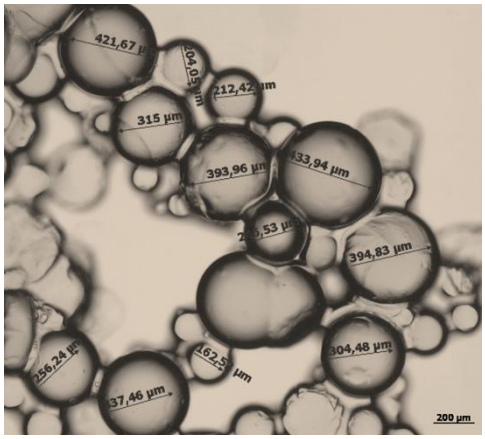

Figure 36 – Image of PEI-functionalized gellan microspheres after its production obtained in the semiotic microscope (5x).

The mean diameter of the microspheres functionalized with PEI is about 304.40 ± 27.59 µm. In general, the microspheres present a round shape, so the water-in-oil emulsion allows a suitable formulation of the microspheres. The PEI-functionalized gellan microspheres have an inferior diameter when compared with the microspheres crosslinked with copper (365.34 ± 17.24 µm) which could be attributed to an effective charge interaction between gellan gum and PEI or to

the chemical coordination effects between copper ion and PEI, resulting in a more compact structure (Patnaik, Arif et al. 2010, Wang, Yang et al. 2019).

4.2.5.1 Gellan microspheres stability analysis

The microspheres stability was studied over time, through evaluation of the mean diameter in the semiotic microscope, mainly, after its production 0, 3, 10 and 20 days. Among the analyzed samples, 5 snaps were taken for each day and the mean diameter was calculated. Figure 37 shows an example of the measures made for the PEI-functionalized microspheres. Table 17 summarizes the mean diameters obtained from the 5 snaps (n = 5) for each sample over time.

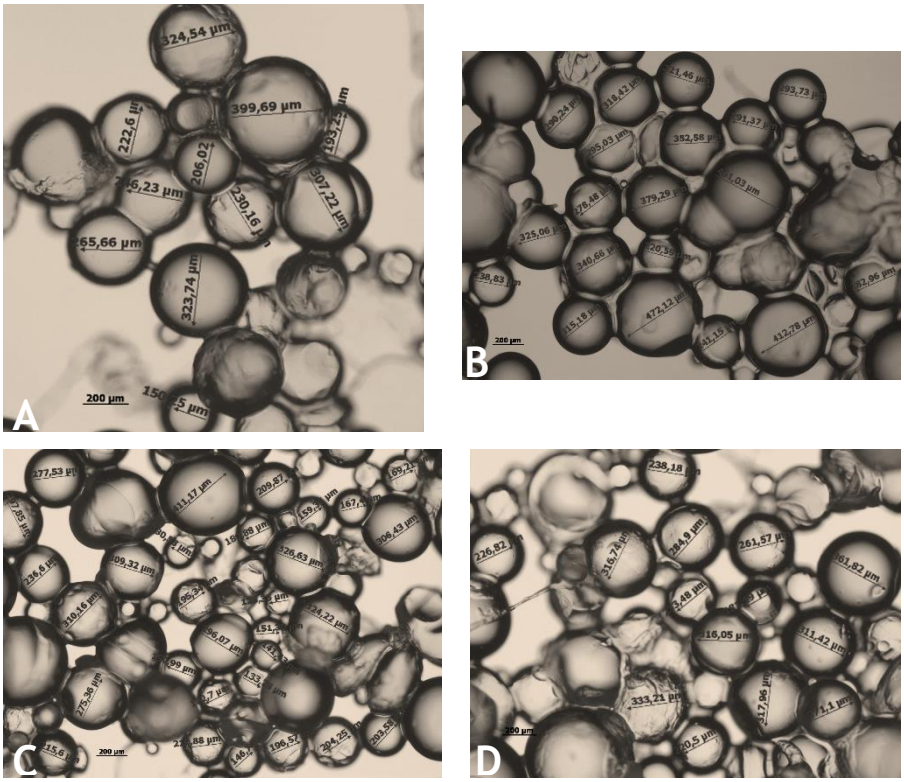

Figure 37 - Images of the PEI-functionalized gellan obtained in the semiotic microscope (5x). A – Snap taken at 0 days; B - Snap taken at 3 days; C - Snap taken at 10 days; D - Snap taken at 20 days.

Table 17 – PEI-functionalized gellan microspheres mean diameter considering the stability over time (n=5).

Days	Mean diameter (µm ± SD)
0	304.40 ± 27.59
3	284.34 ± 28.87
10	257.34 ± 23.88
20	253.37 ± 16.09

In agreement with figure 37 and table 17 the microspheres mean diameter diminishes over time, as reported in the stability analysis of the copper-crosslinked gellan microspheres. This might be attributed to the disintegration of the biggest microspheres over time, only remaining intact the smallest ones, probably due to the swelling phenomenon (Coelho, Eusebio et al. 2019). Nevertheless, there are a lot of microspheres with uniform size, which suggest that in these formulation conditions, the microspheres stability is higher than 20 days.

4.2.5.2 SEM analysis

The morphology and geometry of PEI-functionalized gellan microspheres were evaluated through SEM. Figure 38 illustrates the SEM images captured at different degrees of magnification of the PEI-functionalized gellan microspheres.

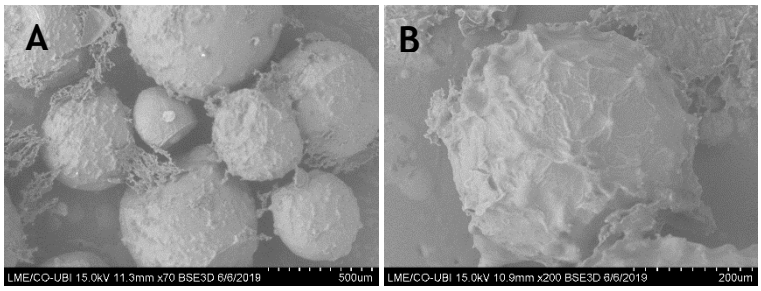

Figure 38 - Representation of the PEI-functionalized gellan microspheres, visualized in SEM at a magnification of x70 (A) and x200 (B).

Considering the SEM images, the PEI-functionalized gellan microspheres are very similar in terms of morphology to the copper-crosslinked gellan microspheres. They present a spherical shape and a consistent structure, in which most have cavities at the surface. In addition, they also have a rough surface morphology but with no sharps edges, which diminishes the occurrence of the "egg-beater effect" during the batch method (Hlady 1999). The microspheres do not have inner pores, suggesting that the binding of the target molecule will only occur with the surface of the microspheres.

4.2.5.3 EDX analysis

After SEM analysis, PEI-functionalized gellan microspheres were examined through energy-dispersive X-ray spectroscopy (EDX) in order to identify the principal elements and also to confirm the presence of nitrogen from the amino groups of PEI. The results are presented in table 18, in which are expressed in normalized concentration by weight percentage of each element (C norm. [wt. %]), in atomic concentration by atomic percentage of each element (C Atom. [at. %]) and there is also represented the error related to the weight percentage at the 2 Sigma level (C Error (2 sigma) [wt. %]).

Table 18 - Chemical characterization of PEI-functionalized gellan microspheres through EDX.

Element	C norm. [wt. %]	C Atom. [at. %]	C error (2 sigma) [wt. %]
Carbon	41.17	47.43	9.34
Oxygen	41.21	35.64	9.68
Nitrogen	16.99	16.79	4.73
Copper	0.62	0.13	0.13
Total	100.00	100.00	

According to the elementary analysis, PEI-functionalized gellan microspheres have two major components, carbon and oxygen, that is already expected since gellan gum is a polysaccharide constituted by a tetrasaccharide unit of two residues of ß-D-glucose, one of ß-D -glucuronate and one of α-L-rhamnose (Prajapati, Jani et al. 2013). PEI is a synthetic polymer with a large number of reactive groups, such as primary, secondary, and tertiary amines (Wang, Yang et al. 2019), so the presence of 17 % of the nitrogen in the PEI-microspheres confirms its functionalization. Nevertheless, it is shown a reduction of copper percentage from 9.33 % (present in the copper-crosslinked microspheres) to 0.62 %, which can be explained by the formation of a coordinated bond between copper ion present in gellan microspheres and the lone pair electrons from the nitrogen atoms of the PEI polymer (Ben El Ayouchia, ElMouli et al. 2019, Dong, Du et al. 2019).

Chapter 5 - Conclusions and future perspectives

Nowadays, the number of patients with diseases caused by viral or bacterial infections has been increasing all over the world. So, it is necessary to develop new strategies that could overcome the limitations of the prophylactic vaccines, thereby answering this problematic. In this way, the DNA vaccines seem to be promising, once they allow the prevention and treatment of diseases and are more safe and effective than the conventional vaccines. The process to obtain a pure DNA vaccine has a high cost to the pharmaceutical industry and an associated environmental impact due to the use of high amounts of chaotropic salts and organic solvents. The batch method is very simple, fast and can be used as an alternative method to capture pDNA since it has the advantage of allowing different materials to be used in particle production. Gellan gum is an anionic exopolysaccharide with great properties, is highly applied in several industries and also has the ability to form strong gels in the presence of divalent cations. Therefore, the aim of this work was to develop a new strategy to capture pDNA from *E. coli* lysates by applying gellan microspheres through the batch method.

Thus, gellan microspheres were produced by a water-in-oil emulsion and reinforced with copper, in which some were also functionalized with PEI. Both formulations present microspheres with spherical shape and consistent structure. Nevertheless, the microspheres functionalized with PEI have a minor diameter in comparison with the copper-crosslinked microspheres, which could be attributed to the coordination bond that could occur between copper and PEI leading to a more compact structure. This structural rearrangement can also explain the elementary composition of the microspheres, once that the microspheres functionalized with PEI have 17 % of amines and only 0.62 % of copper, while the copper-crosslinked microspheres have 9 % of copper. The global surface charge is higher when the microspheres were functionalized with PEI (+ 5 mV) in comparison with the copper-crosslinked microspheres (- 5 mV). This difference could be due to the presence of the amino groups from the PEI.

The capture strategy of pDNA by gellan microspheres without functionalization can occur by interactions with metal ions, mimic the IMAC principles. So, the gellan microspheres were crosslinked with different metal ions and explored in the batch method, in order to understand which one allowed a higher recovery of pDNA. The copper ion used as a crosslinker of gellan microspheres showed to be more adequate to pDNA capture and the best strategy allowed recovery of 15.61 % of pDNA with a purity degree of 2.42 %. The binding step was performed at

pH 5.0, since most of proteins are positively charged, which interact with the gellan negative polymer, avoiding the competition with the pDNA by the interaction with copper ions (positively charged). The elution step was performed at pH 8.0, once it seems to favor the pDNA elution, maintaining proteins bound to the gellan microspheres. Another strategy was developed in order to increase the recovery percentage of pDNA, in which the *E. coli* lysate was clarified by ammonium sulfate precipitation. This precipitation allowed the elimination of RNA of high molecular weight and some proteins, improving the pDNA capture strategy by the increment in the recovery percentage to 32.41 % and also in the purity percentage to 12.43 %, indicating that the impurities affect/compete by the interaction between pDNA and the copper ion. Moreover, it was also developed microspheres functionalized with PEI, to achieve better recovery of pDNA, once the global surface charge shifted to positive. The binding step was promoted at the same pH, around 5.0, but the elution step was performed with pH around 10.5 because the microspheres functionalized with PEI present neutral/negative charge at this pH, which can favor the pDNA elution. This strategy allowed a great improvement of the pDNA recovery to 88.09 %, but only with 3.18 % of purity, which indicates that this operation mode is not selective since it allows the RNA and pDNA binding to the microspheres. The gellan microspheres demonstrated that they can be applied in pDNA capture from crude *E. coli* lysates, without the need to use organic solvents, once they increased the pDNA percentage from 1.07% to 15.61 % or 88.09 %. So, if the main purpose is the total pDNA capture from crude lysates without using salts or organic solvents, the strategy with PEI-functionalized gellan microspheres showed great potential. On the other hand, if the main objective is to capture pDNA with higher purity, it is recommended to perform a previous clarification step with ammonium sulfate prior to capture procedure, where copper-crosslinked microspheres may be applied or also the ones functionalized with PEI.

In the future, it would be interesting to functionalize the gellan microspheres with PEI by covalent interactions through chemical synthesis, since by electrostatic interactions present some limitations being lost PEI ligands through the binding and elution steps. It will also be curious to explore if it would be possible to purify the pDNA obtained from the batch method with a single chromatographic step.

Chapter 6 – Bibliography

Abbas, Z. and S. Marihal (2014). "Gellan gum-based mucoadhesive microspheres of almotriptan for nasal administration: Formulation optimization using factorial design, characterization, and in vitro evaluation." J Pharm Bioallied Sci **6**(4): 267-277.

Abdelhamid Elaissari, C. P., Thierry Delair, Philippe Cros, and Robin Kiirfurstt (1995). "Adsorption and Desorption Studies of Polyadenylic Acid onto Positively Charged Latex Particles." Langmuir **11**(4): 1261-1267.

Abdulrahman, A. and A. Ghanem (2018). "Recent advances in chromatographic purification of plasmid DNA for gene therapy and DNA vaccines: A review." Anal Chim Acta **1025**: 41-57.

Aguero, L., D. Zaldivar-Silva, L. Pena and M. L. Dias (2017). "Alginate microparticles as oral colon drug delivery device: A review." Carbohydr Polym **168**: 32-43.

Aires-Barros, M. R. and A. M. Azevedo (2017). Fundamentals of Biological Separation Processes. Current Developments in Biotechnology and Bioengineering**:** 187-237.

Alex Xenopoulos, P. P. (2014). "Production and purification of plasmid DNA vaccines: is there scope for further innovation?" Expert Review of Vaccines **13**(12): 1537–1551.

Anastassopoulou, J. (2003). "Metal–DNA interactions." Journal of Molecular Structure **651-653**: 19–26.

Andreou, L. V. (2013). "Isolation of plasmid DNA from bacteria." Methods Enzymol **529**: 135-142.

Antila, H. S., M. Harkonen and M. Sammalkorpi (2015). "Chemistry specificity of DNA-polycation complex salt response: a simulation study of DNA, polylysine and polyethyleneimine." Phys Chem Chem Phys **17**(7): 5279-5289.

Armando Tejeda-Mansir, R. M. M. (2008). "Upstream Processing of Plasmid DNA for Vaccine and Gene Therapy Applications." Recent Patents on Biotechnology **2**(3): 156-172.

Babiuk, S. B., Hani (2014). DNA Vaccines. Reference Module in Biomedical Sciences-Diagnosis and Treatment of Viral Diseases. M. Caplan, Elsevier Inc**:** 1-5.

Baumann, P. and J. Hubbuch (2017). "Downstream process development strategies for effective bioprocesses: Trends, progress, and combinatorial approaches." Engineering in Life Sciences **17**(11): 1142-1158.

BeMiller, J. N. (2019). Gellans, Curdlan, Dextrans, Levans, and Pullulan. Carbohydrate Chemistry for Food Scientists. J. N. BeMiller, Elsevier Inc.**:** 271-278.

Ben El Ayouchia, H., H. ElMouli, L. Bahsis, H. Anane, R. Laamari, C. J. Gómez-García, M. Julve and S.-E. Stiriba (2019). "Hyperbranched polyethylenimine-supported copper(II) ions as a macroliganted homogenous catalyst for strict click reactions of azides and alkynes in water." Journal of Organometallic Chemistry **898**: 120881.

Besnard, L., V. Fabre, M. Fettig, E. Gousseinov, Y. Kawakami, N. Laroudie, C. Scanlan and P. Pattnaik (2016). "Clarification of vaccines: An overview of filter based technology trends and best practices." Biotechnol Adv **34**(1): 1-13.

Bhattacharya, S. S., S. Banerjee, P. Chowdhury, A. Ghosh, R. R. Hegde and R. Mondal (2013). "Tranexamic acid loaded gellan gum-based polymeric microbeads for controlled release: in vitro and in vivo assessment." Colloids Surf B Biointerfaces **112**: 483-491.

Biswas, M., S. R. P. Kumar, C. Terhorst and R. W. Herzog (2018). "Gene Therapy With Regulatory T Cells: A Beneficial Alliance." Front Immunol **9**: 554.

Blom, H., M. Bennemo, M. Berg and R. Lemmens (2010). "Flocculate removal after alkaline lysis in plasmid DNA production." Vaccine **29**(1): 6-10.

Bolanos-Garcia, V. M. and O. R. Davies (2006). "Structural analysis and classification of native proteins from E. coli commonly co-purified by immobilised metal affinity chromatography." Biochim Biophys Acta **1760**(9): 1304-1313.

Bower, D. M. and K. L. Prather (2009). "Engineering of bacterial strains and vectors for the production of plasmid DNA." Appl Microbiol Biotechnol **82**(5): 805-813.

Carson, S., H. B. Miller, D. S. Witherow and M. C. Srougi (2019). Lab Session 2 - Purification and Digestion of Plasmid (Vector) DNA. Molecular Biology Techniques. H. B. M. Susan Carson, D. Scott Witherow, Melissa C. Srougi, Elsevier Inc**:** 13-22.

Carter, M. and J. Shieh (2015). Gene Delivery Strategies. Guide to Research Techniques in Neuroscience**:** 239-252.

Chakraborty, S., S. Jana, A. Gandhi, K. K. Sen, W. Zhiang and C. Kokare (2014). "Gellan gum microspheres containing a novel alpha-amylase from marine Nocardiopsis sp. strain B2 for immobilization." Int J Biol Macromol **70**: 292-299.

Charak, S. and R. Mehrotra (2013). "Structural investigation of idarubicin-DNA interaction: spectroscopic and molecular docking study." Int J Biol Macromol **60**: 213-218.

Chunsheng, H., Z. Qinglin, L. Yuxin, C. Xiaochen, W. Yanliang, Z. Tong and W. Zuze (2011). "A continuous cell alkaline lysis, neutralization, and clarification combination process for production of plasmid pUDK-HGF." Biotechnol Appl Biochem **58**(3): 162-165.

Coelho, J., D. Eusebio, D. Gomes, F. Frias, L. A. Passarinha and A. Sousa (2019). "Biosynthesis and isolation of gellan polysaccharide to formulate microspheres for protein capture." Carbohydr Polym **220**: 236-246.

Deshmukh, N. R. and A. M. Lali (2005). "Adsorptive purification of pDNA on superporous rigid cross-linked cellulose matrix." J Chromatogr B Analyt Technol Biomed Life Sci **818**(1): 5-10.

Dhanka, M., C. Shetty and R. Srivastava (2018). "Methotrexate loaded gellan gum microparticles for drug delivery." Int J Biol Macromol **110**: 346-356.

Diogo, M. M., J. A. Queiroz and D. M. Prazeres (2005). "Chromatography of plasmid DNA." J Chromatogr A **1069**(1): 3-22.

Dochez, C., J. J. Bogers, R. Verhelst and H. Rees (2014). "HPV vaccines to prevent cervical cancer and genital warts: an update." Vaccine **32**(14): 1595-1601.

Don J. Brenner, G. R. F., Adrian V. Rake, and Karl E. Johnson (1969). "Batch Procedure for Thermal Elution of DNA from Hydroxyapatite." Analytical Biochemistry **28**: 447-459.

Dong, J., Y. Du, R. Duyu, Y. Shang, S. Zhang and R. Han (2019). "Adsorption of copper ion from solution by polyethylenimine modified wheat straw." Bioresource Technology Reports **6**: 96-102.

Dunbar, C. E., K. A. High, J. K. Joung, D. B. Kohn, K. Ozawa and M. Sadelain (2018). "Gene therapy comes of age." Science **359**(6372): eaan4672.

Durzynska, J., K. Lesniewicz and E. Poreba (2017). "Human papillomaviruses in epigenetic regulations." Mutat Res Rev Mutat Res **772**: 36-50.

E. Moroydor Derun, N. T., F. T. Senberber, A. S. Kipcak, S. Piskin (2014). "The Optimization of Copper Sulfate and Tincalconite Molar Ratios on the Hydrothermal Synthesis of Copper Borates." International Journal of Chemical and Molecular Engineering **8**(10): 1152-1156.

Estevao, D., N. R. Costa, R. M. Gil da Costa and R. Medeiros (2019). "Hallmarks of HPV carcinogenesis: The role of E6, E7 and E5 oncoproteins in cellular malignancy." Biochim Biophys Acta Gene Regul Mech **1862**(2): 153-162.

Eva K. Lindskog, S. F., Till Wenger, Patrick Schulz, (2018). Section II - Upstream Processes Principles and Methods. Biopharmaceutical Processing: Development, Design, and Implementation of Manufacturing Processes. E. L. Günter Jagschies, Karol Łącki, Parrish Galliher, Elsevier Ltd.**:** 111-130.

Fan, Y., J. Yi, X. Hua, Y. Zhang and R. Yang (2017). "Preparation and characterization of gellan gum microspheres containing a cold-adapted beta-galactosidase from Rahnella sp. R3." Carbohydr Polym **162**: 10-15.

Fialho, A. M., L. M. Moreira, A. T. Granja, A. O. Popescu, K. Hoffmann and I. Sa-Correia (2008). "Occurrence, production, and applications of gellan: current state and perspectives." Appl Microbiol Biotechnol **79**(6): 889-900.

Foldvari, M., D. W. Chen, N. Nafissi, D. Calderon, L. Narsineni and A. Rafiee (2016). "Non-viral gene therapy: Gains and challenges of non-invasive administration methods." J Control Release **240**: 165-190.

Fu, K., D. W. Pack, A. M. Klibanov and R. Langer (2000). "Visual Evidence of Acidic Environment Within Degrading Poly(lactic-co-glycolic acid) (PLGA) Microspheres." Pharmaceutical Research **17**(1): 100-106.

G-Biosciences Plasmid Isolation (Alkaline Lysis) - Teacher's Guidebook.

Ghanem, A., R. Healey and F. G. Adly (2013). "Current trends in separation of plasmid DNA vaccines: a review." Anal Chim Acta **760**: 1-15.

Giacca, M. and S. Zacchigna (2012). "Virus-mediated gene delivery for human gene therapy." J Control Release **161**(2): 377-388.

Ginn, S. L., A. K. Amaya, I. E. Alexander, M. Edelstein and M. R. Abedi (2018). "Gene therapy clinical trials worldwide to 2017: An update." J Gene Med **20**(5): e3015.

Goncalves, A. I., L. A. Rocha, J. M. Dias, L. A. Passarinha and A. Sousa (2014). "Optimization of a chromatographic stationary phase based on gellan gum using central composite design." J Chromatogr B Analyt Technol Biomed Life Sci **957**: 46-52.

Grace Hampson, A. T., Steven D Pearson, William B Dreitlein & Chris Henshall (2018). "Gene therapy: evidence, value and affordability in the US health care system." Journal of Comparative Effectiveness Research **7**(1): 15-28.

Guilherme N.M. Ferreira, G. A. M., Duarte M.F. Prazeres and Joaquim M.S. Cabral (2000). "Downstream processing of plasmid DNA for gene therapy and DNA vaccine applications." Trends Biotechnol **18**(9): 380-388.

Gupta, S., P. Kumar and B. C. Das (2018). "HPV: Molecular pathways and targets." Curr Probl Cancer **42**(2): 161-174.

Hage, D. S. (2018). Chromatography. Principles and Applications of Clinical Mass Spectrometry. A. R. H. Nader Rifai, Carl T. Wittwer, Elsevier Inc.**:** 1-32.

Hage, D. S., J. A. Anguizola, C. Bi, R. Li, R. Matsuda, E. Papastavros, E. Pfaunmiller, J. Vargas and X. Zheng (2012). "Pharmaceutical and biomedical applications of affinity chromatography: recent trends and developments." J Pharm Biomed Anal **69**: 93-105.

Hasson, S. S. A. A., J. K. Z. Al-Busaidi and T. A. Sallam (2015). "The past, current and future trends in DNA vaccine immunisations." Asian Pacific Journal of Tropical Biomedicine **5**(5): 344-353.

Hlady, V., Buijs, J., Jennissen, P. H. (1999). Methods for Studying Protein Adsorption. Methods in Enzimology, Academic Press. **309:** 402-429.

Hobernik, D. and M. Bros (2018). "DNA Vaccines-How Far From Clinical Use?" Int J Mol Sci **19**(11): 3605.

Hu, L. L., B. Hu, L. M. Shen, D. D. Zhang, X. W. Chen and J. H. Wang (2015). "Polyethyleneimine-iron phosphate nanocomposite as a promising adsorbent for the isolation of DNA." Talanta **132**: 857-863.

Humans, H. P. I. W. G. o. t. E. o. C. R. t. (2007). IARC Monographs on the Evaluation of Carcinogenic Risks to Humans. **90**.

Hung, C. F., B. Ma, A. Monie, S. W. Tsen and T. C. Wu (2008). "Therapeutic human papillomavirus vaccines: current clinical trials and future directions." Expert Opin Biol Ther **8**(4): 421-439.

Ibraheem, D., A. Elaissari and H. Fessi (2014). "Gene therapy and DNA delivery systems." Int J Pharm **459**(1-2): 70-83.

Igor Tadeu Lazzarotto Bresolin, E. A. M., Sônia Maria Alves Bueno (2009). "Cromatografia de Afinidade por ions metálicos imobilizados (IMAC) de biomoléculas: Aspectos fundamentais e aplicações tecnológicas " Quimíca Nova **32**(5): 1288-1296.

Ishwar B. Bajaj, S. A. S., Parag S. Saudagar and Rekha S. Singhal (2007). "Gellan Gum: Fermentative Production, Downstream Processing and Applications." Food Technology. Biotechnology. **45**: 341–354.

Ishwar B. Bajaj, S. A. S., Parag S. Saudagar and Rekha S. Singhal (2007). "Gellan Gum: Fermentative Production, Downstream Processing and Applications." Food Technol. Biotechnol. **45**(4): 341–354.

Islas-Lugo, F., J. Vega-Estrada, C. A. Alvis, J. Ortega-Lopez and M. Del Carmen Montes-Horcasitas (2016). "Developing strategies to increase plasmid DNA production in Escherichia coli DH5alpha using batch culture." J Biotechnol **233**: 66-73.

J. Porath, P. E. R. F. (1959). "Gel filtration: a method for desalting and group separation." Nature **183**: 1657e1659.

J.Doly, H. C. B. a. (1979). "A rapid alkaline extraction procedure for screening recombinant plasmid DNA." Nucleic Acids Research **7**(6): 1513-1523.

Jason C. Murphy, D. L. J., Kristopher I. White, George E. Fox, and Richard C. Willson (2003). "Nucleic Acid Separations Utilizing Immobilized Metal Affinity Chromatography." Biotechnology Progress **19**: 982−986.

John Duguid, V. A. B., James Benevides, and George J. Thomas, Jr. (1993). "Raman Spectroscopy of DNA-Metal Complexes. 1. Interactions and Conformational Effects of the Divalent Cations: Mg, Ca, Sr, Ba, Mn, Co, Ni, Cu, Pd, and Cd." Biophysical Journal **65**: 1916-1928.

Jorritsma, S. H. T., E. J. Gowans, B. Grubor-Bauk and D. K. Wijesundara (2016). "Delivery methods to increase cellular uptake and immunogenicity of DNA vaccines." Vaccine **34**(46): 5488-5494.

Joye, I. J. and D. J. McClements (2014). "Biopolymer-based nanoparticles and microparticles: Fabrication, characterization, and application." Current Opinion in Colloid & Interface Science **19**(5): 417-427.

Kang, K. S., Pettitt, D. J. (1993). Xanthan, Gellan, Welan and Rhamsan Industrial Gums - Polysaccharides and Their Derivatives. J. B. B. Roy L. Whistler, Elsevier Inc.**:** 341-397.

Kardani, K., A. Bolhassani and S. Shahbazi (2016). "Prime-boost vaccine strategy against viral infections: Mechanisms and benefits." Vaccine **34**(4): 413-423.

Kasturi, S. P., K. Sachaphibulkij and K. Roy (2005). "Covalent conjugation of polyethyleneimine on biodegradable microparticles for delivery of plasmid DNA vaccines." Biomaterials **26**(32): 6375-6385.

Ken Lin, K. D., Chien-Fu Hung, and T-C Wu (2010). "Perspectives for Preventive and Therapeutic HPV Vaccines." J Formos Med Assoc. **109(1)**: 4-24.

Leal, L. B. (2018). Caracterização da urina por espectroscopia vibracional. Mestrado, Universidade do Vale do Paraíba.

Lee, J., S. Arun Kumar, Y. Y. Jhan and C. J. Bishop (2018). "Engineering DNA vaccines against infectious diseases." Acta Biomater **80**: 31-47.

Lee, S. J., A. Yang, T. C. Wu and C. F. Hung (2016). "Immunotherapy for human papillomavirus-associated disease and cervical cancer: review of clinical and translational research." J Gynecol Oncol **27**(5): e51.

Liderfelt, J. and J. Royce (2018). Section III - Recovery Processes, Principles, and Methods. Biopharmaceutical Processing: Development, Design, and Implementation of Manufacturing Processes. E. L. Günter Jagschies, Karol Łącki, Parrish Galliher, Elsevier Ltd.**:** 279-293.

Lindskog, E. K. (2018). Section VI - Industrial Process Design. Biopharmaceutical Processing: Development, Design, and Implementation of Manufacturing Processes. E. L. Günter Jagschies, Karol Łącki, Parrish Galliher, Elsevier Ltd.**:** 625-635.

loannis Giavasis, L. M. H., and Brian McNeil (2000). "Gellan Gum." Critical Reviews in Biotechnology **20**(3): 177-211.

Lowy, D. R. (2016). "HPV vaccination to prevent cervical cancer and other HPV-associated disease: from basic science to effective interventions." J Clin Invest **126**(1): 5-11.

Lucimara A. Forato, R. B. F., Luiz A. Colnago (1997). "Estudo de métodos de aumento de resolução de espectros de FTIR para análise de estruturas secundárias de proteínas " Química Nova **20**(5): 146-150.

Luechau, F., T. C. Ling and A. Lyddiatt (2009). "Primary capture of high molecular weight nucleic acids using aqueous two-phase systems." Separation and Purification Technology **66**(1): 202-207.

Luechau, F., T. C. Ling and A. Lyddiatt (2010). "Two-step process for initial capture of plasmid DNA and partial removal of RNA using aqueous two-phase systems." Process Biochemistry **45**(8): 1432-1436.

Luten, J., C. F. van Nostrum, S. C. De Smedt and W. E. Hennink (2008). "Biodegradable polymers as non-viral carriers for plasmid DNA delivery." J Control Release **126**(2): 97-110.

Lyu, C. J., L. Liu, J. Huang, W. R. Zhao, S. Hu, L. H. Mei and S. J. Yao (2019). "Biosynthesis of gamma-aminobutyrate by engineered Lactobacillus brevis cells immobilized in gellan gum gel beads." J Biosci Bioeng **128**(2): 123-128.

M. M. Diogo, J. A. Q., G. A. Monteiro, S. A. M. Martins, G. N. M. Ferreira, D. M. F. Prazeres (2000). "Purification of a Cystic Fibrosis Plasmid Vector for Gene Therapy Using Hydrophobic Interaction Chromatography." Biotechnology and Bioengineering **68**(5): 576-583.

Malviya, R., P. K. Sharma and S. K. Dubey (2016). "Modification of polysaccharides: Pharmaceutical and tissue engineering applications with commercial utility (patents)." Mater Sci Eng C Mater Biol Appl **68**: 929-938.

Manmohan Singh, M. B., Gary Ott, and Derek O'Hagan (2000). "Cationic microparticles: A potent delivery system for DNA vaccines." Proceedings of the National Academy of Sciences **97**(2): 811–816.

Martinez-Ramirez, I., A. Carrillo-Garcia, A. Contreras-Paredes, E. Ortiz-Sanchez, A. Cruz-Gregorio and M. Lizano (2018). "Regulation of Cellular Metabolism by High-Risk Human Papillomaviruses." Int J Mol Sci **19**(7): 1839.

Mesgari-Shadi, A., M.-H. Sarrafzadeh, B. Divband, J. Barar and Y. Omidi (2018). "Batch adsorption/desorption for purification of scFv antibodies using nanozeolite microspheres." Microporous and Mesoporous Materials **264**: 167-175.

Mittal, S. and L. Banks (2017). "Molecular mechanisms underlying human papillomavirus E6 and E7 oncoprotein-induced cell transformation." Mutat Res Rev Mutat Res **772**: 23-35.

Mohsen, M. M. (2011). "Interaction of DNA and polyethylenimine: Fourier-transform infrared (FTIR) and differential scanning calorimetry (DSC) studies." International Journal of the Physical Sciences **6**(32): 7328 - 7334.

Morris, E. R., K. Nishinari and M. Rinaudo (2012). "Gelation of gellan – A review." Food Hydrocolloids **28**(2): 373-411.

Munier, S., I. Messai, T. Delair, B. Verrier and Y. Ataman-Onal (2005). "Cationic PLA nanoparticles for DNA delivery: comparison of three surface polycations for DNA binding, protection and transfection properties." Colloids Surf B Biointerfaces **43**(3-4): 163-173.

Nandi, G., A. K. Nandi, N. S. Khan, S. Pal and S. Dey (2018). "Tamarind seed gum-hydrolyzed polymethacrylamide-g-gellan beads for extended release of diclofenac sodium using 3(2) full factorial design." Int J Biol Macromol **114**: 214-225.

Narkar, M., P. Sher and A. Pawar (2010). "Stomach-specific controlled release gellan beads of acid-soluble drug prepared by ionotropic gelation method." AAPS PharmSciTech **11**(1): 267-277.

Nesterenko, P. N. and M. D. Palamareva (2019). Liquid Chromatography: Overview. Encyclopedia of Analytical Science. C. P. Paul Worsfold, Alan Townshend, Manuel Miró, Elsevier Inc.: 174-181.

Nunes, J. C., A. M. Morão, C. Nunes, M. T. Pessoa de Amorim, I. C. Escobar and J. A. Queiroz (2012). "Plasmid DNA recovery from fermentation broths by a combined process of micro- and ultrafiltration: Modeling and application." Journal of Membrane Science **415-416**: 24-35.

Osmalek, T., A. Froelich and S. Tasarek (2014). "Application of gellan gum in pharmacy and medicine." Int J Pharm **466**(1-2): 328-340.

Padilla-Zamudio, A., P. Guerrero-German and A. Tejeda-Mansir (2015). "Plasmid DNA primary recovery from E. coli lysates by depth bed microfiltration." Bioprocess Biosyst Eng **38**(6): 1091-1096.

Pandey, A. P. and K. K. Sawant (2016). "Polyethylenimine: A versatile, multifunctional non-viral vector for nucleic acid delivery." Mater Sci Eng C Mater Biol Appl **68**: 904-918.

Patnaik, S., M. Arif, A. Pathak, N. Singh and K. C. Gupta (2010). "PEI-alginate nanocomposites: efficient non-viral vectors for nucleic acids." Int J Pharm **385**(1-2): 194-202.

Patrick P. Berna, N. T. M., Jozef Van Beeumen, Bart Devreese, Jerker Porath, and Mookambeswaran A. Vijayalakshmi (1997). "Residue Accessibility, Hydrogen Bonding, and Molecular Recognition: Metal-Chelate Probing of Active Site Histidines in Chymotrypsins." Biochemistry **36**(23): 6896-6905.

Pérez-Ramos, A., M. Nácher-Vázquez, S. Notararigo, P. López and M. L. Mohedano (2016). Part II - Probiotics in Food. Probiotics, Prebiotics, and Synbiotics. V. R. P. Ronald Ross Watson, Elsevier Inc.: 329-344.

Phong, W. N., P. L. Show, Y. H. Chow and T. C. Ling (2018). "Recovery of biotechnological products using aqueous two phase systems." J Biosci Bioeng **126**(3): 273-281.

Prajapati, V. D., G. K. Jani, B. S. Zala and T. A. Khutliwala (2013). "An insight into the emerging exopolysaccharide gellan gum as a novel polymer." Carbohydr Polym **93**(2): 670-678.

Prather, K. J., S. Sagar, J. Murphy and M. Chartrain (2003). "Industrial scale production of plasmid DNA for vaccine and gene therapy: plasmid design, production, and purification." Enzyme and Microbial Technology **33**(7): 865-883.

Pruthu, K. (2014). "Organic Solvents - Health Hazards." Journal of Chemical and Pharmaceutical Sciences(3): 83-86.

Rappuoli, R. and E. De Gregorio (2016). "Editorial overview: Vaccines: novel technologies for vaccine development." Curr Opin Immunol **41**: v-vii.

Reis, C. P., R. J. Neufeld, S. Vilela, A. J. Ribeiro and F. Veiga (2006). "Review and current status of emulsion/dispersion technology using an internal gelation process for the design of alginate particles." J Microencapsul **23**(3): 245-257.

Rieppo, L., S. Saarakkala, T. Narhi, H. J. Helminen, J. S. Jurvelin and J. Rieppo (2012). "Application of second derivative spectroscopy for increasing molecular specificity of Fourier transform infrared spectroscopic imaging of articular cartilage." Osteoarthritis Cartilage **20**(5): 451-459.

Saha, D. and S. Bhattacharya (2010). "Hydrocolloids as thickening and gelling agents in food: a critical review." J Food Sci Technol **47**(6): 587-597.

Schiffman, M., P. E. Castle, J. Jeronimo, A. C. Rodriguez and S. Wacholder (2007). "Human papillomavirus and cervical cancer." The Lancet **370**(9590): 890-907.

Sciences, G. H. L. (2006). Hydrophobic Interaction and Reversed Phase Chromatography: Principles and Methods, GE Healthcare Life Sciences.

Sciences, G. H. L. (2015). Size Exclusion Chromatography: Principles and Methods, GE Healthcare Life Sciences.

Sciences, G. H. L. (2016). Affinity Chromatography: Specific Groups of Biomolecules, GE Healthcare Life Sciences.

Sciences, G. H. L. (2016). Ion Exchange Chromatography: Principles and Methods, GE Healthcare Life Sciences.

Shi, B., M. Zheng, W. Tao, R. Chung, D. Jin, D. Ghaffari and O. C. Farokhzad (2017). "Challenges in DNA Delivery and Recent Advances in Multifunctional Polymeric DNA Delivery Systems." Biomacromolecules **18**(8): 2231-2246.

Siddhesh D. Patil, D. G. R., Diane J. Burgess (2005). "DNA-based Therapeutics and DNA Delivery Systems: A Comprehensive Review." The AAPS Journal **7**(1): 61-77.

Slivac, I., D. Guay, M. Mangion, J. Champeil and B. Gaillet (2017). "Non-viral nucleic acid delivery methods." Expert Opin Biol Ther **17**(1): 105-118.

Songock, W. K., S. M. Kim and J. M. Bodily (2017). "The human papillomavirus E7 oncoprotein as a regulator of transcription." Virus Res **231**: 56-75.

Sousa, A., A. M. Almeida, U. Cernigoj, F. Sousa and J. A. Queiroz (2014). "Histamine monolith versatility to purify supercoiled plasmid deoxyribonucleic acid from Escherichia coli lysate." J Chromatogr A **1355**: 125-133.

Sousa, A., F. Sousa and J. A. Queiroz (2012). "Advances in chromatographic supports for pharmaceutical-grade plasmid DNA purification." J Sep Sci **35**(22): 3046-3058.

Sridharan, K. and N. J. Gogtay (2016). "Therapeutic nucleic acids: current clinical status." Br J Clin Pharmacol **82**(3): 659-672.

Sun, H., X. Zhu, L. Zhang, Y. Zhang and D. Wang (2010). "Capture and release of genomic DNA by PEI modified Fe3O4/Au nanoparticles." Mater Sci Eng C Mater Biol Appl **30**(2): 311-315.

T. Alexakis, D. K. B., D. Quong, A. Groboillot, I. O'Neill, D. Poncelet, R. J. Neufeld (1995). "Microencapsulation of DNA Within Aiginate Microspheres and Crosslinked Chitosan Membranes for In Vivo Application " Applied Biochernistry and Biotechnology **50**: 93-106.

Tan, L., D.-S. Kim, I.-K. Yoo and W.-S. Choe (2007). "Harnessing metal ion affinity for the purification of plasmid DNA." Chemical Engineering Science **62**(21): 5809-5820.

Thatcher, S. A. (2018). Nucleic Acid Isolation. Principles and Applications of Molecular Diagnostics. A. R. H. Nader Rifai, Carl T. Wittwer, Elsevier Inc.**:** 35-46.

Thomas, M. A. (2012). Surface Area: The Most Underutilized Particle Property in Pharma. PSG Pharmafocus. **10:** 1-5.

Tolmasky, M. E. (2017). Plasmids. Reference Module in Life Sciences, Elsevier.

Tüzmen, N., F. Akdoğan, T. Kalburcu, S. Akgöl and A. Denizli (2010). "Development of the magnetic beads for dye ligand affinity chromatography and application to magnetically stabilized fluidized bed system." Process Biochemistry **45**(4): 556-562.

Valente, J. F., A. Sousa, J. A. Queiroz and F. Sousa (2014). "Selective purification of supercoiled p53-encoding pDNA with L-methionine-agarose matrix." Anal Biochem **459**: 61-69.

Valente, J. F. A., A. Sousa, V. M. Gaspar, J. A. Queiroz and F. Sousa (2018). "The biological performance of purified supercoiled p53 plasmid DNA in different cancer cell lines." Process Biochemistry **75**: 240-249.

Van Alstine, J. M., G. Jagschies and K. M. Łącki (2018). Section III - Recovery Processes, Principles, and Methods. Biopharmaceutical Processing: Development, Design, and Implementation of Manufacturing Processes. E. L. Günter Jagschies, Karol Łącki, Parrish Galliher, Elsevier Ltd.**:** 207-220.

Van Alstine, J. M., G. Jagschies and K. M. Łącki (2018). Section III - Recovery Processes, Principles, and Methods. Biopharmaceutical Processing: Development, Design, and Implementation of Manufacturing Processes. E. L. Günter Jagschies, Karol Łącki, Parrish Galliher, Elsevier Ltd.**:** 221-239.

Vermeulen, L. M. P., T. Brans, S. C. De Smedt, K. Remaut and K. Braeckmans (2018). "Methodologies to investigate intracellular barriers for nucleic acid delivery in non-viral gene therapy." Nano Today **21**: 74-90.

Viarisio, D., L. Gissmann and M. Tommasino (2017). "Human papillomaviruses and carcinogenesis: well-established and novel models." Curr Opin Virol **26**: 56-62.

Virgen-Ortíz, J. J., J. C. S. dos Santos, Á. Berenguer-Murcia, O. Barbosa, R. C. Rodrigues and R. Fernandez-Lafuente (2017). "Polyethylenimine: a very useful ionic polymer in the design of immobilized enzyme biocatalysts." Journal of Materials Chemistry B **5**(36): 7461-7490.

Voß, C. (2007). Production of plasmid DNA for pharmaceutical use. Biotechnology Annual Review, Elsevier. **13:** 201-222.

Wang, M., Q. Yang, X. Zhao and Z. Wang (2019). "Highly efficient removal of copper ions from water by using a novel alginate-polyethyleneimine hybrid aerogel." Int J Biol Macromol **138**: 1079-1086.

Xiang, Y., N. N. L. Oo, J. P. Lee, Z. Li and X. J. Loh (2017). "Recent development of synthetic nonviral systems for sustained gene delivery." Drug Discov Today **22**(9): 1318-1335.

Yamashita, Y., R. Miyahara and K. Sakamoto (2017). Emulsion and Emulsification Technology: Theoretical Principles and Applications. Cosmetic Science and Technology. R. Y. L. Kazutami Sakamoto, Howard I. Maibach, Yuji Yamashita, Elsevier Inc.**:** 489-506.

Yang, A., J. Jeang, K. Cheng, T. Cheng, B. Yang, T. C. Wu and C. F. Hung (2016). "Current state in the development of candidate therapeutic HPV vaccines." Expert Rev Vaccines **15**(8): 989-1007.

Yang, J., H. Liu and X. Zhang (2014). "Design, preparation and application of nucleic acid delivery carriers." Biotechnol Adv **32**(4): 804-817.

Yang, X., Y. Hou, T. Gong, L. Sun, J. Xue and Y. Guo (2019). "Concentration-dependent rheological behavior and gelation mechanism of high acyl gellan aqueous solutions." Int J Biol Macromol **131**: 959-970.

Yeo-Teh, N. S. L., Y. Ito and S. Jha (2018). "High-Risk Human Papillomaviral Oncogenes E6 and E7 Target Key Cellular Pathways to Achieve Oncogenesis." Int J Mol Sci **19**(6): 1706.

Zaman, A., Z. Arif and K. Alam (2017). "Fructosylation induced structural changes in mammalian DNA examined by biophysical techniques." Spectrochim Acta A Mol Biomol Spectrosc **174**: 171-176.

Zhang, S., Y. Xu, B. Wang, W. Qiao, D. Liu and Z. Li (2004). "Cationic compounds used in lipoplexes and polyplexes for gene delivery." J Control Release **100**(2): 165-180.

Zhang, Y. and G. Lozano (2017). "p53: Multiple Facets of a Rubik's Cube." Annu Rev Cancer Biol **1**: 185-201.

Zia, K. M., S. Tabasum, M. F. Khan, N. Akram, N. Akhter, A. Noreen and M. Zuber (2018). "Recent trends on gellan gum blends with natural and synthetic polymers: A review." Int J Biol Macromol **109**: 1068-1087.

Zimdahl, R. L. (2015). Recombinant DNA. Six Chemicals That Changed Agriculture. R. L. Zimdahl, Elsevier Inc.**:** 135-164.